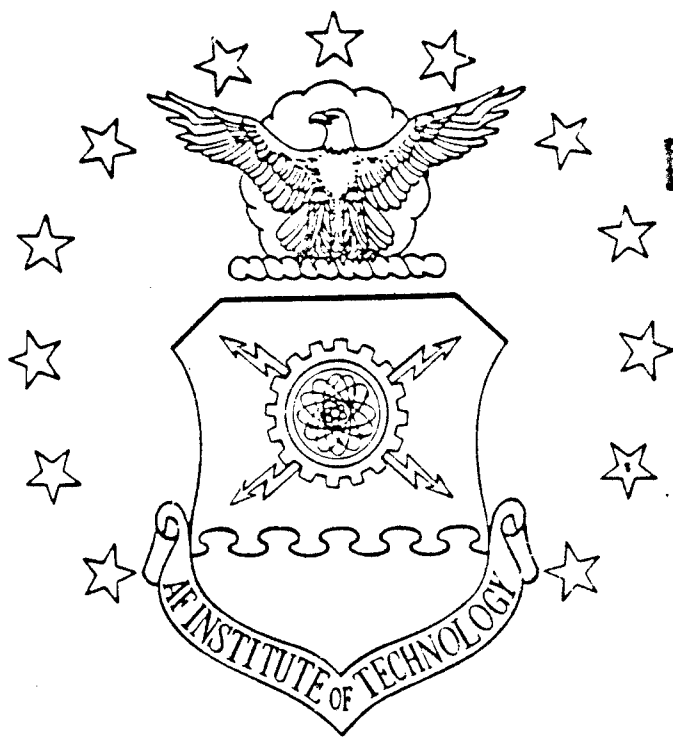DTIC FILE COPY

DTIC
S ELECTE D
JUN 2 3 1988
R H

ANGLE OF ATTACK AND SIDESLIP ESTIMATION
USING AN
INERTIAL REFERENCE PLATFORM

THESIS

JOSEPH E. ZEIS, JR.
CAPTAIN, USAF
AFIT/GAE/AA/88J-2

20030204160

DEPARTMENT OF THE AIR FORCE

AIR UNIVERSITY

AIR FORCE INSTITUTE OF TECHNOLOGY

Wright-Patterson Air Force Base, Ohio

88 6 23 053

AFIT/GAE/AA/88J-2

ANGLE OF ATTACK AND SIDESLIP ESTIMATION
USING AN
INERTIAL REFERENCE PLATFORM

THESIS

JOSEPH E. ZEIS, JR.
CAPTAIN, USAF
AFIT/GAE/AA/88J-2

DTIC

JUN 2 3 1988

◌H

AFIT/GAE/AA/88J-2

ANGLE OF ATTACK AND SIDESLIP ESTIMATION

USING AN

INERTIAL REFERENCE PLATFORM

THESIS

Presented to the Faculty of the School of Engineering

of the Air Force Institute of Technology

Air University

In Partial Fulfillment of the

Requirements for the Degree of

Master of Science in Aeronautical Engineering

Joseph E. Zeis, Jr., B.S.

Captain, USAF

June 1988

PREFACE

The purpose of this research is to develope and flight test concepts for the estimation of angle of attack (α) and sideslip (β) using an inertial reference platform. This development was further broken down into real-time, inflight estimation of α and post-flight estimation of α and β. Following theoretical development, the concepts were tested with NASA F-15A flight data and examined real-time during a NASA Highly Integrated Digital Engine Control (HIDEC) flight test using the F-15A aircraft.

Angle of attack is a critical parameter in the maneuverable, high performance aircraft of today. Yet many errors are present in the current methods of obtaining this angle. An accurate method of α and β estimation could eliminate the need for such probes, and allow these quantities to be used for a broad range of applications. An inflight estimator was developed for computational speed and accuracy using inertial navigation system linear accelerations and angular rates. A second system based on linear recursive modeling was developed for post-flight estimation of α and β. The data and programs specified in this research are applicable only to those aircraft mentioned, but the methods of estimation are universal.

I would like to thank my thesis advisors, Dr. Robert Calico and Maj. Daniel Gleason for their help and direction in this project. In addition, I am indebted to NASA for allowing me the use of their facilities and test aircraft for this work. The superb efforts of NASA flight control engineer Heather Lambert turned a theory into reality.

ii

TABLE OF CONTENTS

TABLE OF CONTENTS (CONCLUDED)

LIST OF FIGURES

LIST OF FIGURES (CONCLUDED)

LIST OF TABLES

LIST OF SYMBOLS AND ABBREVIATIONS

Symbol	Title	Units
A	Stability matrix	--
a_{BZ}	Normal acceleration in body axis	feet/sec^2
B	Control matrix	--
$\bar{c}$	Mean aerodynamic chord of wing	feet
$C_{L_{WB}}$	Wing-body coefficient of lift	--
C_{m_o}	Zero lift pitching moment coefficient	--
g	acceleration of gravity	feet/sec^2
H	Matrix of available measurements	--
h	Altitude	feet
I	Identity matrix	--
Ix	Moment of inertia about x axis	slug-feet^2
Iy	Moment of inertia about y axis	slug-feet^2
Iz	Moment of inertia about z axis	slug-feet^2
Ixz	Cross-product of inertia	slug-feet^2
KG	Kalman gain matrix	--
L	Total aircraft lift	pounds
L_T	Tail contribution to lift	pounds
L_{WB}	Lift of wing-body combination	pounds
M	Mach number	--
m	Moment about y axis (pitching moment)	foot-pounds
m_o	Zero-lift pitching moment	foot-pounds
N	Moment about z axis (yawing moment)	foot-pounds

Symbol	Title	Units
n	Load factor	g
p	Roll rate	radians/sec
PM	Error covariance prior to measurement	- -
PP	Error covariance after measurement	- -
Q	Matrix of model uncertainty	- -
q	Pitch rate	radians/sec
R	Matrix of measurement uncertainty	- -
r	Yaw rate	radians/sec
s	Wing area	feet
T	Error range or twice the given accuracy	- -
u	Body axis velocity in x direction	feet/sec
V	True airspeed	feet/sec
V_A	Airmass velocity	feet/sec
V_B	Body axis velocity	feet/sec
V_I	Inertial velocity	feet/sec
V_V	Wind velocity	feet/sec
X	State vector	- -
XM	State estimate prior to measurement	- -
XP	State estimate after measurement	- -
X_{WB}	Distance from center of gravity to wing-body aerodynamic center	feet
X_T	Distance from center of gravity to horizontal tail aerodynamic center	feet
Z	Measurement vector	- -

x

Symbol	Title	Units
α	Angle of attack	degrees
α_o	Initial angle of attack guess	degrees
β	Angle of sideslip	degrees
δ	Control input	--
σ^2	Variance	--
θ	Pitch angle	degrees
ϕ	Roll angle	degrees
ψ	Heading angle	degrees

SUBSCRIPTS AND SUPERSCRIPTS

Symbol	Title	Units
T	Transpose	--
o	Trim value	--
$\hat{}$	Perturbation value	--
$.$	Time derivative	--
$'$	Primed lateral derivative	--
x	x direction	--
y	y direction	--
z	z direction	--
N	North direction	--
E	East direction	--
W	West direction	--

Symbol	Title	Units

ABBREVIATIONS

Symbol	Title	Units
a	Aileron	--
AOA	Angle of attack	degrees
CADC	Central air data computer	--
C.L.	Chord line of wing	--
E	Elevator	--
HIDEC	Highly integrated digital engine control	
INS	Inertial navigation system	--
IRS	Inertial reference system	--
Lat	Lateral	--
Long	Longitudinal	--
Rd	Rudder	--
RMS	Root mean squared error	--
Rw	Relative wind	--
T	Thrust	--
X_u	Partial derivative example: $\dfrac{\delta X}{\delta u}$	--
(K)	At time K	seconds
(K - 1)	At time step prior to K	seconds

ABSTRACT

Throughout aviation history, pilots and engineers have had to rely on mechanical angle of attack (α) and sideslip (β) probes to determine an aircraft's position relative to the airmass. Recent advances in the stability, accuracy and reliability of inertial navigation and reference systems now allow angle of attack and sideslip information to be calculated from internal aircraft systems and a central air data computer. Conflicting requirements for inflight angle of attack information and post-flight angle of attack and sideslip data reduction demand two seperate methods. Inflight algorithms require fast, accurate angle of attack, with no assumptions on vertical wind. Post-flight usage, however, demands great accuracy with no assumptions on either sideslip or vertical windage. From the aircraft equations of motion, angle of attack and sideslip algorithms will be developed, with velocity and rate inputs of the type expected from an aircraft central air data computer and inertial navigation system. A computer program will then be developed to validate these equations. A Kalman filter algorithm will also be designed to aid in estimating data output from these sources.

Flight test will consist of two parts. Initally, velocity, rate, acceleration, and aircraft position signals will be picked off a standard inertial reference system on a NASA F-15A aircraft. These signals will be processed using the algorithms developed, and estimated angle of attack will be output. These outputs will be compared with those

predicted by the inflight and post-flight algorithm for accuracy and usability. A demonstration will then be conducted on the NASA F-15A to determine usability and accuracy of inertially derived angle of attack information in a highly maneuvering environment.

Conclusions will include both the usability and accuracy of inertially derived angle of attack and sideslip. Applications for accurate and reliable angle of attack and sideslip are many. Three-dimensional windage can be readily predicted as a result of this research, along with airborne windshear detection and stall warning systems. Elimination of mechanical angle of attack and sideslip probes, with their inherent inaccuracy, failure rates, and time lag, will also allow for angle of attack information to be used as reliable feedback in automatic aircraft control systems.

ANGLE OF ATTACK AND SIDESLIP ESTIMATION
USING AN
INERTIAL REFERENCE PLATFORM

I. Introduction

OVERVIEW The orientation of an aircraft's velocity vector
relative to the airmass surrounding it can be described by
two angles, the angle of attack (alpha or α) and the angle of
sideslip (beta or β). Since all aerodynamic forces and
moments depend on these two angles, they are critical
parameters in stability and control flight testing. Indeed,
angle of attack, and to a lesser extent sideslip, are
extremely important parameters to pilots of high performace
aircraft in an operational environment. Angle of attack is
continuously monitored in air-to-air maneuvering and during
approach to landing In addition, the two angles are
utilized for stall inhibitor and alpha limiter subsystems in
advanced flight control systems. But angle of attack and
sideslip are extremely difficult to measure precisely.
Throughout the brief history of aviation, both pilots and
engineers have had to rely on mechanical angle of attack and
sideslip devices to determine those critical angles in the
three-dimensi al airmass. If angle of attack and sideslip
could be accur ly estimated both in the dynamic inflight
environment, and during post-flight data analysis sessions, a
great deal of difficulty in performing calibrations, creating
correction curves, and calculating performance derivatives
could be eliminated. An accurate, real-time knowledge of

angle of attack and sideslip could aid the pilot in a variety
of ways, just as accurate post-flight estimations of both
critical angles could aid the flight test engineer.

PROBLEM   Currently, angle of attack and sideslip are
measured by external probes mounted on the forward fuselage
of operational aircraft.   These rotating mechanical probes
have slots which then align the probes to the local airflow,
thus providing an estimate of the true angle of attack of the
wing-body combination in the airmass. Flight testing, to a
great degree, relies on pitot probe mounted angle of attack
and sideslip vanes. The mounting of probes far ahead on the
fuselage eliminates some of the error due to local flow
effects, but many problems still exist with external angle of
attack (AOA) and sideslip probes and vanes. First, being
away from the center of gravity of the aircraft, the rotating
probes are subject to pitch, yaw, and roll motion-induced
errors which vary with Mach number and maneuver, increasing
the difficulty of calibration dramatically[1:4]. Second,
being mechanical pick-off devices, these probes have a
definite time lag that hampers their use in flight controls
and autopilot applications[2:443]. This time lag can produce
extremely undesirable characteristics in most flight.
controls.   Third, several airplanes, most notably F-16 and
F-111 aircraft have been lost due to failure of the angle of
attack probe inflight[3].   This has been due to the
requirement for stall inhibitor systems which attempt to
prevent the aircraft from exceeding a specified angle of
attack.   The flight controls will respond to a high AOA with
a pitch down maneuver to reduce the sensed extreme angle of
attack.   If both probes have failed in flight, the aircraft
could pitch down for no reason, other than the false AOA

derived from the failed probe[4:1-51]. For such a vital instrument on a high performace aircraft, single probe failure could result in aircraft loss. Finally, the very accuracy of the mechanical probe in determining angle of attack and sideslip is difficult to determine. Thacker found errors in angle of attack over the subsonic range to be on the order of 1.5 to 2 times the actual value of alpha, and sideslip error of 1.75 to 2.4 times actual beta values for the USAF/CALSPAN NT-33A, varying with Mach number[1:2]. The F-16 flight control system currently calculates angle of attack with twin double-slotted probes to an accuracy of approximately 0.4 to 0.5 degrees over the entire flight regime[3]. These probe errors are applicable to all probed aircraft in the subsonic range of flight. The realm of supersonic flight makes greater demands on the use of probes and vanes to determine angles of attack and sideslip. Increased performance dictates a greater requirement for knowledge of these angles. However, at extremely high speeds, penalties from drag and aerodynamic heating require a "cleaner" method for angle of attack and sideslip determination without reference to external devices in the airflow. Indeed, the increased reliance on angle of attack and sideslip information at these critical speeds and flight conditions places a strong requirement on sensor redundancy for critical flight control systems. That requirement could be fulfilled by such an internal AOA and sideslip estimation system.

SOLUTION   Angle of attack and sideslip can be determined with a high degree of accuracy from inertial reference systems and central air data computers. The current generation of ring laser gyro inertial navigation systems (INS) and inertial reference systems (IRS) have accuracies in

pitch, roll and heading angles on the order of 5.6×10^{-4}
radians(.032 deg.) and angular rate measurment accuracies on
the order of 7.5×10^{-4}radians/second(.043 degrees/sec)
[5:86-89]. The newest generation ring laser gyro INS units
are even better, with accuracies of 2.0×10^{-6}radians[6].
Normal acceleration can be measured to an accuracy of 2
feet/sec^2[5]. Using the three INS rates, accelerations, and
central air data computer (CADC) inputs, the angle of attack
can be estimated with a moment summation and lift model.
This lift can then be compared to the current aircraft weight
model and measured load factor. An angle of attack
estimation can then be generated based on the required load
factor. For post-flight evaluation, the INS rates and Euler
angles can be input to a extended Kalman estimator for ground
reconstruction of angle of attack and sideslip.

The speed of the digital INS, combined with its accuracy
and reliability provide the following advantages. Primarily,
if angle of attack can indeed be estimated with a high degree
of certainty, the speed of the INS/computer calculations
implies that the information can be used in conjunction with
advanced flight control systems as a feedback quantity. Being
internal to the aircraft and extremely accurate, the INS will
eliminate local flow and Mach effects that must now be
corrected in raw external probe data. Finally, the
reliability of the current INS systems, and even higher
reliability of the ring laser INS's, adds sensor redundancy
to probe derived AOA systems. As the mean time between
failures (MTBF) of INS's increases, it could become the
primary source of angle of attack and sideslip data.

A post-flight derived angle of attack and sideslip can
be used readily to calibrate probes and aid in the estimation
of stability derivatives without lengthy trim shots. Alpha

and beta derived immediately following flight from INS and
CADC data can save valuable flight time, effort and
substantial computer resources.

SCOPE The purpose of this thesis is to develop an accurate
method for estimating angle of attack and sideslip using
signals available from a standard INS. The estimation
algorithm is broken into two parts, the inflight and the
post-flight algorithms. The inflight algorithm must
accurately (to .5 degrees) measure angle of attack in real
time, suitable for use in a flight control application. An
update rate of 30 to 60 cycles per second will allow flight
control usage of the derived information. This dictates
quick, simple and accurate calculations from INS and CADC
inputs only. A by-product of alpha esitmates should be the
accurate calculation of three-dimensional winds. The
post-flight algorithm must accurately (to 0.25 degrees)
estimate AOA and sideslip using INS angles and rates. These
desired accuracies are based on 200 percent improvement on
current uncorrected probe accuracies of 2 degrees over the
entire flight regime. This information would be input to a
linear recursive estimator for reconstruction of the required
data. There is no requirement, however, for real time data.
In this way, complicated estimation algorithms can be applied
to determine the most accurate angle of attack and sideslip,
along with windage, for flight test interests.

The algorithms will be developed with these specific
purposes in mind. A complete flight test program will
determine the usefulness and accuracy of the angle of attack
and sideslip estimates. This testing will first evaluate
estimation in straight and level flight, and gentle turning
maneuvers. This will be followed by examination of the

- 5 -

algorithms in a highly maneuvering environment at increased
AOA and load factors. The results will be compared to a
computer simulation of the angle of attack and sideslip
required for the specific maneuver, as well as probe and vane
measured alpha and beta.

The objectives of this project are:

1. Develop a post-flight algorithm for
    determination of angle of attack and sideslip
    with reference to INS and CADC outputs only,
    making no assumptions on vertical wind or
    sideslip. The estimations should be accurate to
    .25 degrees. Then, apply a Kalman filter
    to post flight data for accurate AOA
    and sideslip.

2. Validate by computer simulation the angle of
    attack and sideslip recovered by the Kalman
    filter.

3. Develop an inflight algorithm to determine
    angle of attack with reference to INS and CADC
    outputs only, assuming sideslip is zero. The
    data must be real time and accurate to .5
    degrees.

4. Demonstrate algorithms with flight test data.

5. Determine through flight test where the
    algorithms are no longer valid estimators.

II. BACKGROUND

PREVIOUS APPROACHES Four basic approaches have been used to
estimate angle of attack. Freeman's method [7] in 19??
utilized accelerometers only, with no inertial hardware The
additional aircraft dynamics were then estimated by control
surface deflection pickoff devices and basic aircraft
equations of motion. An angle of attack processor then took
inputs of flight condition, accelerations, and surface
position to estimate angle of attack for the required
maneuver. This method required extensive modeling of
stability derivatives. Tail aerodynamics were needed to
implement the algorithm. Surface position indicators were
used to formulate the model of the aerodynamic response of
the tail surfaces. Pitch, roll, mach and G-loading
limitations were placed on the estimator to simplify this
complex modeling into a managable system of equations for
processing. This method relied heavily on aerodynamic
modeling using stability derivatives and surface position to
evaluate the maneuver being performed and estimate an angle
of attack required. While accurate to approximately .5
degrees angle of attack over the flight range specified in
the limitations [7:38], INS information could eliminate the
need for such extensive aero modeling and surface position
pickoff, with improved accuracy over a less constrained
flight envelope.

A second algorithm, requiring less extensive aerodynamic
modeling, is provided by Petrov and Studnev, et al [8]. This
method requires precise modeling of the coefficients of lift and
drag and accelerometers to model aerodynamic performance in

gliding flight [8:3]. The linearized equations are
applicable only for small alpha and beta (less than 10
degrees) and do not provide the angles throughout the
maneuvering envelope [8:5].

Perhaps the most detailed work has been accomplished by
Olhausen, using INS outputs for YF-16 flight test [9]. The
method uses INS accelerometer and velocity measurments, along
with Euler angle measuments. Basic aircraft equations of
motion were solved using appropriate order Runge-Kutta
integration techniques. This method is effective, but like
most, it requires the assumption that sideslip and vertical
windage are zero. Used primarily for flight test
applications, the algorithm develops problems determining
winds in steep turns where sideslip is not negligible.

The fourth method, and the one used by Thacker [1], is
state-space estimation. Thacker only used two states, $\hat{\theta}$ and
$\hat{q}$. In this model, $\hat{\theta}$ represents the pitch angle and $\hat{q}$ is the
pitch rate. These quantities are perturbation values about
some nominal flight condition. The two states were shown by
Thacker to successfully determine angle of attack to
approximately .5 degrees. Logically, a more accurate math
model of the aircraft dynamics should result in more accurate
determinations of angle of attack. In addition, a model of
the lateral dynamics of the same aircraft should also yield
comparable results with sideslip. The usual model of an
unaugmented aircraft consists of 4 states in both the
decoupled longitudinal and lateral modes. Although varied,
this mathematically more accurate system can be one with $\hat{V}$,
$\hat{\alpha}$, $\hat{q}$, and $\hat{\theta}$, where $\hat{\alpha}$ is angle of attack, $\hat{V}$ is true
airspeed, $\hat{\theta}$ is pitch angle, and $\hat{q}$ is pitch rate. Again,
these quantities are perturbation values. They are, in other
words, the changes in those variables from some steady state

- 8 -

values. Accurate inputs can be obtained for q and θ from the INS, with a moderately accurate V from the CADC (off by the angle of attack rotation). Alpha would then be estimated by a Kalman estimator. This state-space estimator has several disadvantages. The system must model about 34 stability derivatives, depending on the accuracy desired in the result. These derivatives are naturally based on Mach, altitude, flight condition, and require mathematical changes for flap deflection. This extensive math modeling, along with the computational time required to solve the system of equations, currently precludes this method for real time inflight estimator applications.

PROPOSED APPROACH Angle of attack and sideslip estimation has two inherently opposing requirements, speed and accuracy. Speed of calculation is a critical requirement for flight control usage of alpha, as well as for pilot information and three dimensional windage derivation. Calculations must be minimized, with a judicious use of assumptions, while retaining accuracy to .5 degrees. On the other hand, flight test standards require an accurate knowledge of alpha, beta, and three-dimensional winds. This information is not time critical, and can be post-flight processed for analysis at a later time. These requirements drive the need for two types of estimators, a rapid estimator method for inflight use, and a very accurate estimator method for flight test analysts after the fact. I propose to develop these two methods of angle of attack and sideslip estimation, and flight test their validity.

Freeman's work with the alpha estimator provides a good basis for the inflight, real-time portion of the alpha estimator problem. Incorporation of INS rates, angles and

- 9 -

accelerations can dramatically reduce the requirement for extensive stability derivative modeling, and increase the accuracy and calculation speed. However, the flight envelope imposed by Freeman must be expanded for a wider range of inflight applications. A new algorithm based on total lift and aircraft moments will be eveloped. No assumptions will be made concerning the existence of a vertical wind, and accurate three-dimensional windage output will be a criterion for acceptable operation of the inflight alpha estimator.

With calculation speed not a factor for the post-flight estimator, the state-space method provides a basis for alpha, beta, and three-dimensional windage estimation, with no assumptions made on any of these three quantities. The more extensive, 4 component state-space model of 34 derivatives for decoupled longitudinal and lateral response modes can be easily used. This would also require application of a linear recursive Kalman estimator to take the limited INS and CADC inputs to estimate the alpha and beta obtained in the maneuvers performed. 3-d windage profiles can then readily be calculated for test engineering usage.

III. INFLIGHT ANGLE OF ATTACK ESTIMATION THEORY

BASIC LIFT EQUATIONS Angle of attack is directly related to the coefficient of lift of the wing-body combination. If the total lift on the wing-body is obtained, angle of attack may be subsequently computed. Total lift is the sum of the lift of the wing-body combination acting at the corresponding wing-body aerodynamic center, and the lift of the tail, acting at the aerodynamic center of the empennage.
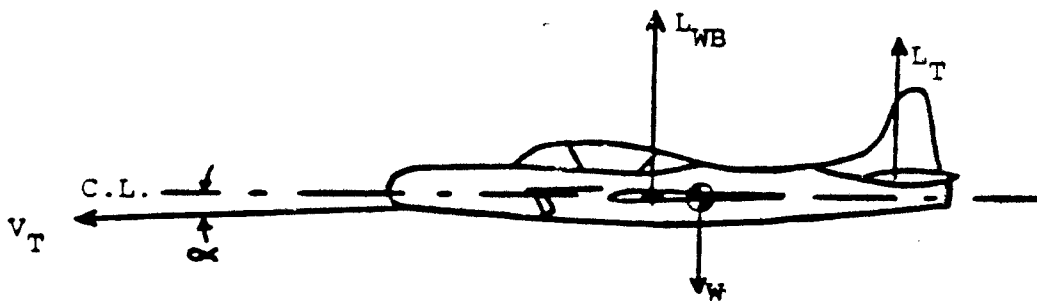
Figure 1.   Basic Longitudinal Aerodynamic Forces

Denoting this lift of the wing-body combination as L_{WB} , the lift of the tail as L_T, the total lift, L, is given by:

$$L = L_{WB} + L_T \tag{1}$$

But total lift can also be defined by:

$$L = nW \tag{2}$$

where n is load factor and W is total aircraft weight.
Then:

$$nW = L_{WB} + L_T \qquad (3)$$

Wing-body lift can be expressed in a standard non-dimensional coefficient $C_{L_{WB}}$, where:

$$C_{L_{WB}} = \frac{L_{WB}}{(\frac{1}{2}\rho V^2)S} \qquad (4)$$

where ρ is atmospheric density at flight altitude, V is true airspeed, and S is wing area.

Rearranging:

$$L_{WB} = C_{L_{WB}} (\tfrac{1}{2}\rho V^2)S \qquad (5)$$

so that in terms of load factor:

$$nW = C_{L_{WB}} (\tfrac{1}{2}\rho V^2)S + L_T \qquad (6)$$

MOMENT SUMMATION Lift on the tail must be modeled next.
This can be accomplished by applying an analagous equation,
but the effects of elevator deflection, downwash, and surface
position pickoffs, as well as wake effects must be
considered. These effects are difficult to account for due
to the inaccuracies of determining exact tail deflection, as
well as the errors in aerodynamic modeling of the flow over
the empennage, and the resulting forces. While it is
possible to model downwash and analytically determine tail
lift, the equations quickly become unmanagable in even slight

- 12 -

maneuvering. In addition, the algorithm would then vary extensively with tail surface control design. The simpler and more direct method is the calculation of the lift contribution of the tail surfaces as determined through aircraft moments.

The moment action on the total aircraft can be described adequately by the zero-lift pitching moment, wing-body lift, and the moments due to the tail lift. Since the lift is always perpendicular to the relative wind, the resulting moments and arms are shown in Figure 2.
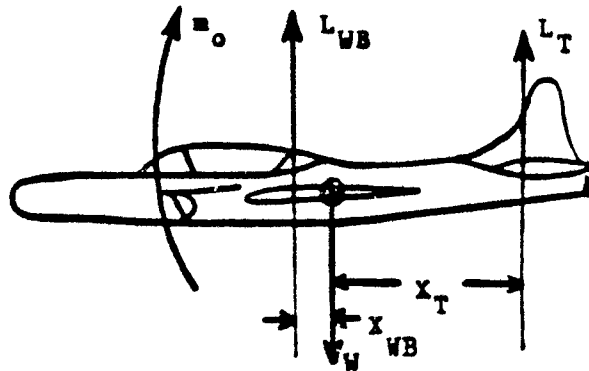
Figure 2. Moments Acting on an Aircraft in Flight

where m_o is the zero-lift pitching moment about the quarter-chord and X_T is the distance between the center of gravity of the aircraft and the aerodynamic center of the horizontal tail. X_{WB} is the corresponding distance between the center of gravity of the aircraft and the wing-body aerodynamic center. It is assumed that the weight acts through the center of gravity, and is therefore not a contributing factor in any moment equation. This is a valid

assumption in that the aircraft in flight will generally
rotate about its center of gravity. Therefore, any moment
summation about the center of gravity eliminates weight of
the aircraft as a contributing factor in the moment
equation. A normal static margin will place the center of
gravity less than ten percent of the mean aerodynamic chord
away from the aerodynamic center. A further assumption is
that the lift of the wing-body combination acts at a single
point called the wing-body aerodynamic center. These two
basic assumptions are generally held to be true for
conventional aircraft throughout a large portion of their
flight regimes. In addition, centerline thrust is assumed,
resulting in no moments due to thrust, as well as drag.
This assumption is valid for NT-33A and other fighter- type
aircraft investigations, but may require correction in
tanker/transport applications.

The term m_O as used here refers to the zero-lift pitching
moment of the wing-body-tail combination. As such, the
conditions at zero lift require that lift of the wing-body
offset the lift of the tail. Thus the terms L_T and L_{VB}
actually refer to incremental lift from the zero-lift
condition. However, the zero-lift values of wing-body and tail
lift are negligible when compared to total wing-body and tail
lift in 1-g flight. The simplification will therefore be
made that L_T and L_{VB} are total lift terms and not incremental
terms from the zero-lift condition. So the summation of moments
yields:

$$\Sigma m = m_O - L_T X_T + L_{VB} X_{VB} \qquad (7)$$

where X_{VB} is the wing-body static margin as defined by the
expression:

$$X_{VB} = (h - h_{VB})\bar{c} \qquad (8)$$

- 14 -

But a standard alternate formula for the total sum of the moments is given in McRuer [2:220].

$$\Sigma m = \dot{q}I_Y + pr(I_X - I_Z) - r^2 I_{XZ} + p^2 I_{XZ} \qquad (9)$$

where q is pitch acceleration, p is roll rate and r is yaw rate, all quantities available directly from a USAF standard INS. I_X, I_Y, and I_Z are respective principle moments of inertia to the X, Y, and Z axes and I_{XZ} is the applicable cross product of inertia calculated in the body axis.

If we neglect the cross products and rate-squared terms as negligible, equation (8) becomes:

$$\Sigma m = \dot{q}I_Y + pr(I_X - I_Z) \qquad (10)$$

This is a valid assumption due to the relative size of the cross-products. The NT-33A data [15:22] shows a cross product of 480 slug-feet^2 compared to a difference in I_X and I_Z of 20,000 slug-feet^2 . The yaw rate squared term will always be less than 1 radian/second, and it is assumed that roll rates will be less than 1 radian/second also. A typical transport aircraft, the Convair 880M [15:200], specifies this cross-product as 0, indicating that it can be ignored for the purposes of this investigation. Now, only the moments of inertia need to be modeled throughout the flight regime.

So, combining equations (7) and (9) yields:

$$\dot{q}I_Y + pr(I_X - I_Z) = m_0 - L_T X_T + L_{VB} X_{VB} \qquad (11)$$

Now solving for L_T :

$$L_T = \frac{-\dot{q}I_Y - pr(I_X - I_Z) + m_0 + L_{VB} X_{VB}}{X_T} \qquad (12)$$

This equation for the lift of the tail provides several advantages. The algorithm does not require extensive aerodynamic modeling of tail effects. The theory is based entirely on the effect of the developed tail lift on the aircraft pitch, roll and yaw motions. In that light, there is no downwash calculation error or surface position indicator requirement. Indeed, the algorithm doesn't care if the horizontal tail surface is a conventionally flapped elevator, a full-flying stabilator with variable trim tabs, or even a differential stabilator with roll control mixing.

Equation (11) can now be introduced into equation (6) with the result:

$$nW = C_{L_{WB}}(\tfrac{1}{2}\rho V^2)S + \left[\frac{-\dot{q}I_Y - pr(I_x - I_z) + C_{mo}(\tfrac{1}{2}\rho V^2)S\bar{c} + L_{WB}X_{WB}}{X_T}\right] \quad (13)$$

or

$$X_T nW = X_T C_{L_{WB}}(\tfrac{1}{2}\rho V^2)S\left[1 + \frac{X_{WB}}{X_T}\right] + \left[-\dot{q}I_Y - pr(I_x - I_z) + C_{m_o}(\tfrac{1}{2}\rho V^2)S\bar{c}\right] \quad (14)$$

where:

$$C_{m_o} = \frac{m_o}{(\tfrac{1}{2}\rho V^2)S\bar{c}} \quad (15)$$

Solving for $C_{L_{WB}}$ yields the primary equation for the estimator.

- 16 -

$$C_{L_{WB}} = \frac{nWX_T + qI_Y + pr(I_x - I_z) - C_{m_o}(\frac{1}{2}\rho V^2)S\bar{c}}{(\frac{1}{2}\rho V^2)SX_T \left[1 + \dfrac{X_{WB}}{X_T}\right]} \qquad (16)$$

It can then be noted that angle of attack is a function of $C_{L_{WB}}$

$$\alpha = Fn(C_{L_{WB}}, M, h) \qquad (17)$$

with M being Mach and h being altitude.

This functional relationship can be developed for each specific aircraft to be estimated. Mach number and altitude are direct CADC outputs, while $C_{L_{WB}}$ can be derived from equation (16).

The ratio of X_{WB} to X_T is on the order of .02 for most conventionally stable aircraft. Thus the entire correction factor for the moment due to the lift of the wing-body combination is approximately 1.02 to 1.05, yielding a 2 to 5 percent error if neglected entirely. This term will be kept, however, to increase in-flight angle of attack estimation accuracy, but will be assumed to be a constant. This neglects the center of gravity shift as fuel is burned or stores are released. But, this shift from an assumed medium center of gravity will present an α estimate error of less than 1 percent, judging by normal static margin shifts of conventional aircraft through a normal flight mission.

Also, the change in coefficient of lift with a change in α is assumed to be instantaneous, with no associated

dynamics. Thus the angle of attack required for a specific coefficent of lift to exist, as determined by aircraft accelerations and moments, may be calculated at any point in time.

LOAD FACTOR DETERMINATION   A required input to equation (16) to determine $C_{L_{WB}}$ is load factor (n). The load factor is defined as the ratio of the acceleration of the aircraft normal to the flight path within the plane of symmetry to the acceleration of gravity. INS linear acceleration would then yield only acceleration normal to the aircraft within the plane of symmetry. With zero angle of attack, the relationship of a_z and n in level flight is:

$$a_z = -(n - 1)g \qquad (18)$$

there a_z is normal acceleration to the aircraft and g is the acceleration of gravity at the earth's surface, which is assumed to be a constant for the flight conditions examined.
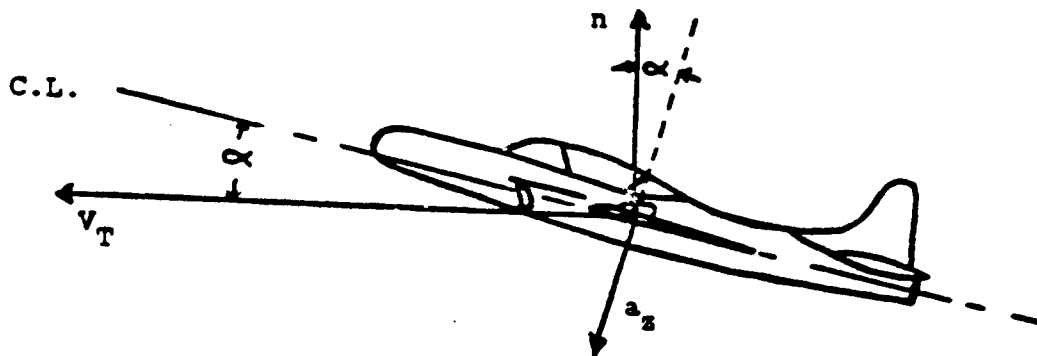
Figure 3.   Relationship of Load Factor and Normal
            Acceleration

This equation can be reasonably corrected for large angle of attack and flight path angle and the existence of roll ϕ by rotating the acceleration vector to a position normal to the flight path. Figure 3 depicts the difference in orientation of the load factor and normal acceleration to the flight path.

In straight and level flight, normal acceleration is 0, but load factor is 1. However, at a climb angle of 90 degrees, this load factor, while normal acceleration is 0, becomes 0 also. The same is true in a bank of 90 degrees while maintaining a steady course. Normal acceleration is 0, and load factor is also 0. This change from normal acceleration to load factor, accounting for large pitch and roll angles can be found by rotating the body normal acceleration to flight path normal acceleration, a_{wz}, in the wind axis system.

So, using the transformation matrix L_{wb} from body to wind frames:

$$\begin{bmatrix} a_x \\ a_y \\ a_z \end{bmatrix}_W = L_{wb} \begin{bmatrix} a_x \\ a_y \\ a_z \end{bmatrix}_B \tag{19}$$

where:

$$L_{wb} = \begin{bmatrix} \cos\alpha\cos\beta & \sin\beta & \sin\alpha\cos\beta \\ -\cos\alpha\sin\beta & \cos\beta & -\sin\alpha\sin\beta \\ -\sin\alpha & 0 & \cos\alpha \end{bmatrix} \tag{20}$$

- 19 -

However, it is immediately evident that prior knowledge of
angle of attack and sideslip is required for this rotation.
As this is only used for a small correction factor
to obtain an accurate load factor, n, some simple
approximations may be used for α and β. For this
case only, sideslip is assumed 0. A no-wind angle of attack
can be quickly computed using direct INS data. While not
accurate for estimator purposes, this approximate α can
serve very well to correct body axis accelerations to
approximate fligh path accelerations for use in equation
(19). The equations for quickly obtaining this α_G are
presented in the next section on No-wind Angle of Attack.
Using this α_G and assuming zero sideslip for the
transformation matrix purposes only, L_{vB} becomes:

$$L_{vb} = \begin{bmatrix} \cos\alpha_G & 0 & \sin\alpha_G \\ 0 & 1 & 0 \\ -\sin\alpha_G & 0 & \cos\alpha_G \end{bmatrix} \qquad (21)$$

Then, using the transformation matrix, normal acceleration in
the wind axis system is:

$$a_{vz} = -(\sin\alpha_G)a_{Bx} + (\cos\alpha_G)a_{Bz} \qquad (22)$$

But normal acceleration in the wind axis may also be written
as:

$$a_{vz} - (\text{component of } g)_{vz} = -ng \qquad (23)$$

So to find the component of gravity in the z direction in the wind axis, another transformation matrix is used to rotate g from the vertical reference frame to the wind axis. It should be noted that wind Euler angles are used in this transformation. However, for the purposes of this estimate of n, body axis Euler angles from the INS will be used. L_{vv} is:

$$L_{vv} = \begin{bmatrix} \cos\theta\cos\psi & \cos\theta\sin\psi & -\sin\theta \\ \sin\phi\sin\theta\cos\psi & \sin\phi\sin\theta\sin\psi & \sin\phi\cos\theta \\ -\cos\phi\sin\psi & +\cos\phi\cos\psi & \\ \cos\phi\sin\theta\cos\psi & \cos\phi\sin\theta\sin\psi & \cos\phi\cos\theta \\ +\sin\phi\sin\psi & -\sin\phi\cos\psi & \end{bmatrix} \quad (24)$$

Heading angle is not a factor in this determination, so it is assumed to be 0. Again, α is assumed to be small (below 20 degrees) and β is assumed to be 0, so $\theta = \theta_v$ and $\phi = \phi_v$. L_{vv} becomes:

$$L_{vv} = \begin{bmatrix} \cos\theta & 0 & -\sin\theta \\ \sin\phi\sin\theta & \cos\phi & \sin\phi\cos\theta \\ \cos\phi\sin\theta & -\sin\phi & \cos\phi\cos\theta \end{bmatrix} \quad (25)$$

Then the component of g in the z direction in wind axis is:

$$g_{vz} = (\cos\phi\cos\theta)g \quad (26)$$

Substituting equations (22) and (26) into equation (23)

yields the following equation for load factor determination.

$$(\cos\alpha_G)a_{Bz} - (\sin\alpha_G)a_{Bx} = -n g + g\cos\theta\cos\phi \qquad (27)$$

where α_G is the initial angle of attack guess, θ and ϕ are pitch and roll angles.

Solving for n in terms of body axis accelerations and Euler angles yields:

$$n = \frac{-(\cos\alpha_G)a_{Bz} + (\sin\alpha_G)a_{Bx}}{g} + (\cos\theta)(\cos\phi) \qquad (28)$$

This load factor can, derived from INS accelerations and Euler angles, become an input to the primary estimator equation (16). α_G, or the approximate angle of attack, is the only value that needs to be calculated for use in the load factor equation (28). A no-wind assumption will allow quick computation of this rough guess.

NO-WIND ANGLE OF ATTACK A no-wind angle of attack can be immediately obtained from the INS. All inertial velocities are actually groundspeeds over the locally flat earth. If we assume for this guess only that wind is negligible as compared to groundspeed, the INS groundspeeds will also be true airspeeds, and an initial α_G can be derived from inertial velocities in the X, Y, and Z directions.

$$v_{Bx} = (\cos\theta \cos\psi)v_{IN} + (\cos\theta \sin\psi)v_{IE} - (\sin\theta)v_{IZ} \qquad (29)$$

$$
\begin{aligned}
v_{By} = &(-\cos\phi \sin\psi + \sin\phi \sin\theta \cos\psi)v_{IN} + \\
&(\cos\phi \cos\psi + \sin\phi \sin\theta \sin\psi)v_{IE} + \\
&(\sin\phi \cos\theta)v_{IZ}
\end{aligned}
\qquad (30)
$$

- 22 -

$$v_{Bz} = (\sin\phi \, \sin\psi + \cos\phi \, \sin\theta \, \cos\psi)v_{IN} \quad + \tag{31}$$
$$(-\sin\phi \, \cos\psi + \cos\phi \, \sin\theta \, \sin\psi)v_{IE} \, +$$
$$(\cos\phi \, \cos\theta)v_{IZ}$$

These body velocities can then be evaluated to find an approximate angle of attack using the body axis relationship:

$$\alpha_G = \arctan\left[\frac{v_{Bz}}{v_{Bx}}\right] \tag{32}$$

This no-wind guess of angle of attack is then used only to make the small rotational correction on normal acceleration to the load factor.

THREE DIMENSIONAL WINDAGE CALCULATION With angle of attack recovered from the functional equation (17), airmass velocities of the aircraft can be calculated in north, east and down axes.

$$v_{AN} = (\cos\psi \, \cos\theta \, \cos\alpha \, \cos\beta + \cos\psi \, \sin\theta \, \sin\phi \, \sin\beta + \tag{33}$$
$$\cos\psi \, \sin\theta \, \cos\phi \, \sin\alpha \, \cos\beta - \sin\psi \, \cos\phi \, \sin\beta +$$
$$\sin\psi \, \sin\phi \, \sin\alpha \, \cos\beta)V$$

$$v_{AE} = (\sin\psi \, \cos\theta \, \cos\alpha \, \cos\beta + \sin\psi \, \sin\theta \, \sin\phi \, \sin\beta + \tag{34}$$
$$\sin\psi \, \sin\theta \, \cos\phi \, \sin\alpha \, \cos\beta + \cos\psi \, \cos\phi \, \sin\beta -$$
$$\cos\psi \, \sin\phi \, \sin\alpha \, \cos\beta)V$$

$$v_{AZ} = (-\sin\theta \, \cos\alpha \, \cos\beta + \cos\theta \, \sin\phi \, \sin\beta + \tag{35}$$
$$\cos\theta \, \cos\phi \, \sin\alpha \, \cos\beta)V$$

where v_{AN}, v_{AE}, and v_{AZ} are airmass velocities of the aircraft in the direction specified and V is the true

airspeed from the CADC.

Assuming sideslip is zero, equations (33), (34), and (35) become:

$$V_{AN} = (\cos\psi \cos\theta \cos\alpha + \cos\psi \sin\theta \cos\phi \sin\alpha + \sin\psi \sin\phi \sin\alpha)V \quad (36)$$

$$V_{AE} = (\sin\psi \cos\theta \cos\alpha + \sin\psi \sin\theta \cos\phi \sin\alpha - \cos\psi \sin\phi \sin\alpha)V \quad (37)$$

$$V_{AZ} = (-\sin\theta \cos\alpha + \cos\theta \cos\phi \sin\alpha)V \quad (38)$$

The INS groundspeeds subtracted from these airmass velocities then give the wind component in each direction.

$$V_{WN} = V_{AN} - V_{IN} \quad (39)$$

$$V_{WE} = V_{AE} - V_{IN} \quad (40)$$

$$V_{WZ} = V_{AZ} - V_{IZ} \quad (41)$$

FLOW DIAGRAM The overall components of the inflight estimator would act together to first compute the no-wind guess of angle of attack. At this point, all the information necessary for estimation of actual angle of attack would be available from the INS, the CADC, and the model of the current aircraft weight and configuration. A CADC output would be used to determine the values for the 5 stability derivatives that must be modeled for varying flight conditions. The angle of attack would then be computed by the estimator. This angle of attack and the INS groundspeeds

could then be used to find a three-dimensional wind, given
the current true airspeed.   The flow diagram in figure 4
depicts this action.
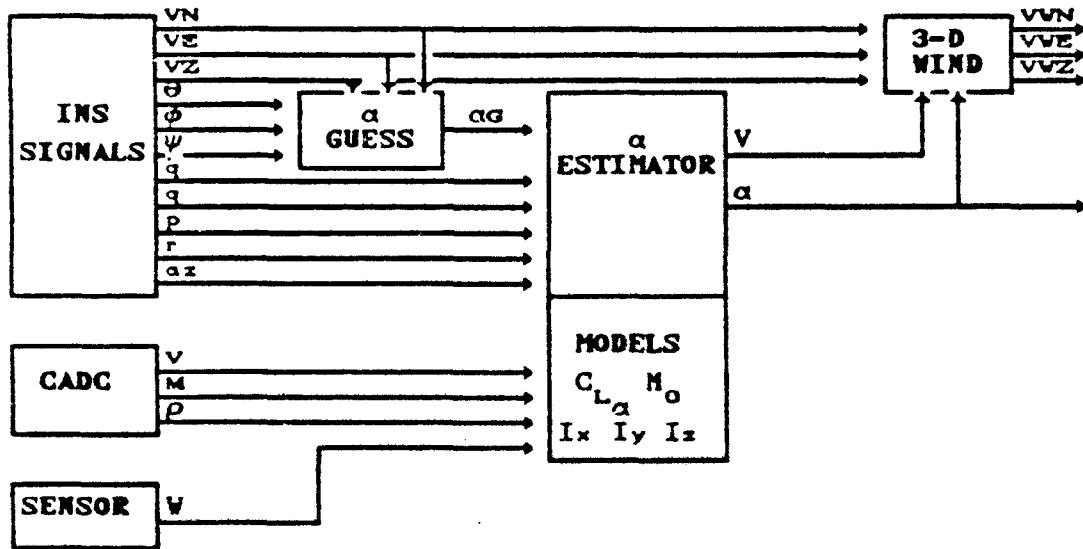
Figure 4.   Inflight Estimator Flow Diagram

IV. POST FLIGHT ESTIMATOR THEORY

BASIC EQUATIONS OF MOTION   The body axis system provides a
convenient system for measurement of perturbed angle of
attack and sideslip from a trimmed condition.   The
conventions of this body system are presented in figure 5.
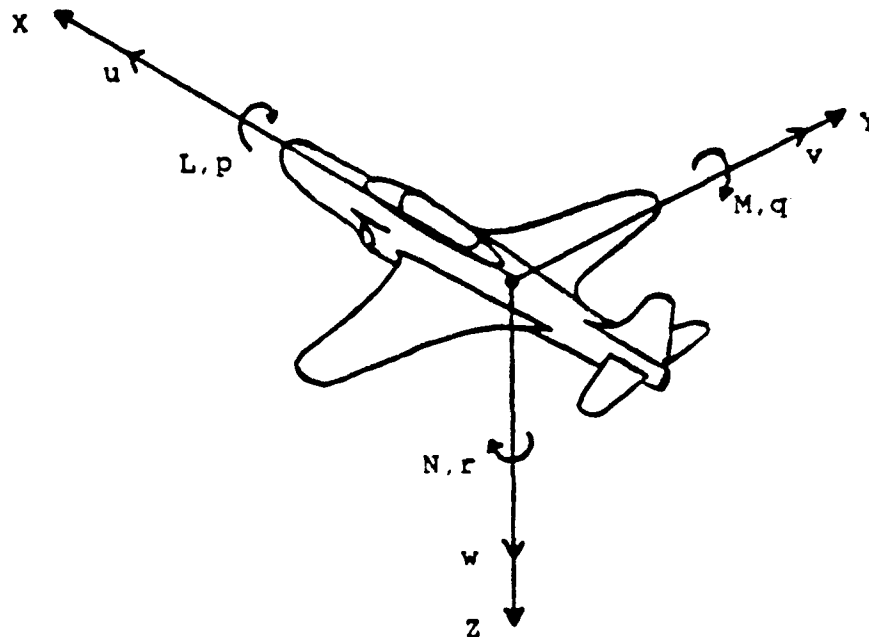
Figure 5.   Body Axis System

In the body axis system, the angle of attack can be related
by the ratio of vertical velocity, w, to longitudinal
velocity, u.
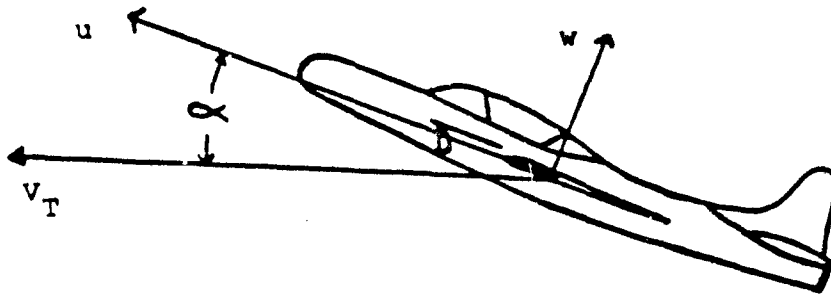
Figure 6.   Angle of Attack as a Velocity Ratio

Assuming a perturbation away from the trimmed condition,
this ratio takes the form:

$$\alpha = \arctan\left[\frac{w}{u}\right] \qquad (42)$$

In order to determine these velocities during maneuvers,
perturbation equations of motion can be developed to
simulated the interaction of pitch rates and angles on the
velocities, U and V. Development of dimensional perturation
equations of motion can be found in McRuer[2]. Four
linearized equations of motion can be derived for use in an
angle of attack estimator algorithm. The first of these is
the longitudinal velocity perturbation equation.

$$\dot{\hat{u}} = x_u\hat{u} + x_v\hat{w} + x_{\dot{v}}\dot{\hat{w}} + (x_q - w_0)\hat{q} - g\cos\theta_0(\hat{\theta}) + x_{\delta E}\delta E + x_{\delta T}\delta T \qquad (43)$$

where the dimensional derivatives are described in the
glossary of terms. Assuming x_v to be small, the u equation

can be written as:

$$\dot{\hat{u}} = x_u \hat{u} + x_v \hat{w} + (x_q - w_o)\hat{q} - g\cos\theta_o(\hat{\theta}) + x_{\delta E}\delta E + x_{\delta T}\delta T \qquad (44)$$

The normal velocity equation is formed in a like manner.

$$\dot{\hat{w}} - z_v\dot{\hat{w}} = z_u\hat{u} + z_v\hat{w} + (z_q + u_o)\hat{q} - g\sin\theta_o(\hat{\theta}) + z_{\delta E}\delta E + z_{\delta T}\delta T \qquad (45)$$

This can be subsequently reduced to:

$$\dot{\hat{w}} = \frac{z_u\hat{u}}{(1-z_v)} + \frac{z_v\hat{w}}{(1-z_v)} + \frac{(z_q+u_o)\hat{q}}{(1-z_v)} - \frac{g\sin(\theta_o)\hat{\theta}}{(1-z_v)} +$$

$$\frac{z_{\delta E}\delta E}{(1-z_v)} + \frac{z_{\delta E}\delta E}{(1-z_v)} \qquad (46)$$

And, in the same manner, pitch acceleration is:

$$\dot{\hat{q}} = m_u\hat{u} + m_v\hat{w} + m_q\hat{q} + m_v\dot{\hat{w}} + m_{\delta E}\delta E + m_{\delta T}\delta T \qquad (47)$$

where $\dot{\hat{w}}$ is defined by equation (45). Substituting equation (45) into equation (47) gives:

$$\dot{\hat{q}} = \left[m_u + \frac{m_v z_u}{(1-z_v)}\right]\hat{u} + \left[m_v + \frac{m_v z_v}{(1-z_v)}\right]\hat{w} + \left[m_q + \frac{m_v(z_q+u_o)}{(1-z_v)}\right]\hat{q} -$$

$$\left[\frac{m_v g \sin\theta_o}{(1-z_v)}\right]\hat{\theta} + \left[m_{\delta E} + \frac{m_v z_{\delta E}}{(1-z_v)}\right]\delta E + \left[m_{\delta T} + \frac{m_v z_{\delta T}}{(1-z_v)}\right]\delta T \qquad (48)$$

A fourth equation simply supplies the identity:

$$\dot{\hat{\theta}} = \hat{q} \qquad (49)$$

Equations (44), (46), (48), and (49) can now be compiled into standard state-space matrix notation of:

$$\dot{\hat{X}} = A \cdot \hat{X} + B \cdot \hat{U} \qquad (50)$$

Filling in the stability derivatives gives the form of the A and B matrices.

$$
\begin{bmatrix} \dot{\hat{u}} \\ \dot{\hat{w}} \\ \dot{\hat{q}} \\ \dot{\hat{\theta}} \end{bmatrix}
=
\begin{bmatrix}
x_u & x_w & x_q - w_0 & -g\cos\theta_0 \\
\dfrac{z_u}{(1-z_{\dot{w}})} & \dfrac{z_w}{(1-z_{\dot{w}})} & \dfrac{z_q + u_0}{(1-z_{\dot{w}})} & \dfrac{-g\sin\theta_0}{(1-z_{\dot{w}})} \\
m_u + \dfrac{m_{\dot{w}} z_u}{(1-z_{\dot{w}})} & m_w + \dfrac{m_{\dot{w}} z_w}{(1-z_{\dot{w}})} & m_q + \dfrac{m_{\dot{w}}(z_q + u_0)}{(1-z_{\dot{w}})} & \dfrac{-m_{\dot{w}} g\sin\theta_0}{(1-z_{\dot{w}})} \\
0 & 0 & 1 & 0
\end{bmatrix}
\begin{bmatrix} \hat{u} \\ \hat{w} \\ \hat{q} \\ \hat{\theta} \end{bmatrix}
+
$$

$$
\begin{bmatrix}
x_{\delta E} & x_{\delta T} \\
\dfrac{z_{\delta E}}{(1-z_{\dot{w}})} & \dfrac{z_{\delta T}}{(1-z_{\dot{w}})} \\
m_{\delta E} + \dfrac{m_{\dot{w}} z_{\delta E}}{(1-z_{\dot{w}})} & m_{\delta T} + \dfrac{m_{\dot{w}} z_{\delta T}}{(1-z_{\dot{w}})} \\
0 & 0
\end{bmatrix}
\begin{bmatrix} \delta E \\ \delta T \end{bmatrix}
\qquad (51)
$$

In an analagous manner to the development of
longitudinal perturbation equations, lateral perturbation
equations can be defined to estimate sideslip. Beta can be
defined also by a ratio of velocities, in this case, lateral
velocity to true airspeed.
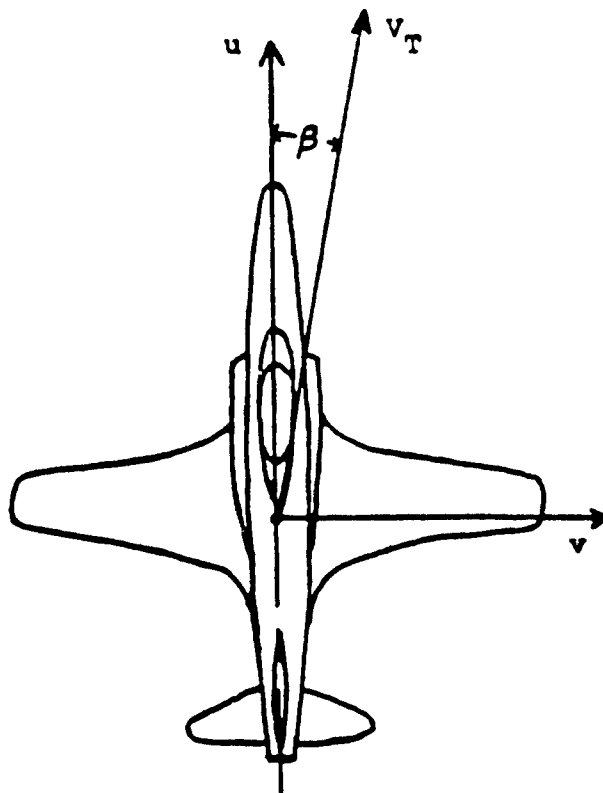
Figure 7.   Sideslip as a Velocity Ratio

This ratio can be expressed by the following equation:

$$\beta = \arcsin\left[\frac{v}{V}\right] \tag{52}$$

Thus lateral perturbation equations can be resolved to the following four equations:

$$\dot{\hat{v}} - Y_{\dot{v}}\dot{\hat{v}} = Y_v\hat{v} + (Y_p + w_0)\hat{p} + (Y_r - u_0)\hat{r} + g\cos(\theta_0)\hat{\phi} +$$
$$Y_{\delta A}\delta A + Y_{\delta Rd}\delta Rd \qquad (53)$$

$$\dot{\hat{p}} = L_v'\hat{v} + L_p'\hat{p} + L_r'\hat{r} + L_{\dot{v}}'\dot{\hat{v}} + L_{\delta A}'\delta A + L_{\delta Rd}'\delta Rd \qquad (54)$$

$$\dot{\hat{\phi}} = \hat{p} \qquad (55)$$

$$\dot{\hat{r}} = N_v'\hat{v} + N_p'\hat{p} + N_r'\hat{r} + N_{\dot{v}}'\dot{\hat{v}} + N_{\delta A}'\delta A + N_{\delta Rd}'\delta Rd \qquad (56)$$

Assuming that $Y_{\dot{v}} = 0$, $Y_p = 0$, $Y_r = 0$, $L_{\dot{v}}' = 0$, and that $N_{\dot{v}}' = 0$, the above set of lateral equations reduce to:

$$\dot{\hat{v}} = Y_v\hat{v} + w_0\hat{p} + g\cos(\theta_0)\hat{\phi} - u_0\hat{r} + Y_{\delta A}\delta A + Y_{\delta Rd}\delta Rd \qquad (57)$$

$$\dot{\hat{p}} = L_v'\hat{v} + L_p'\hat{p} + L_r'\hat{r} + L_{\delta A}'\delta A + L_{\delta Rd}'\delta Rd \qquad (58)$$

$$\dot{\hat{\phi}} = \hat{p} \qquad (59)$$

$$\dot{\hat{r}} = N_v'\hat{v} + N_p'\hat{p} + N_r'\hat{r} + N_{\delta A}'\delta A + N_{\delta Rd}'\delta Rd \qquad (60)$$

This in matrix notation described by equation (50) is:

$$\begin{bmatrix} \dot{v} \\ \dot{p} \\ \dot{\phi} \\ \dot{r} \end{bmatrix} = \begin{bmatrix} Y_v & v_0 & g\cos\theta_0 & -u_0 \\ L'_v & L'_p & 0 & L'_r \\ 0 & 1 & 0 & 0 \\ N'_v & N'_p & 0 & N'_r \end{bmatrix} \begin{bmatrix} \hat{v} \\ \hat{p} \\ \hat{\phi} \\ \hat{r} \end{bmatrix} + \begin{bmatrix} Y_{\delta A} & Y_{\delta Rd} \\ L'_{\delta A} & L'_{\delta Rd} \\ 0 & 0 \\ N'_{\delta A} & N'_{\delta Rd} \end{bmatrix} \begin{bmatrix} \delta A \\ \delta Rd \end{bmatrix} \qquad (61)$$

These stability derivatives for both longitudinal and lateral A and B matrices can be evaluated for the flight condition of interest. The numeric A and B matrices can then be discretized for use in a discrete Kalman estimator program.

ESTIMATOR THEORY Both state-space models (51) and (61) will approximate their respective longitudinal and lateral systems in perturbed motions. Implied in this is the assumption that the systems are linear and excited by small perturbations about a trim condition. Equation (50) describes a state model completely, provided all states are available for measurement. This single equation system is:

$$\dot{\hat{X}} = A \cdot \hat{X} + B \cdot \hat{U} \qquad (50)$$

However, all the states of any given system may not be available for measurement. In this case, the model consists of 2 equations, with the second describing the available measurements. This system is formed as:

$$\dot{\hat{X}} = A \cdot \hat{X} + B \cdot \hat{U} \qquad (62)$$
$$\hat{Z} = H \cdot \hat{X} \qquad (63)$$

where $\hat{Z}$ is the measurement vector and H is the matrix of the available measurement components. In both the longitudinal and lateral cases studied here, not all the states are available for measurement. In the longitudinal case, only θ and q are available from the INS. In the lateral case, the only measurements are r, ϕ , and p. This then dictates the H matrix of available measurement components for use in equation (63).

$$H_{LONG} = \begin{bmatrix} 0 & 0 & 1 & 0 \\ 0 & 0 & 0 & 1 \end{bmatrix} \qquad (64)$$

$$H_{LAT} = \begin{bmatrix} 0 & 1 & 0 & 0 \\ 0 & 0 & 1 & 0 \\ 0 & 0 & 0 & 1 \end{bmatrix} \qquad (65)$$

A second alteration to the basic system equation (50) is the presence of noise in both the modeling process and the measuring process. The modeling cannot take into account every condition and outside action that may possibly affect the states. Also, the model itself may not completely depict the exact action of the states in response to a specified input. This inaccuracy inherent in the model itself can be accounted for by adding a process noise. The errors are random, and centered about a zero mean of the actual values. Thus these errors can be represented by a gaussian noise

- 33 -

system which will be called V . This noise will be defined
by a variance, σ_v^2 , with a mean of 0.0. In additor, the
available measurements are also corrupted by noise. This
noise is uncorrelated, gaussian, with zero mean. This noise
V can be described by a variance, σ_v^2 , analagous to the
process noise describe previously. The measurment noise,
affecting the measuring device itself, affects the accuracy
and consistency of the measurement. Table 1 depicts the
accuracies of a USAF standard INS. The jitter value is added
to the accuracy to produce an error range, T. It then
follows that the variance of the Gausssian approximation, σ^2,
is $\frac{1}{12}(2T)^2$ for use in the measurement uncertainty matrix,
R.

Table I.

USAF Standard INS Measurement Accuracies

SIGNAL	UNIT	ACCURACY	JITTER
θ	rad	.00028	.0001
ϕ	rad	.00028	.0001
p	rad/sec	.00075	.00035
q	rad/sec	.00075	.00035
r	rad/sec	.00075	.00035

Assuming that the matrices Q and R are stationary, the

resulting R matrix is:

$$R_{LONG} = \begin{bmatrix} 4.81 \times 10^{-8} & 0 \\ 0 & 4.03 \times 10^{-7} \end{bmatrix} \qquad (66)$$

$$R_{LAT} = \begin{bmatrix} 4.02 \times 10^{-7} & 0 & 0 \\ 0 & 4.81 \times 10^{-8} & 0 \\ 0 & 0 & 4.03 \times 10^{-7} \end{bmatrix} \qquad (67)$$

A similar Q matrix contains the uncertainty values for the model itself. These covariances will be the subject of later filter tuning requirements.

The Kalman estimator makes initial estimates of the states prior to the measurement, and then subsequent estimates after the measurement. These estimates are provided by the initial conditions placed on the states, followed by subsequent values of XP, the Kalman predicted state vector. The full derivation of the Kalman equations can be found in Gelb[12]. The prediction equation takes the form:

$$XM(K) = A \cdot XP(K-1) + B \cdot U(K-1) \qquad (68)$$

where XM is the state estimate prior to the measument.

In a likewise manner, the error covariance prior to the measurment can be calculated, using an initial best estimate of covariance, by:.

$$PM(K) = A \cdot PP(K-1) \cdot A^T + B \cdot Q \cdot B^T \qquad (69)$$

where PM is the error covariance prior to the measurement and PP is the error covariance after the measurement, at time $(K - 1)$.

With these estimates, the Kalman gain, KG, to be applied to the post-measurement error covariances and state estimation can be found. This Kalman gain matrix is calculated from the expression:

$$KG(K) = PM(K).H^T \left[H.PM(K).H^T + R \right]^{-1} \qquad (70)$$

The predicted error covariance, given the next measurement, is calculated as:

$$PP(K) = \left[I - KG(K).H \right] PM(K-1) \qquad (71)$$

and the corresponding state estimate is calculated as:

$$XP(K) = XM(K) + KG(K) \left[Z(K) - H.XM(K) \right] \qquad (72)$$

Now given a full state estimate in both longitudinal and lateral modes, α and β are estimated from the perturbation and true velocities by:

$$\alpha(K) = \text{arcTAN} \left[\frac{w_o + w(K)}{u_o + u(K)} \right] \qquad (73)$$

$$\beta(K) = \text{arcSIN} \left[\frac{v_o + v(K)}{V} \right] \qquad (74)$$

rhere w_o , u_o , and v_o are trim values and V is the CADC
calculated true airspeed.

PROGRAMS DKF AND DKFLAT A discrete Kalman filter program by
Gleason [13] was used to perform the above calculations.
This program was modified for angle of attack and sideslip
determination into two separate, parallel programs, DKF and
DKFLAT. A sample listing of DKF is given in appendix A.
DKFLAT is identical to DKF with the exception of the sideslip
subroutine BETA, which is listed in appendix B. The programs
take true angle of attack and true airspeed, and the
discretized A matrix for lateral and longitudinal modes.
Step elevator or thrust changes are input for the
longitudinal responses in DKF, resulting in a trace of
computed angle of attack, and estimated angle of attack using
only the two measurements of θ and q . Step rudder and
aileron inputs are inserted to DKFLAT, resulting in a trace
of computed β and the estimated β using the three
measurements of r, ϕ, and p.

FILTER TUNING The Q matrix can now be modified to provide
the proper degree of uncertainty to the model. A good
starting point for Q seems to be the same uncerta' ty values
as in R. At this point, a covariance analysis can be
performed to match computed root mean squared (RMS) error to
the true RMS of the system. This will provide the optimal
estimator for use with actual flight test data.
     The true RMS is the difference between the filter
estimate and the true value of the system.
The difference between the two quantities is due to the
weighting given to the measurements as opposed to the model,

judged by model formulation and sensor capability. These
weightings can be varied through choice of R and Q matrices,
based on known measurement errors and modeling
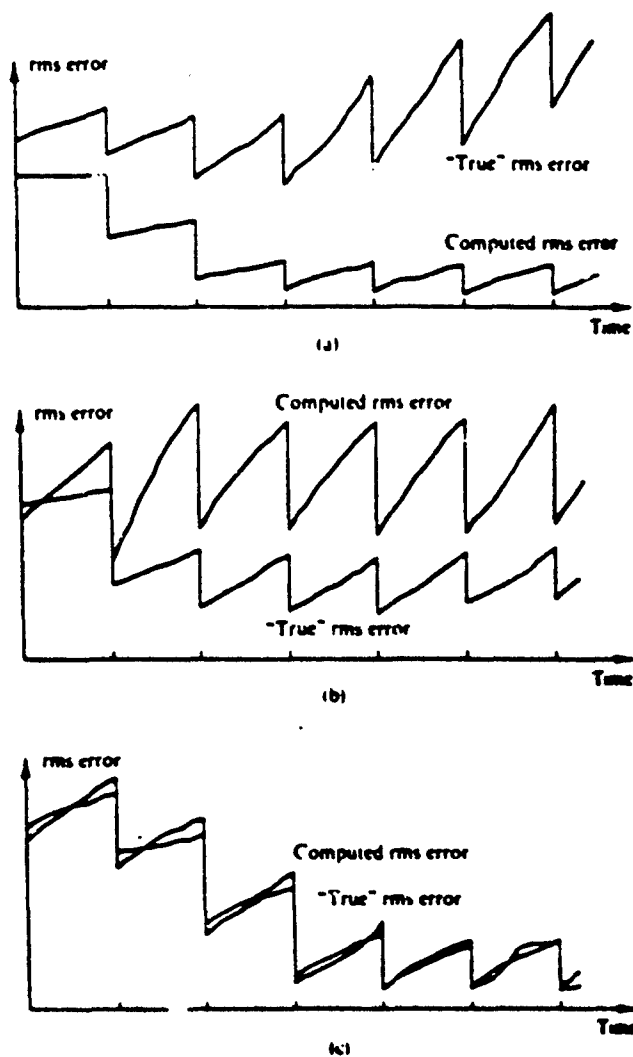
Figure 8.   Covariance Analysis for Kalman Filter Tuning

inadequacies.   R is fixed by the physical constraints of the
given INS accuracies and jitters.   Q can be adjusted, though,
until approximate RMS equality is obtained.   Figure 8a shows
the result of low measurement weighting, while 8b depicts too

much weighting on the actual measurement. Figure 8c depicts,
therefore, a tuned Kalman estimator, with correct weightings
applied to the measurement versus the model. The true RMS is
approximately equal to the computed RMS in this tuned case.
At this point, the Kalman estimator is ready for test runs to
verify its operation.

V. ESTIMATOR VALIDATION

VALIDATION OBJECTIVE The basic objective of the estimator validation phase is to ensure that both estimators have been formulated correctly, with a minimum error under known, static conditions. The aerodynamic data available will allow a study of the effects of assumptions and neglected higher order terms on the overall accuracy of both estimator systems, in the absence of noise and jitter associated with actual systems. A comparison of the estimated angle of attack and sideslip to actual alpha and beta is the overall goal of the validation. Once both algorithms have been verified, a simulation will be accomplished to determine the estimator characteristics in a dynamic environment, close to actual flight conditions. The simulator-derived angle of attack and sideslip can also be compared to estimated values to study the impact of neglected dynamic effects.

INFLIGHT ESTIMATOR VALIDATION Six inflight points were used to verify the ability of the inflight estimator to recover α and β under stable flight conditions. NT-33A data from the National Aeronautics and Space Administration (NASA) contained in a handling qualities report [15] was the reference data for this phase of the validation.

The NT-33A aircraft is a programmable, variable stability aircraft modified from a basic T-33 jet trainer. This two-place aircraft is capable of a wide range of flight conditions, and a great deal of aerodynamic data has been recorded for use in studies of this type.

In a clean aircraft configuration with a nominal flight control system, 6 data points were established, as shown in

- 40 -

Table II, to relate α, altitude, Mach, and angle of attack.

Table II.   Static Inflight Angle of Attack Test Points
NT-33A Aircraft

DATA POINT	3	4	5	6	7	8
$\frac{1}{2}\rho V^2$ (psi)	247	819	62.7	222	440	129
$C_{L_{WB}}$	.2539	.0891	.9477	.2805	.1504	.4698
MACH	.4	.7	.3	.55	.75	.65
ALTITUDE(FT)	0	0	20k	20k	20k	40k
α_{TRUE}(RADS)	.016	-.016	.164	.014	-.005	.043

A multiple linear regression analysis for 2 independent variables was performed to show angle of attack as a function of $C_{L_{WB}}$ and Mach.   The altitude variance was not sufficient to provide a good correlation for its incorporation into the regression formula.   This analysis was accomplished by a least squares method using the HP-41C hand computer.   The regression for the NT-33A in clean configuration provided the following formula:

$$\alpha(RAD) = -.02 + .2(C_{L_{WB}}) - .03(M) \qquad (75)$$

For each of the 6 flight points, the $C_{L_{WB}}$ required for flight was found through the primary estimator equation (16). In straight and level flight for each of the points, the load factor is 1, by definition, with no pitch, roll or yaw rates or accelerations.   Equation (16) then reduces to:

$$C_{L_{WB}} = \frac{WX_T - C_{mo}(\frac{1}{2}\rho V^2)S\bar{c}}{(\frac{1}{2}\rho V^2)SX_T\left[1 + \dfrac{X_{WB}}{X_T}\right]} \qquad (76)$$

The $C_{L_{WB}}$ required for straight and level flight is calculated by this equation. This is then input to the regression formula (75) with the simulated CADC input of Mach and true airspeed. Estimated angle of attack can then be calculated. A comparison of these estimated angles of attack to the documented angles of attack was then performed.

Table III. Static Inflight Estimator Validation
NT-33A Aircraft

DATA POINT	3	4	5	6	7	8
α_{TRUE} (DEG)	.899	-.899	9.402	.802	-.295	2.498
α_{EST} (DEG)	1.08	-1.328	9.198	1.123	-.712	3.120
$\Delta ERROR$ (DEG)	.176	-.429	-.204	.321	.414	.622

Table III depicts the error in the estimation from documented values. With just 6 data points, the average error over the flight range is .15 degrees with a maximum error of .622 degrees at flight condition 6. However, this flight condition is the only data point at 40,000 feet, resulting in significant least square error in the regression analysis, even with altitude not an explicit parameter in equation (76). Throwing out that data point results in an average angle of attack error of 0.0557 degrees over the remaining range of

- 42 -

flight data points. This regression formula is valid over the linear portion of the lift curve. It can be extended to the stall region depending on the extent of the non-linear lift region. A rapidly stalling wing-body combination could be modeled accurately to α_{stall}, while a flat stall region would induce angle of attack errors over the entire range of the lift curve.

COMPUTER TEST PROGRAMS Two independent methods were used to verify actual angle of attack and sideslip prior to examination of the Kalman filter operation in the post-flight estimator. These programs, called LONG and LAT, represent a decoupled system for modeling the longitudinal and lateral modes of response. Input into LAT and LONG consists of flight condition, control inputs, initial conditions and stability derivatives of the body axis system. Then program then forms the continuous A and B matrices in body axis and outputs the associated eigenvalues and eigenvectors for verification with actual aircraft data. Forced system response to step inputs are calculated using a Taylor series expansion to second order, with output frequency of 30 samples per second on angle of attack and sideslip. At this point, the continuous A and B matrices can be discretized and input into the discrete Kalman filter programs, DKF and DKFLAT, representing the longitudinal and lateral estimators, respectively. Using the same step control inputs as in LAT and LONG, the α and β response is calculated through the transition matrix method. These responses can then be compared, and if formulated corectly, should agree to an extremely close degree. For a .5 degree step elevator input, the correlation is excellent, as shown in figure 9.

Now, DKF and DKFLAT can be used to verify the ability of

DKF AND LONG MODEL COMPARISON

NT-33A 2 DEG STEP ELEVATOR (FLT CON 6)
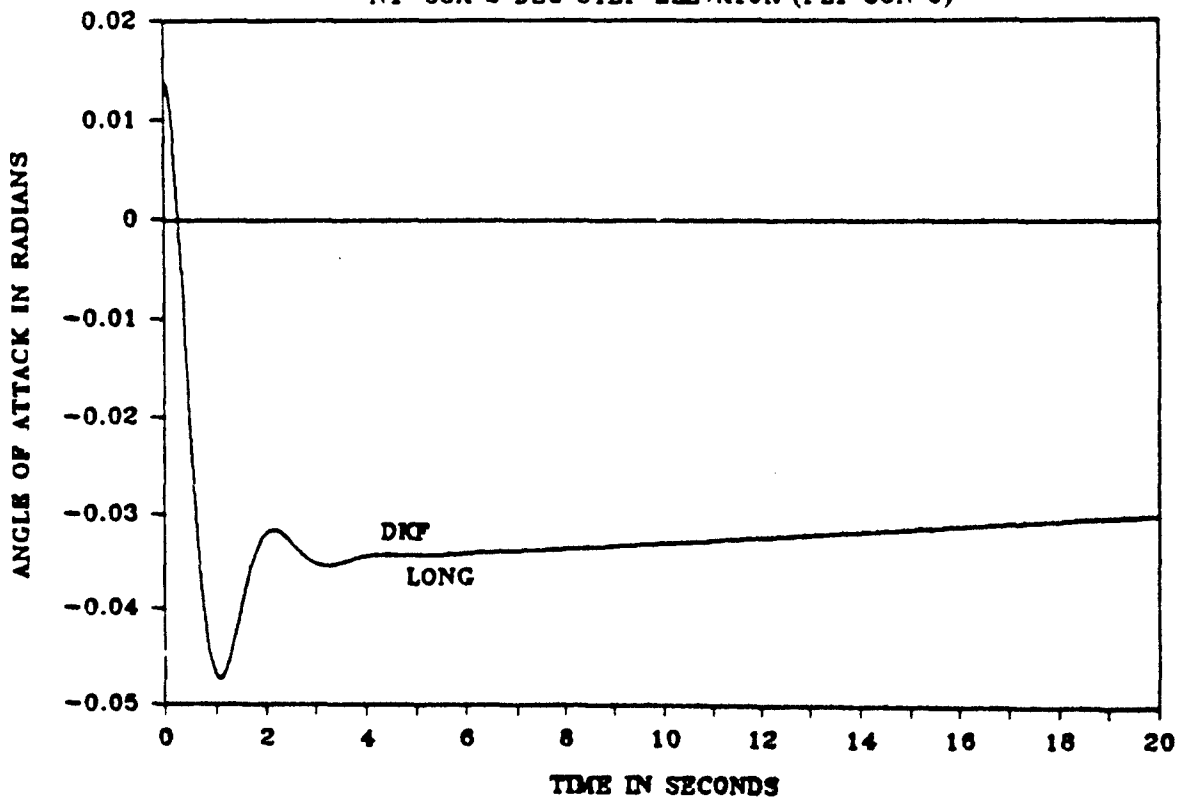
Figure 9.   Comparison of LONG and DKF Derived Angle of Attack

a Kalman estimator to recover accurate angle of attack and sideslip with less than full state, noise-corrupted measurement. Initially, computer generated white noise was modified to a intensity equal to the expected error in the INS measurement signals. This Gaussian noise was then added to the exact state outputs, and these states became noise corrupted measurements of the modeled maneuver for which predicted α and β traces were calculated. The Kalman filter then operates on the available state measurements, estimating the remaining states, based on aircraft model accuracy and measurement uncertainty, as discussed in chapter IV. Angle of attack and sideslip were then calculated from the states and estimated states. When predicted α and β are plotted versus Kalman estimated α and β, the ability of the Kalman filter to recover these parameters becomes evident and quantifiable.

POST-FLIGHT VALIDATION TEST RUNS The post-flight estimator uses perturbations from trim values to calculate α and β. As such, a single trim flight condition was used as a baseline data point. This condition was flight condition 6 of Table II, using the NT-33A aircraft data.

Table IV. Post-Flight Validation Test Points

DATA POINT	1	2	3	4	5
INPUT	.5°ELEV	2°ELEV	.5°RUD	2°RUD	2°AIL

The runs produced a set of six figures (Figure 10 through Figure 15) depicting the modeled response versus the

NT-33A FLIGHT CONDITION 6
2 DEG STEP ELEV INPUT(INS COVARIANCE)
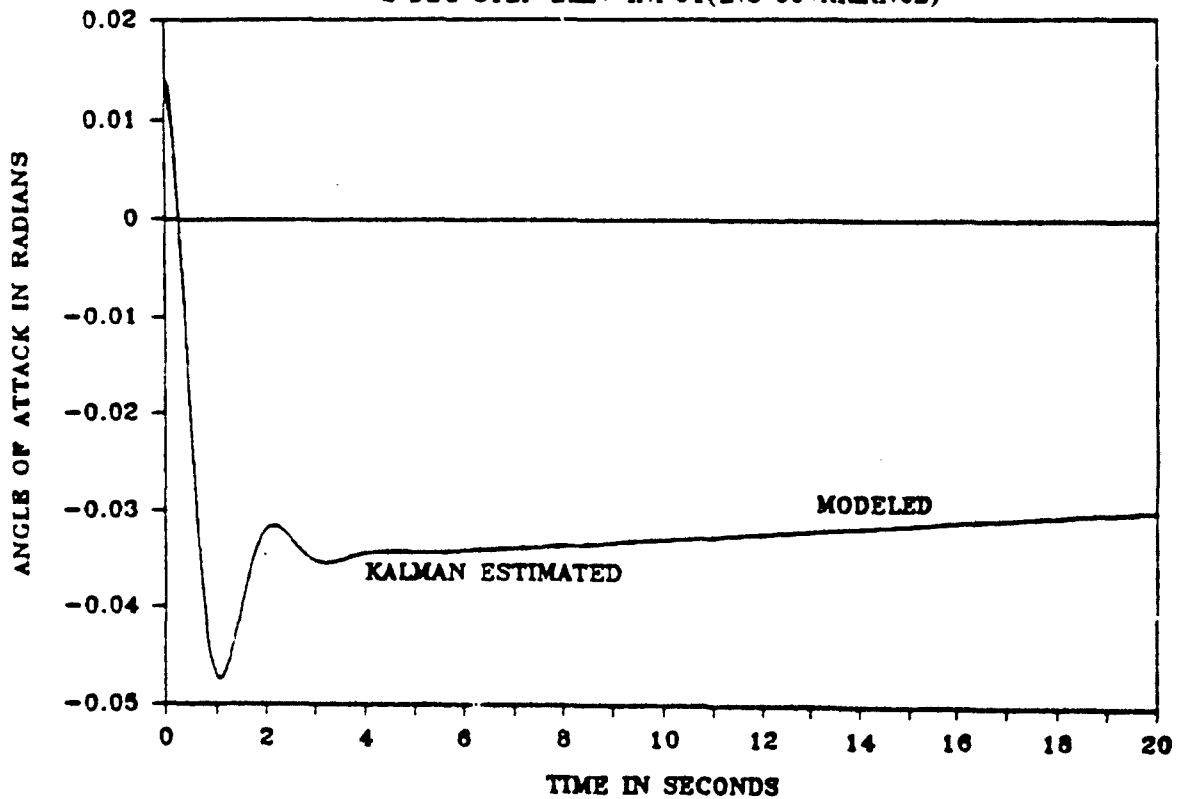
Figure 10.   Angle of Attack Recovery using INS Covariance
         Model

Kalman predicted response.

RESULTS OF VALIDATON RUN   Initial validations runs were made
with the INS measurement error covariance model established
in Chapter IV.   These covariances were input into DKF and
DKFLAT Q and R matrices to determine the ability of the
Kalman estimator to recover angles of sideslip and attack
with noisy INS measurements.   For these initial test runs, Q
and R were assumed to be the same, reflecting similar
measurement and process noises.   However, the accuracy of the
INS, as judged by the covariances that were calculated,
provided an interesting result.   The Kalman filter, with a 2
degree step elevator input, calculated the exact angle of
attack as the model, within the range of the noise.   Figure
10 depicts this result, showing the estimated angle of attack
superimposed on the modeled angle of attack.   The two are
identical traces, with imperceptible error.   This is hardly
surprising, considering the magnitude of the measurement
covariance values calculated in the Post-Flight Theory
chapter.   The noise in measurement is extremely small.   These
values were on the order of 10^{-8} radians for Euler angles and
10^{-7} radians/second for the rates.   This leads to the
conclusion that indeed angle of attack and sideslip can be
accuately estimated with less than full state measurement.   A
properly tuned Kalman estimator can make up for less than
full-state, noise-corrupted measurement, and in turn allow
for accurate estimates of α and β, with an equivalently
accurate INS.

        However, a worst case analysis should also be done to
allow for unknown errors and noises in the system or model.
This was also accomplished, using the raw accuracy and jitter
values as inputs to the covariance matrices for model and
measurement.   The results depict an accurate system as well,

- 47 -

NT-33A FLIGHT CONDITION 6

1/2 DEGREE STEP ELEVATOR INPUT
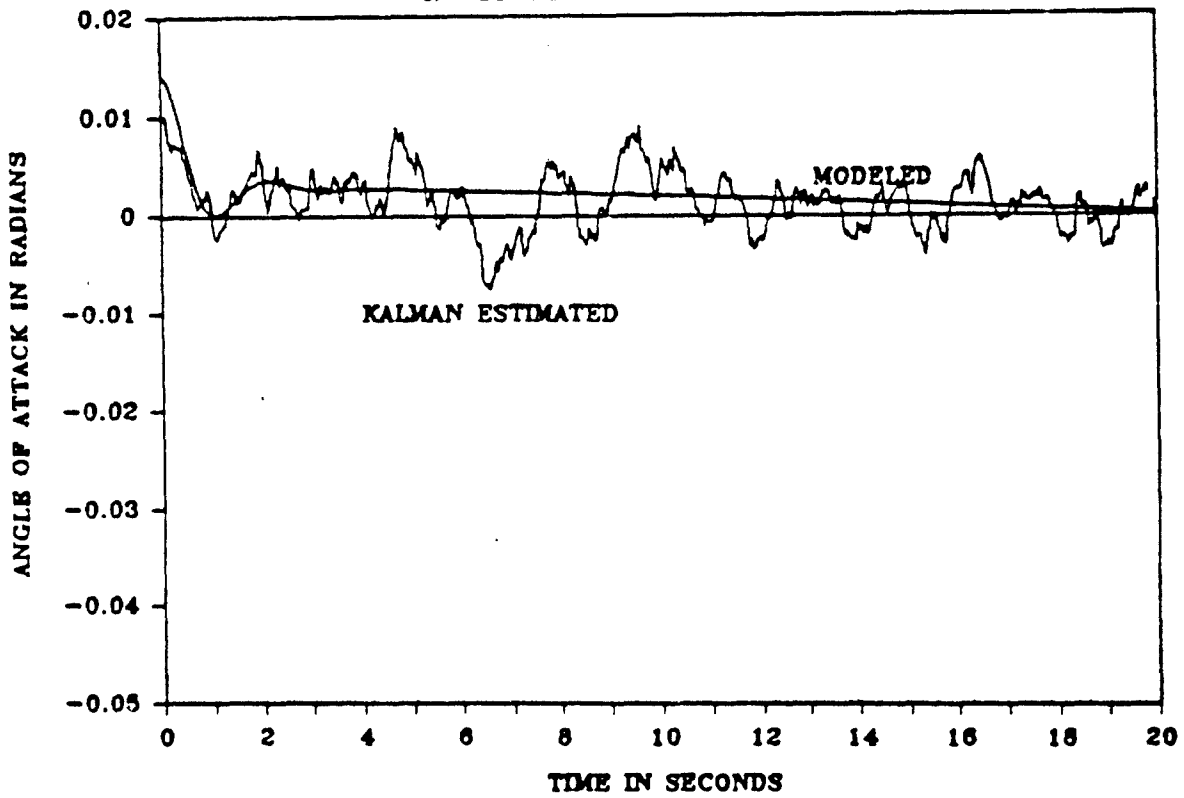
Figure 11.   Angle of Attack Recovery (.5 degree Elevator)

NT−33A FLIGHT CONDITION 6

2 DEGREE STEP ELEVATOR INPUT
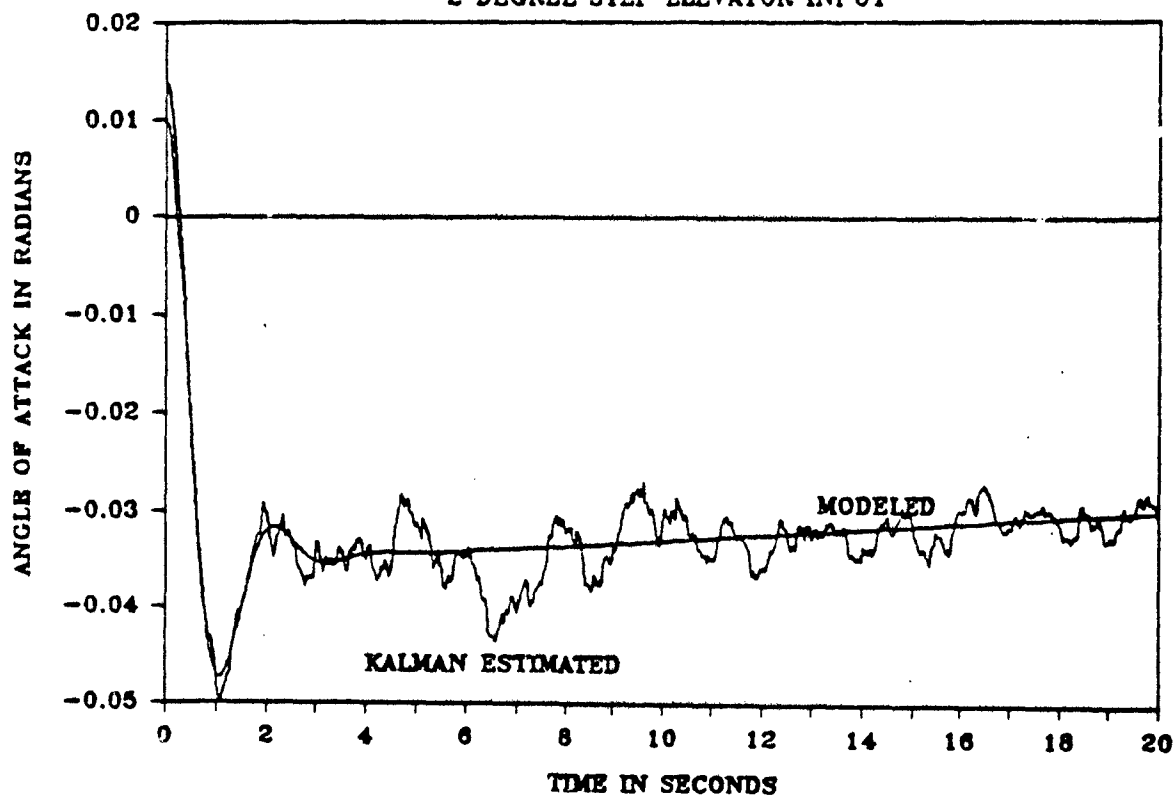
Figure 12.   Angle of Attack Recovery (2 degree Elevator)

- 49 -

Figure 13.   Sideslip Recovery (.5 degree Rudder)

NT-33A FLIGHT CONDITION 6
2 DEGREE STEP RUDDER INPUT
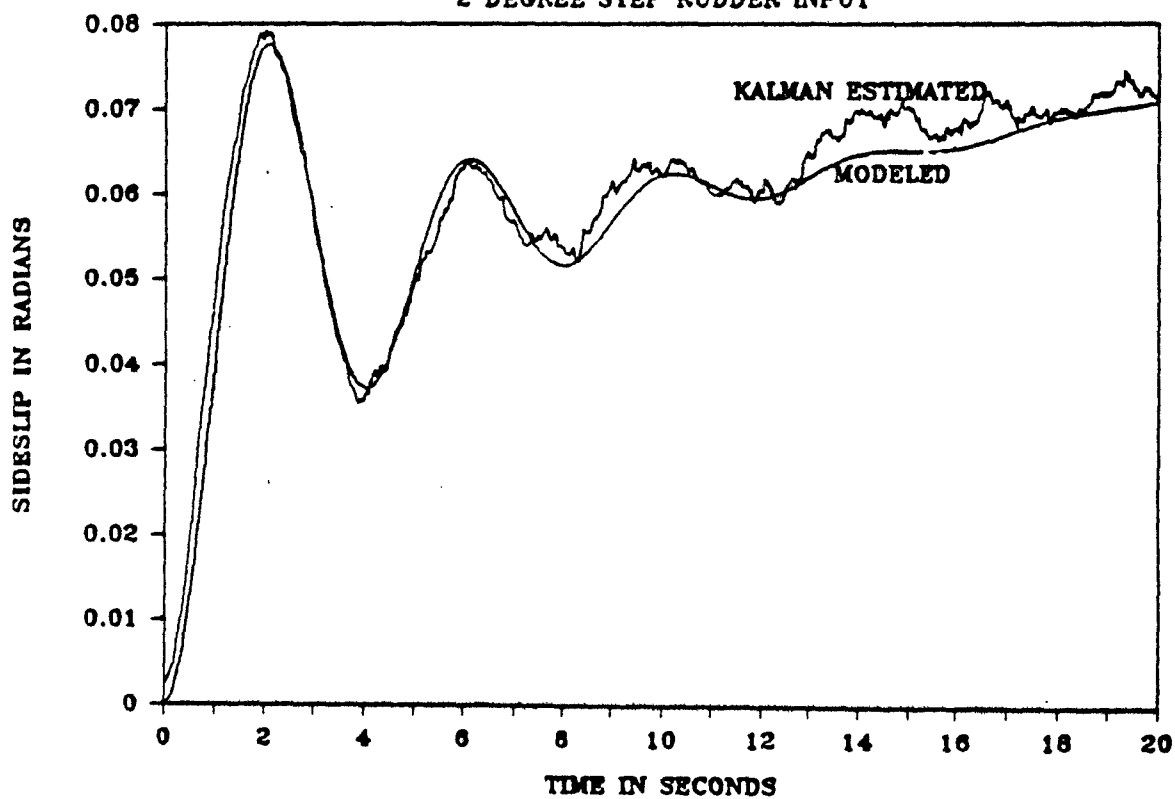
Figure 14.   Sideslip Recovery (2 degree Rudder)

NT−33A FLIGHT CONDITION 6

2 DEGREE STEP AILERON INPUT
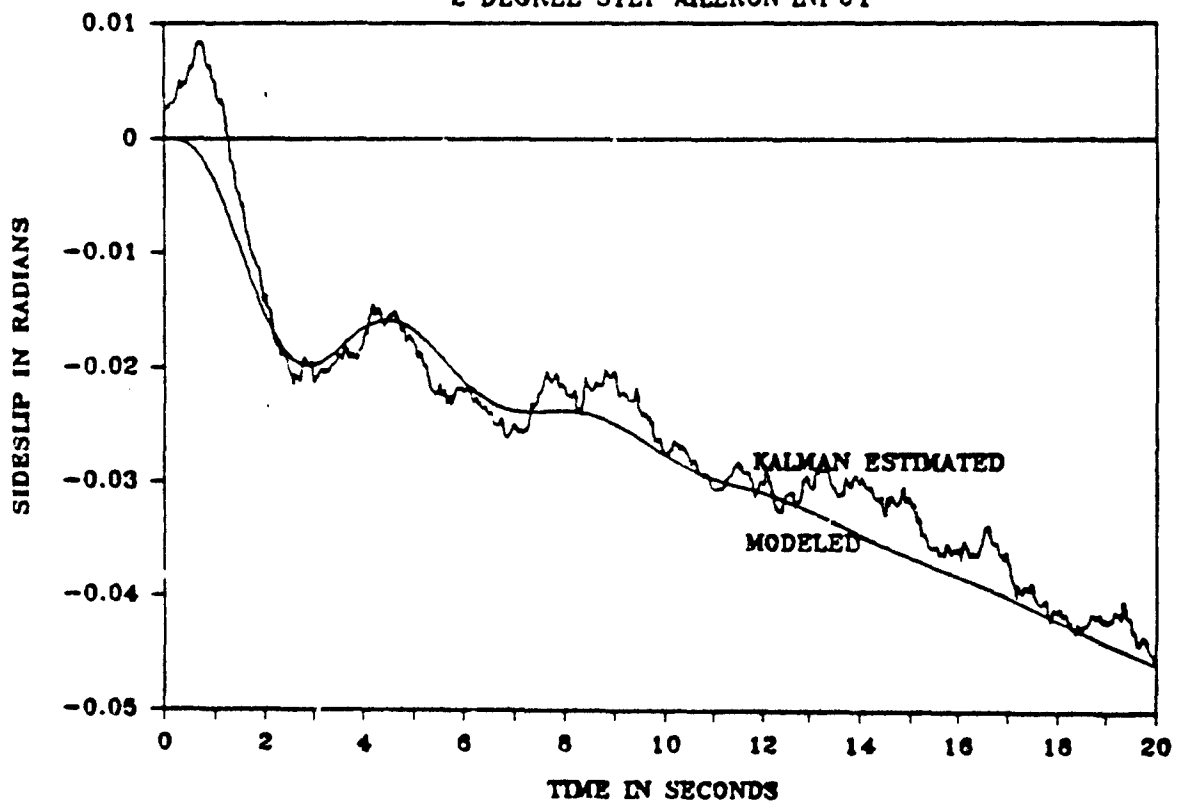
Figure 15.   Sideslip Recovery (2 degree Aileron)

- 52 -

though these covariances are 3 orders of magnitude less accurate than the calculated covariances. Figures 11 through 15 depict these worst case runs. The overall accuracy of the estimations is at the worst, .5 degrees in the longitudinal responses, and .4 degrees in the lateral modes. With less accurate measurements, as this scenario implies, tuning the Kalman filter becomes vastly more important. As these measurements were made from a model, there was no opportunity to actually tune, other than to make a good initial guess of model accuracy. This best guess was the input of measurement covariances into the model covariance matrix. While this is a good starting point for covariance analysis of a physical system [11], a real world system must be examined to tune the filter accurately. However, without such tuning, both modes of the filter are estimating the respective angles of attack and sideslip to about 1/2 degree. A best guess of the true real life performance of the post-flight estimator probably lies somewhere between the caluclated INS covariance analysis and the gross input of INS accuracy values. This is the area that must be examined through flight test with actual ring laser gyro equipment.

VI. FLIGHT TEST

TEST PHILOSOPHY   The purpose of the flight test is to ensure proper operation of the inflight angle of attack routine using actual flight data. This flight data collection is critical to ensure operation with noise-corrupted input data. The noisy nature of the actual INS measurements, coupled with possible unknown or assumed effects, will test the ability of the algorithm to recover the necessary data, and perform proper computations to calculate angle of attack. Unlike simulated data, however, no true angle of attack is known. Measured angle of attack from calibrated vanes, normal aircraft instrumentation, and computer modeled performance will be correlated against the INS derived α. This information will provide an acceptable measure of the accuracy of the INS derived values against the more conventional approaches in obtaining α.

The initial flight test consisted of low performance longitudinal maneuvering flight data tape anlysis only. The reason for this is two-fold. First, it will demonstrate the applicability of these methods for α determination in large, transport type aircraft. As these aircraft do not engage in high-g maneuvering or extreme flight attitudes, the basic assumptions should hold throughout the nominal flight regime. The applicability of these determination techniques will be demonstrated for large aircraft in both the inflight and flight test analysis phases. Secondly, nominal inflight accuracy should give an indication of the proper formulation of the estimator. The absence of high-g, coupled flight conditions allows a straight forward evaluation of the

estimator. The robustness of the estimator in maneuvering flight will be discussed in Chapter VII. This flight test was conducted in cooperation with NASA and in conjuction with a NASA propulsion test flight.

TEST AIRCRAFT   Initial flight test was accomplished using a NASA F-15A aircraft manufactured by the McDonnell Douglas Corporation. This aircraft, S/N 10281, is an F-15A air-superiority fighter modified for digital engine and control testing. It is a single seat aircraft powered by two Pratt and Whitney F-100 engines. Flight controls consist of twin vertical stabilizers mounting a single rudder on each. Lateral control is effected by ailerons on the outboard wing surfaces, aided by split stabilators, with pitch controlled by symmetrical stabilator action. The specific aircraft is shown inflight in Figure 16. For further information on the basic aircraft, consult T.O. 1F-15A-1 [17]. The basic aircraft layout and critical dimensions are depicted in Appendix E.

INSTRUMENTATION   The NASA F-15A Highly Integrated Digital Engine Control (HIDEC) was instrumented with a calibrated yaw-angle of attack-pitot-static (YAPS) head. This vane provided the baseline α information that the inflight estimator was evaluated against. In addition, the flight test boom also provided pitot pressure for calculation of true airspeed within the central air data computer (CADC). This aircraft was also configured with production angle of attack probes which were used as a secondary comparison of the angle of attack estimator. The external instrumentation of the F-15A HIDEC is depicted in Figure 17.

The aircraft was fitted with a USAF standard inertial navigation system. This system, a Litton Systems, Inc.

Figure 16: NASA F-15A HIDEC in Flight
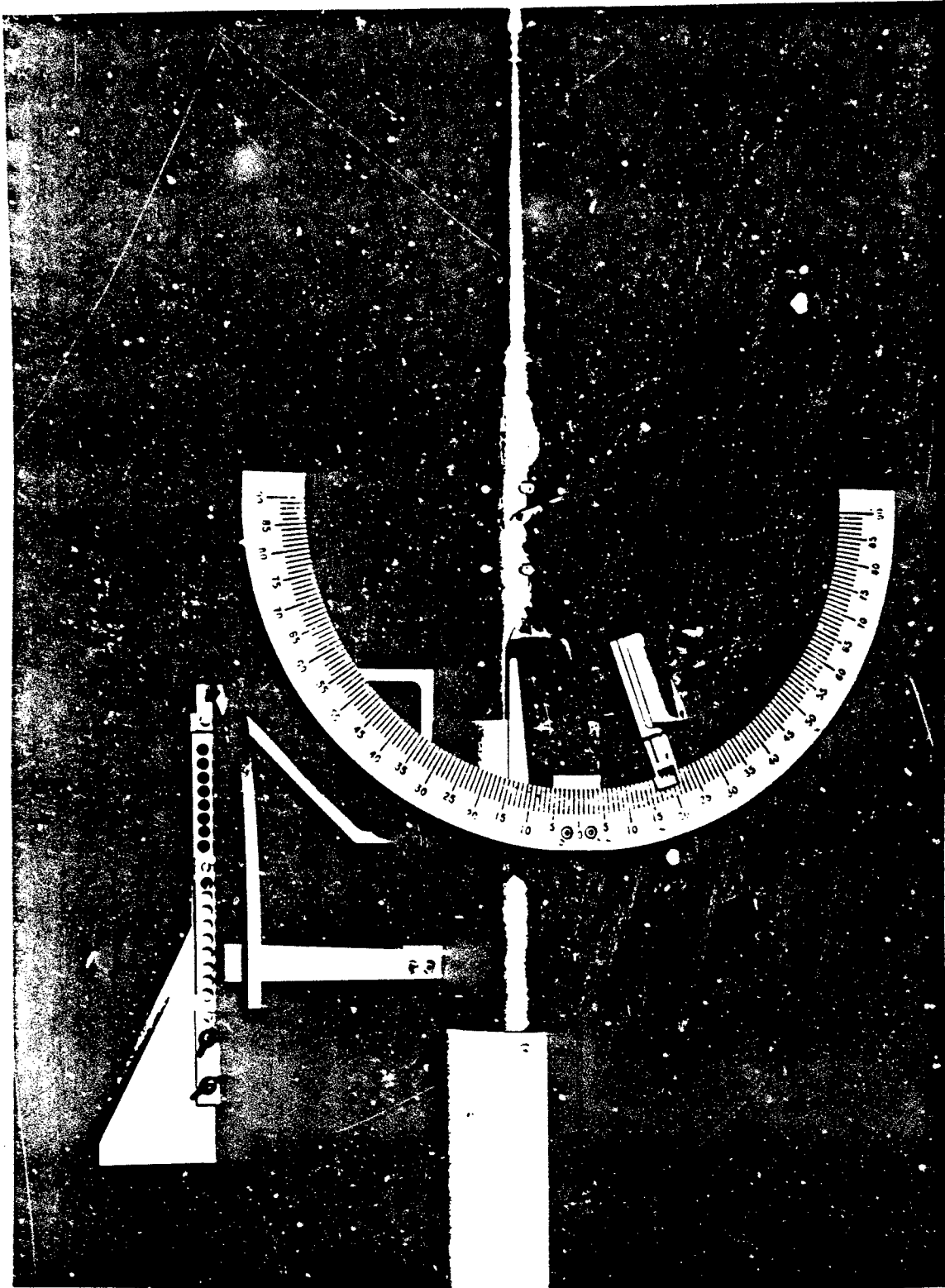
Figure 17: F-15A HIDEC YAPS Noseboom

ASN-109 inertial navigation set, is a fully self-contained
dead reckoning navigation system. It continuously computes
aircraft position by double integration from a known starting
point. Aircraft ground speed and attitude are interim
computations prior to position computation. This INS
consists of three major components. The first is the actual
inertial measuring unit (IMU) which houses the gyros and
accelerometers to sense aircraft motion. The second is the
IMU mount which provides precision mounting and alignment of
the system to the aircraft body axis. The third component is
the navigation control indicator which interfaces the INS to
the central computer of the aircraft and also allows pilot
control of the functions of the system. The INS was fully
instrumented and a list of signals available is contained in
Appendix F.

Weight was available through production fuel sensors on
board the aircraft which measure fuel remaining in each tank
to an accuracy of 200 lbs. The weight of the aircraft could
then be easily calculated, knowing basic aircraft weight,
serviced fluid weight, stores weight, and the changing fuel
weight.

Mach number and altitude signals were obtained from the
Sperry AN/ASK-6 air data computer, along with true airspeed.
Air density was calculated through the standard exponential
atmosphere equation for input into the primary estimator
equation. Overall, no signals were used which would not be
obtainable through current, INS-equipped production aircraft
instrumentation.

All required stability derivatives were modeled from
flight test data obtained in USAF technical reports. C_L,
C_{m_0}, center of gravity motion and all moments of inertia data

plots are included in Appendix G. In addition, all
computer-derived models are also included for comparison
purposes in the same appendix.

DATA REDUCTION All inflight data was reduced using the NASA
ELEXI computer system. Aircraft data telemetry was retrieved
from the computer for the specific maneuvers required. This
data consisted of time tagged values for all signals
specified in the estimator flow chart. The basic estimator
program, as implemented in FORTRAN 77, was altered to allow
use in the time tagged, sequential mode of operation on the
ELEXI system. This consideration was important in that the
inflight estimator was designed for real time operation, and
the ELEXI provided that capability in reducing flight data.
Once the data was calculated sequentially, the results were
plotted and compared to YAPS boom α at the same time tag.
FORTRAN coding of the inflight α estimator for use on the
ELEXI is included in Appendix H.

TEST METHODS AND CONDITIONS The optimum flight test
technique for stable longitudinal flight at varying angle of
attack was determined to be the level acceleration. In
general, the aircraft was stabilized on conditions in the
slow speed regime with engines at the planned military or
maximum power settings. This procedure required a climbing
entry to the test point. The aircraft was then allowed to
accelerate to its maximum speed while maintaining constant
altitude and one-g flight. This required a constant
reduction in angle of attack throughout the level
acceleration maneuver.

Three level acceleration test points were planned to
evaluate estimator angle of attack. Additionally, Mach and

altitude effects were investigated using military and maximum
accelerations at three different altitudes.   Level
acceleration test points are summarized in Table V.

TABLE V.
LEVEL ACCELERATION EVALUATION

TEST POINT	ALTITUDE	POWER	MACH BAND
1	20,000	MIL	0.5 - 0.9
2	10,000	MIL	0.4 - 0.9
3	40,000	MAX	0.5 - 1.5

The next logical step in the buildup process to evaluate
the inflight α estimator is to introduce abruptness into the
estimation process, while still restricting maneuvers to the
longitudinal modes within the plane of gravity.   The
wings-level, constant g pitch-up flight test technique was
considered the optimum for this phase of the flight test.
This technique required the aircraft to be stabilized at a
constant aim altitude and Mach number.   The aircraft was
abruptly pitched to a series of positive and negative
constant g values, much like a roller coaster.   This
technique was accomplished within a standard 2,000 foot data
band.   Three test points were evaluated during this phase and
are summarized in Table VI.
        The final stage of the quantitative flight test
evaluation of the angle of attack estimator is examination of
out-of-plane maneuvers.   The purpose of this phase of testing
is to remove the gravity vector from the longitudinal plane

- 60 -

TABLE VI.

ABRUPT PITCH EVALUATION

TEST POINT	ALTITUDE	MACH	AIM LOAD FACTOR
4	40,000	0.7	+3.0
5	40,000	0.7	-0.5
6	40,000	0.7	-1.0

of the aircraft and judge the effect of load factor and
banked flight of the estimator. The wind-up turn was judged
to be the best flight test technique for this flight test
goal. In this maneuver, the aircraft is trimmed at a given
Mach ,and altitude. The aircraft is then steadily banked
into a constant Mach turn while slowly increasing load factor
to the desired end point. This maneuver takes place within a
2000 foot data band, as a descent is required to maintain
constant Mach at a trim power setting. Two test points were
identified for examination of the effect of g and bank angle
on the estimator. The wind-up turn test points are defined
in Table VII.

TABLE VII.

WIND-UP TURN EVALUATION

TEST POINT	ALTITUDE	MACH	AIM LOAD FACTOR
7	20,000	0.9	+3.0
8	20,000	0.9	+5.0

RESULTS AND ANALYSIS

The results of the military power level acceleration in test point 1 are depicted in Figure 18. This acceleration was from 0.5 to 0.9 Mach at 20,000 FT. The data is presented as two angle of attack traces. The first is AINF, or alpha infinity, as derived from the YAPS boom. The second is AWB, or alpha wing-body, representing the output of the inflight α estimator based on equation (17). Also accompanying the α traces are Mach and altitude data throughout the maneuver. This data will accompany all level acceleration data traces examined in this section.

There are two areas of interest in Figure 18. The most obvious is the initial portions of the α data traces, where an approximately 1.3 degree noise in estimator angle of attack is apparent. The actual level acceleration maneuver does not begin until 17 seconds into the data trace. This initial, high angle of attack regime is the climb into the maneuver at slow flight. This slow flight is characterized by thrust set at test power, in this case military setting. The result is slow, climbing flight in moderate buffet, with some internal vibration present. The difference between α sources is reasonably constant during this entry into the acceleration. Initial skepticism of the estimator would give more credence to the YAPS boom α than the estimator. It should be realized that there is no absolute source of angle of attack in this test. However, the α estimator would be susceptible to airframe buffet and vibration, cluttering the normal load factor signal at these low speed conditions. It is of note, though, that the α estimator does follow the peaks of the YAPS boom α exactly, remaining within 1.5 degrees until the initiation of the pushover at the beginning of the level acceleration, occurring at 15 seconds

- 62 -
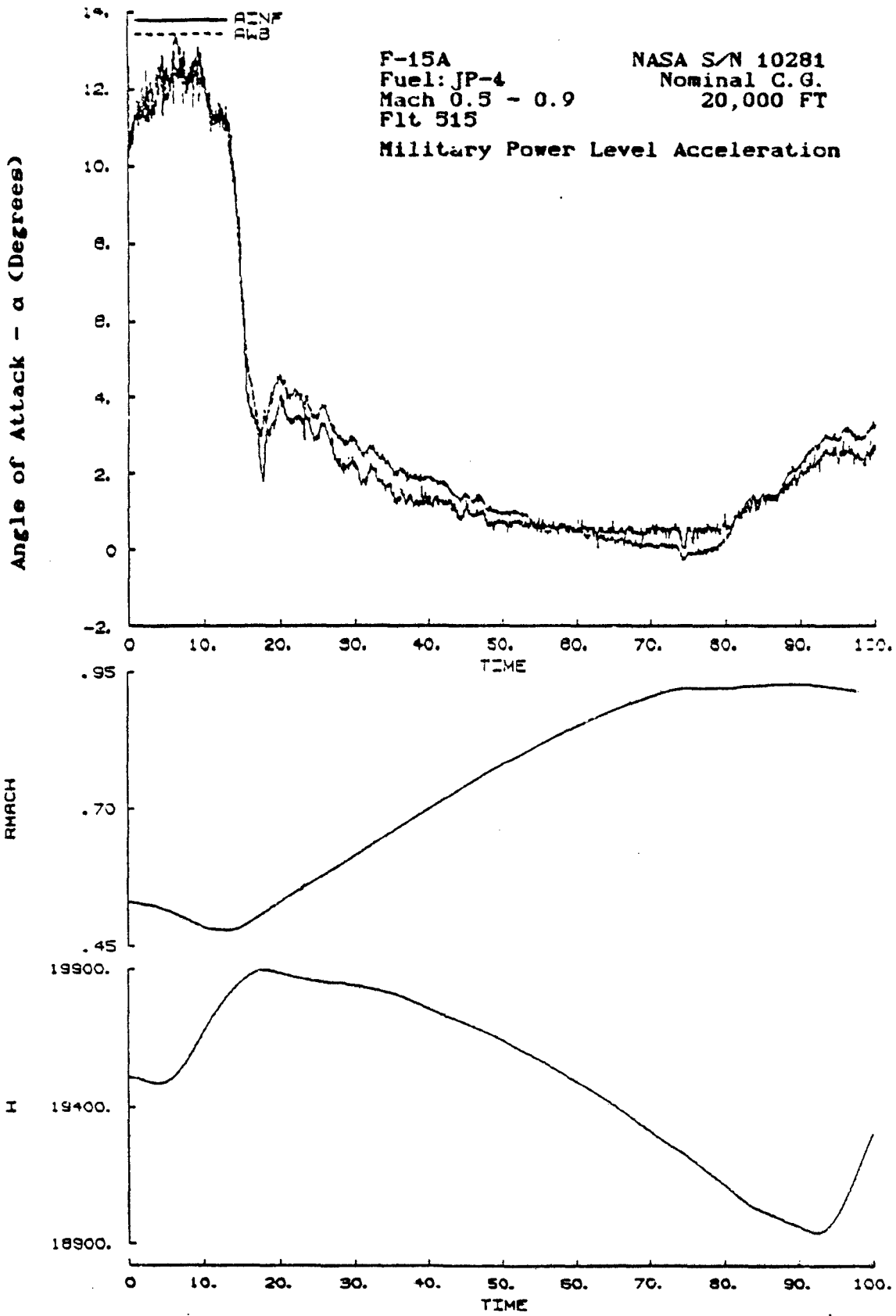
Figure 18. Test Point 1 Level Acceleration Results

into the trace. The YAPS boom appears to be the the most
accurate source during this slow flight phase.

Once the level acceleration has begun, the two angles of
attack remain within 0.5 degrees of each other throughout the
rest of the maneuver. For the first half of the
acceleration, the inflight α estimator is below the YAPS
boom α. At 0.82 Mach, the traces coincide, with estimated α
becoming larger than boom α for the remainder of the trace.
They do stay generally within 0.5 degrees during this
exchange. Overall, the two angle of attack traces coincide
well, with the exception of the entry into the maneuver,
during slow flight in moderate buffet.

Figure 19 depicts the results of a military power level
acceleration to 0.9 Mach at 10,000 FT. Spikes in this, and
subsequent figures indicate data dropout. Again, the same
two phases of the level acceleration are notable in this
figure. During the slow flight entry into the acceleration,
angle of attack traces differ by approximately 2 degrees.
The inflight α estimator follows the peaks of the YAPS boom α
exactly, but the true α is difficult to ascertain for this
flight regime. However, once the manuever begins at 20
seconds into the data trace, the angles of attack coincide
well, again within 0.5 degrees. This is the attempted
specification to which the estimator was designed to meet.
Again, the crossover of α traces occurs in the 0.8 Mach
regime, as was noted in the previous level acceleration.
This crossover can most likely be attributed to the
regression of the lift curve. Recall that α was defined as a
function of Mach and C_L. At 0.82 Mach, the regression
appears almost exact, while at other points, there is some
deviation from the exact lift curve. It is important to note
at this point also that no divergence occurs as the higher

- 64 -
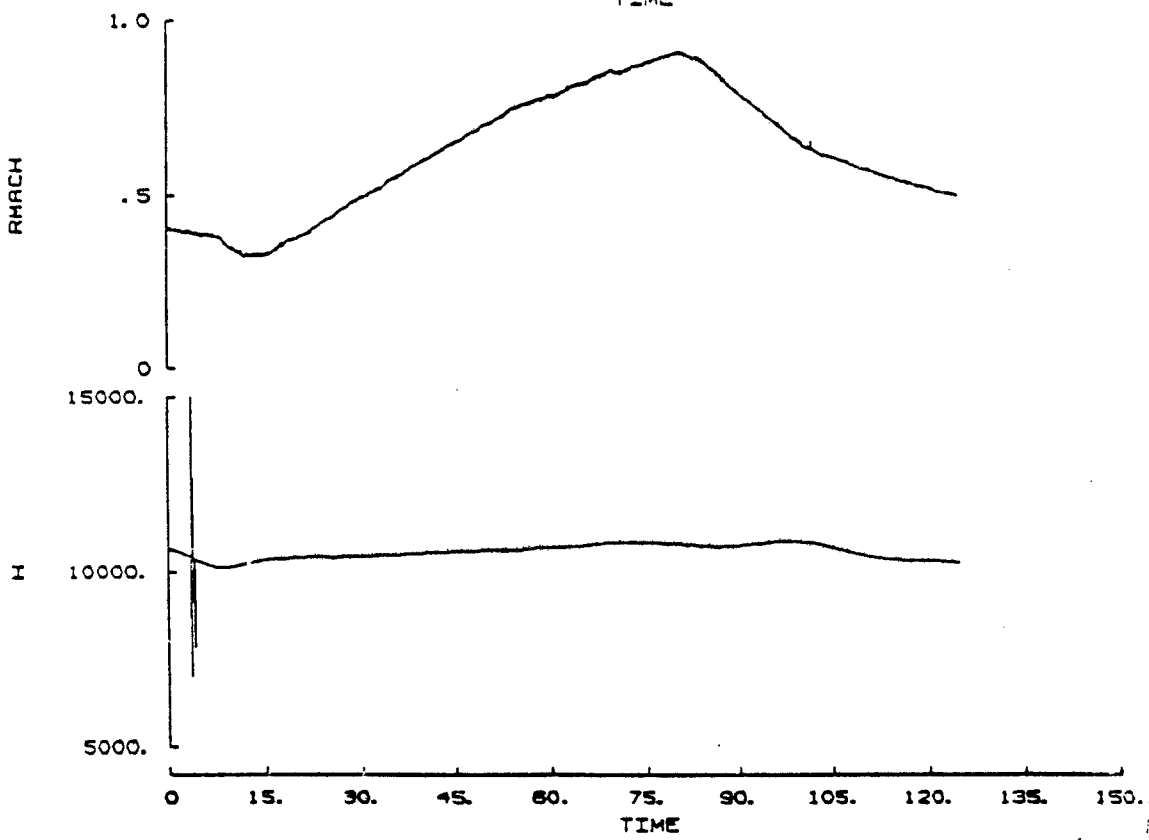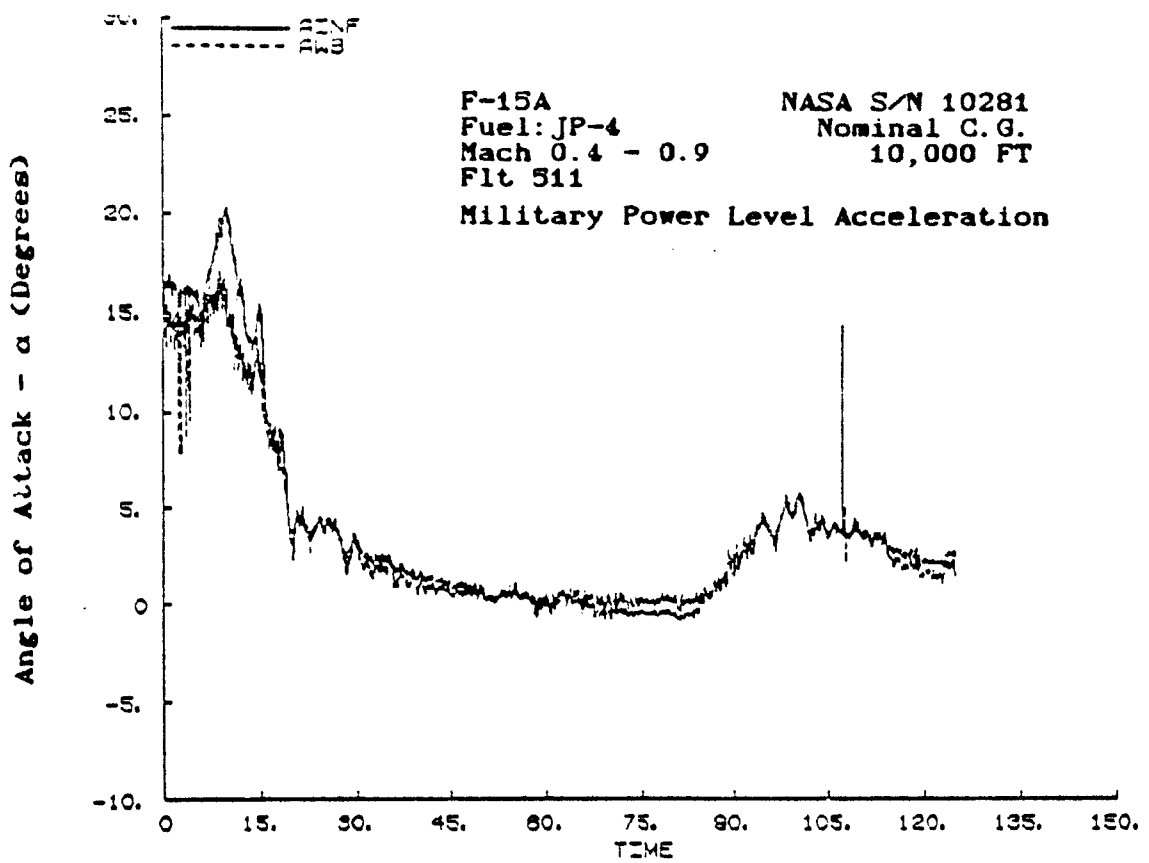
Figure 19. Test Point 2 Level Acceleration Results

subsonic Mach numbers are approached, indicating a
reasonably good fit of Mach number in the high subsonic
regime.

The maximum power level acceleration to Mach 1.5 in
test point 3 also showed good estitmator correlation to YAPS
boom angle of attack in the subsonic regime. Estimator
tracking can be seen in Figure 20, including Mach and
altitude traces. Pitch maneuvers tracked well through almost
17 degrees boom angle of attack. Again, the aircraft is in
slow flight, accompanied by moderate buffet, while performing
the climbing entry to the level acceleration. This is the
most likely cause of noisy normal accelerometer output at the
high angles of attack. Throughout the remainder of the
subsonic portion of the manuever, both α traces correspond
nicely, even during some large angle of attack excursions. A
point of note occurs at the jump to supersonic flight at 118
seconds into the trace. At this point, the traces begin to
diverge at a rate proportional to the Mach number. The
inflight α estimator was not modeled for supersonic flight
and this could be the simple cause. However, the traces tend
to coincide in terms of deviations from a steady condition.
In other words, a 0.5 degree jump in YAPS boom angle of
attack is matched at the identical time segment by a 0.5
degree jump in estimator angle of attack. This again
indicates proper formulation of the estimator, but any YAPS
boom supersonic errors present make it impossible to quantify
estimator errors due to lack of supersonic modeling. In
addition, the closeness of the traces indicate at this point
that altitude has little to no effect on the α_{VB} model.
Recall that the approximation was made to eliminate altitude
from the model. Initial flight test shows that this was an
acceptable approximation of the true model.
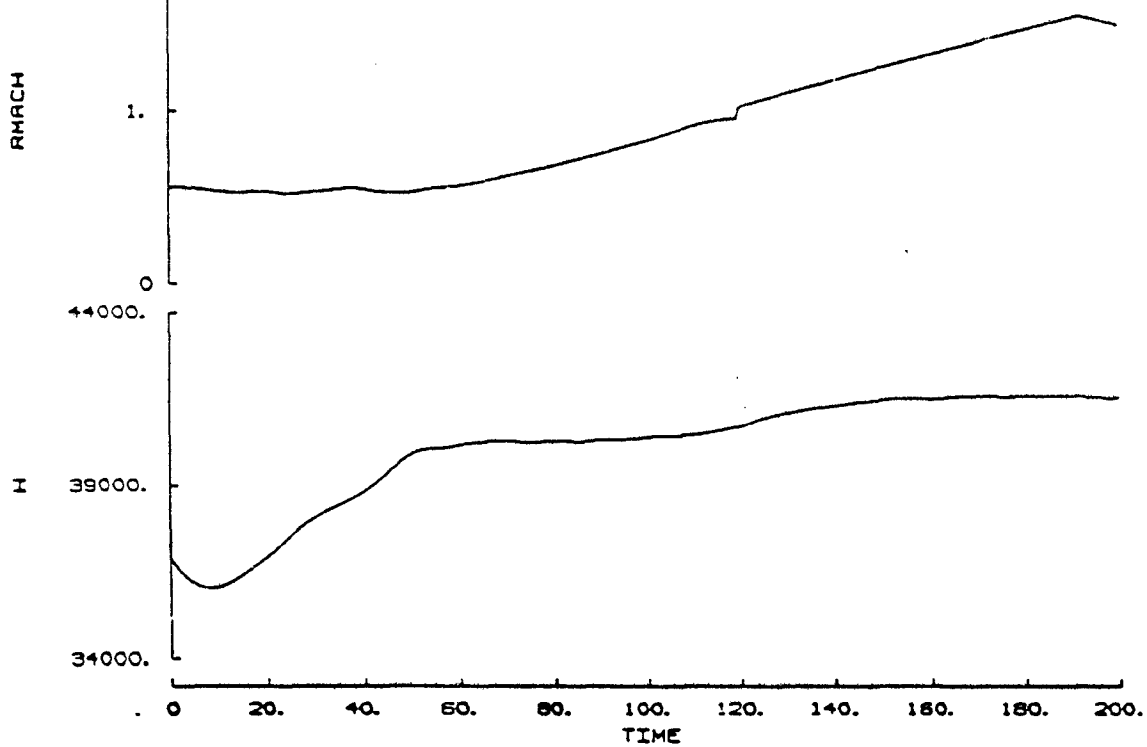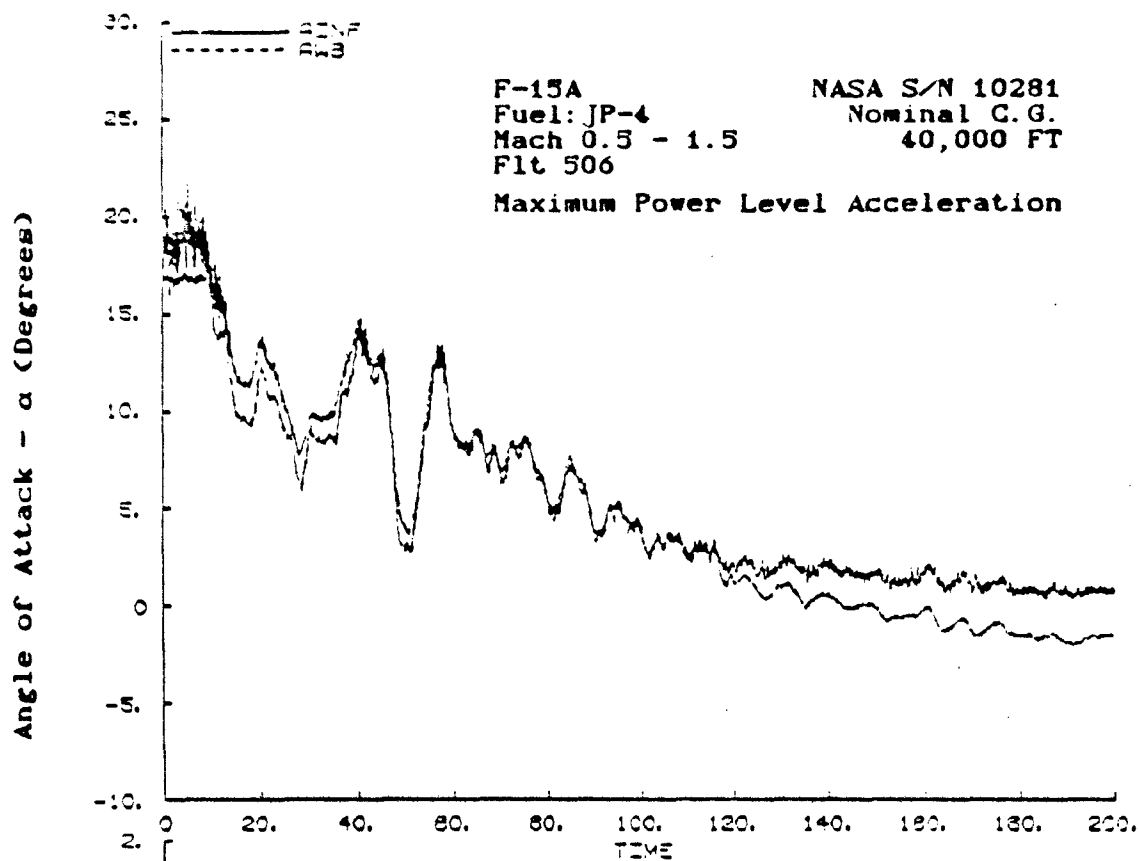
Figure 20.   Maximum Power Level Acceleration Results

Figure 21 depicts the results of the abrupt pitch evaluation. The upper graph shows estimator/YAPS angle of attack correlation, while the lower graph shows corresponding normal load factor. This figure includes all abrupt pitch test points. Of immediate note is the closeness with which estimator a follows boom a below approximately 16 degrees angle of attack. Negative g excursions match almost identically. The lack of high angle of attack modeling is the cause of the deviation at the peak of the high g points, as was noticed in the initial portions of the level accelerations. However, the close correlation of the separate angle of attack sources through rapid changes in angle of attack and load factor do support the basic concept of this form of a estimator. It can indeed accurately recover angle of attack with at least 0.5 degrees of precision in upright, purely longitudinal motion.

The wind up turn evaluation did uncover some angle of attack deviations in the estimator. Figure 22 depicts the 3 g wind up turn results, along with normal load factor achieved in the maneuver. In this figure, there is some definite deviation during the sustained, high g portion of the maneuver. Although the traces match in terms of peak locations, they differ by almost a degree at the sustained g point. Although the YAPS boom a does not provide an absolute, true a, it should be the weighted preference. However, the boom a does show almost 0.5 degrees worth of noise in its signal, while the estimator is slighly smoother. The same result is true with the 5 g wind up turn presented in Figure 23. YAPS boom angle of attack is consistently lower than estimator a at the higher sustained g plateau, although its signal is much cleaner than the preceeding graph. Again, the peaks of each source match well, with no

- 68 -
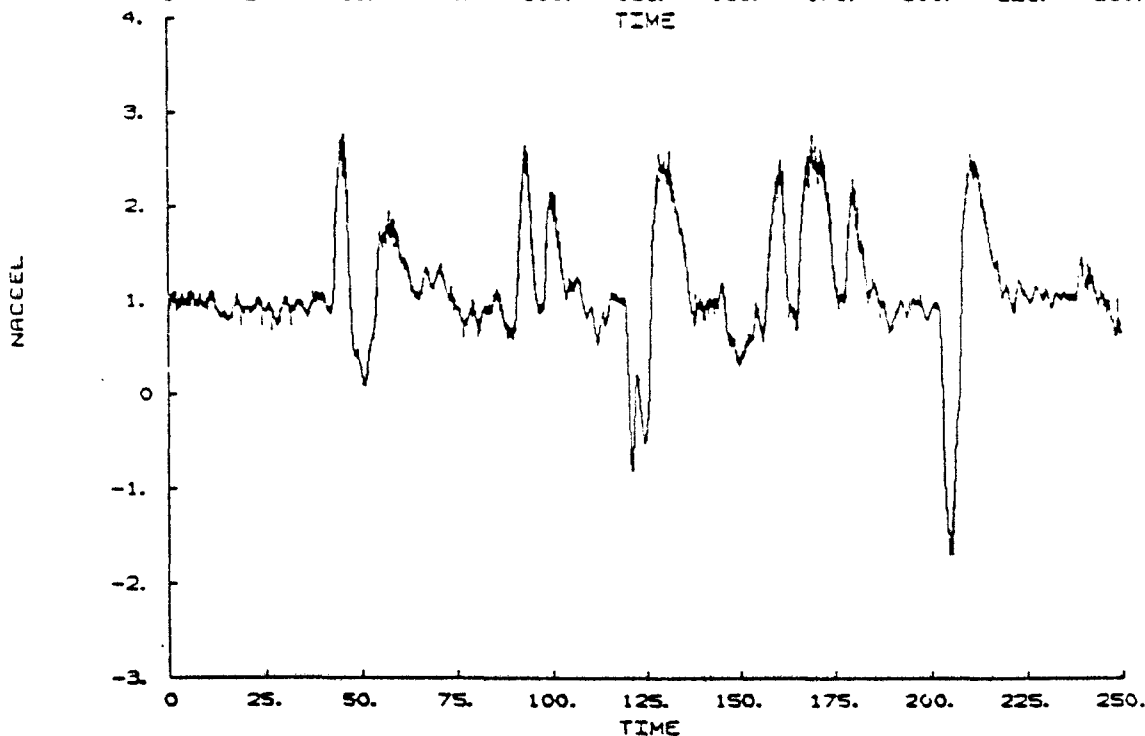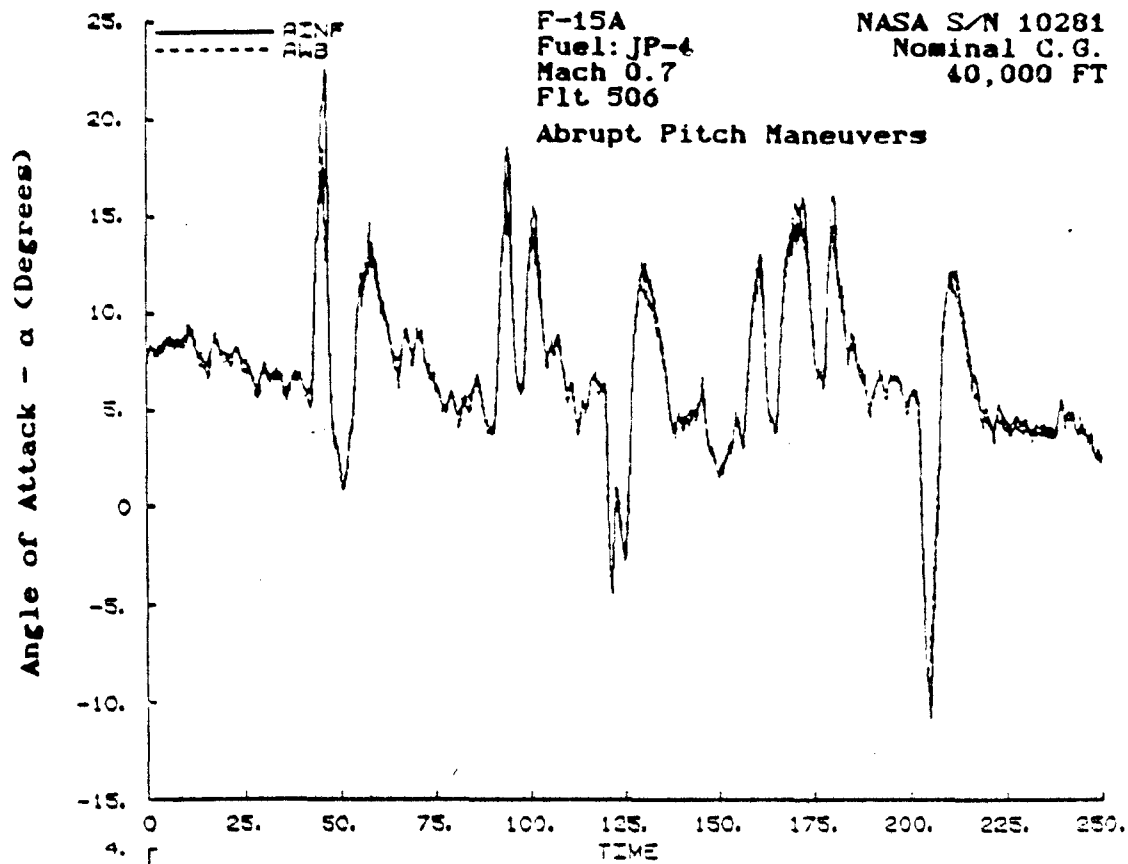
Figure 21.   Abrupt Pitch Maneuver Results
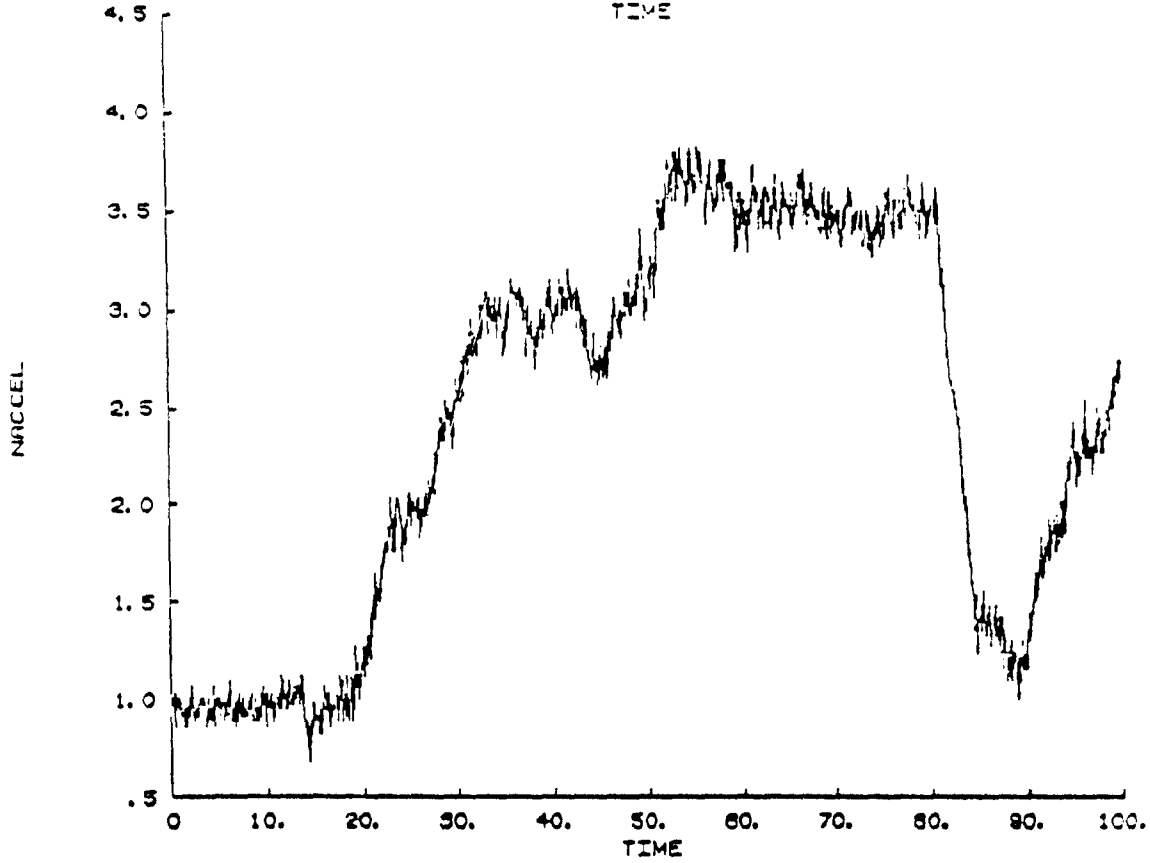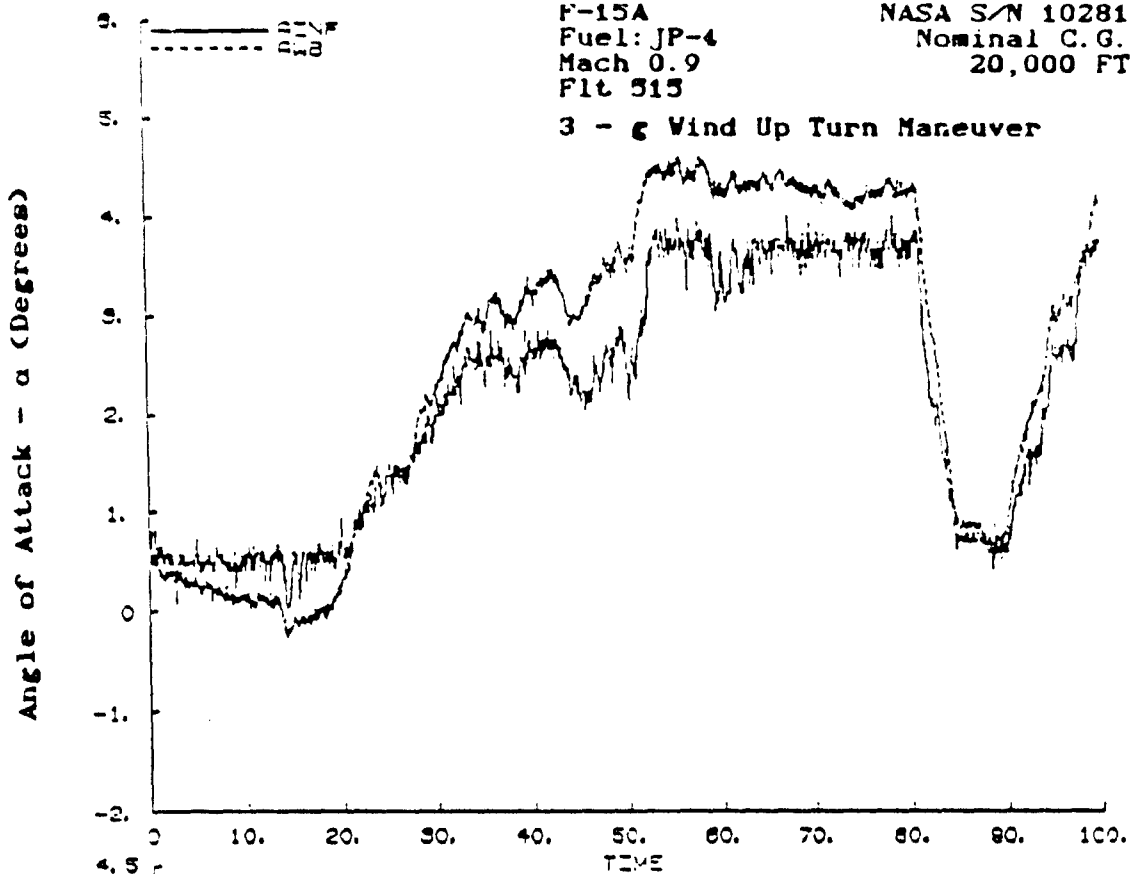
Figure 22.   Test Point 7 - 3 g Wind Up Turn Results
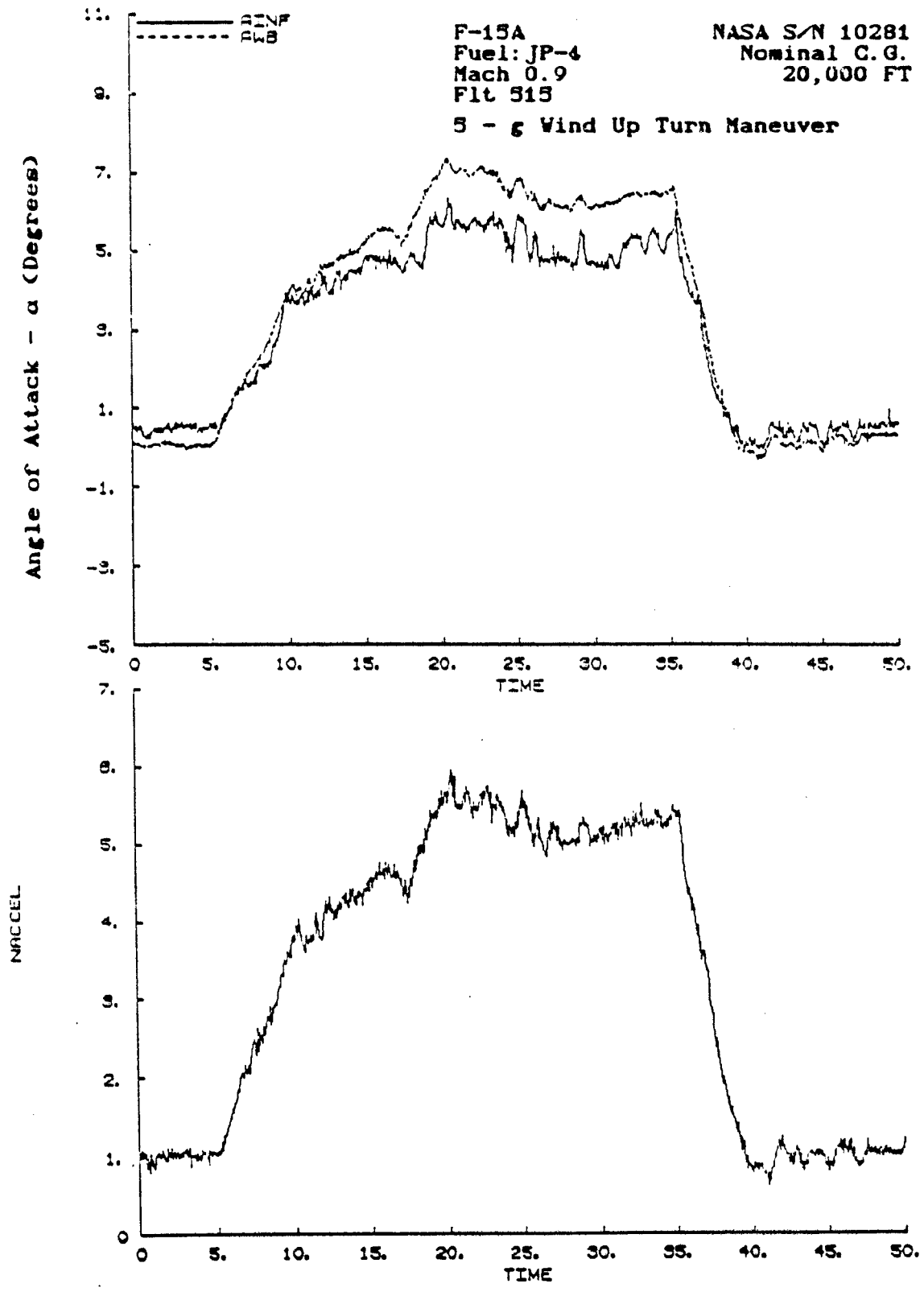
Figure 23.   Test Point 8 - 5 g Wind Up Turn Results

lag noticable in the estimator. The lift curve used as the model was not corrected for load factor, and was a trimmed lift curve. This could account for the deviations at the sustained higher load factors, and indicate a requirement for a closer wing-body model of angle of attack. Another possibility is error in out of plane load factor calculation. This could be the result of actual accelerometer output as opposed to theoretical accelerations about the center of gravity. The result is an alteration in equation (28) to replace the $\cos\theta\cos\phi$ term with 1.0 as these angles are accounted for due to normal accelerometer bias of 1 g. This bias is included in all normal accelerometers to take into account the gravitational pull of the earth. In straight and level, unaccelerated flight, the normal accelerometer reads 0.0 ft/sec^2 acceleration of the aircraft center of gravity. However, the aircraft is indeed under 32.2 ft/sec^2 or 1 g acceleration due to the earth's pull.

Overall, the α estimator correlated to the YAPS boom α well. Under most conditions, the results were within the specified 0.5 degree deviation. Where the deviations were greater than that value, the estimator errors were explainable and indicate a need to form a more precise $C_{L_{WB}}$ model than a linear regression on two independent variables as was accomplished for this research. A full, maneuvering flight demonstration will indicate the degree to which the current model and equations are adequate for high g, rolling flight out of the longitudinal plane of motion.

VII.   MANEUVERING FLIGHT DEMONSTRATION

PURPOSE   The robustness of the inflight estimator is evaluated in this phase of the flight test through a series of highly dynamic maneuvers in varying planes.   The overall goal is to highlight weaknesses in the inflight estimator and examine regimes of flight where the estimator assumptions, as currently proposed, break down.   The most likely area of trouble was determined to be out-of-plane, or three-dimensional, fighter maneuvering of the type expected in basic air-to-air or air-to-ground combat.   This is therefore the emphasis during the robustness check of the inflight α estimator.

SCOPE   The purpose of this portion of the flight test was demonstration only.   The attempt was made to devise a single flight test technique to quickly and efficiently demonstrate any possible area of weakness in the angle of attack estimator.   In other words, this portion of the investigation was to highlight areas to troubleshoot the estimator algorithm or to point where future investigations should be directed.

MANEUVER   The robustness check was only accomplished at one flight condition due to constrained flight test time.   The maneuver that was developed was therefore a dynamic one encompassing all expected problem areas such as loaded rolls and longitudinal pulls out of the local horizontal plane.   The modified split-S maneuver was performed in conjunction with a NASA propulsion test.   The actual NASA flight test card is included in Appendix I.

The overall robustness maneuver can be divided into four

- 73 -

distinct segments.   Initially, the aircraft is flown in a
true north heading.   Once established on conditions, a 30
degree banked, climbing turn at 2 g's is begun.   This is
indeed a climbing turn, as a level 30 degree turn requires
only 1.2 g's.   Upon stabilization in this turn, the pilot
then rolls inverted in the same direction as rolling into the
2 g turn initially.   At this point, the pilot then begins a
sustained 4 g pull in a split-S maneuver, recovering in an
upright, wings level attitude.   The robustness maneuver thus
evaluates a climbing, loaded turn, a pure roll out of the
local horizontal plane, and a loaded pull with the gravity
vector constantly moving throughout the aircraft axis system.
The robustness test points are summarized in Table VIII.

TABLE VIII.

ROBUSTNESS EVALUATION

TEST POINT	ALTITUDE	MACH	ROLL DIRECTION
9	20,000	0.7	RIGHT
10	20,000	0.7	LEFT

RESULTS AND ANALYSIS   The results of the first robustness
maneuver are depicted in Figure 24.   Pitch, roll and yaw
rates are presented with the estimator and YAPS boom α
traces.   The initial roll into the maneuver begins at 2
seconds into the trace.   The initial difference between the
higher estimator trace and the YAPS boom trace is
approximately 0.7 degrees.   As with the loaded rolls
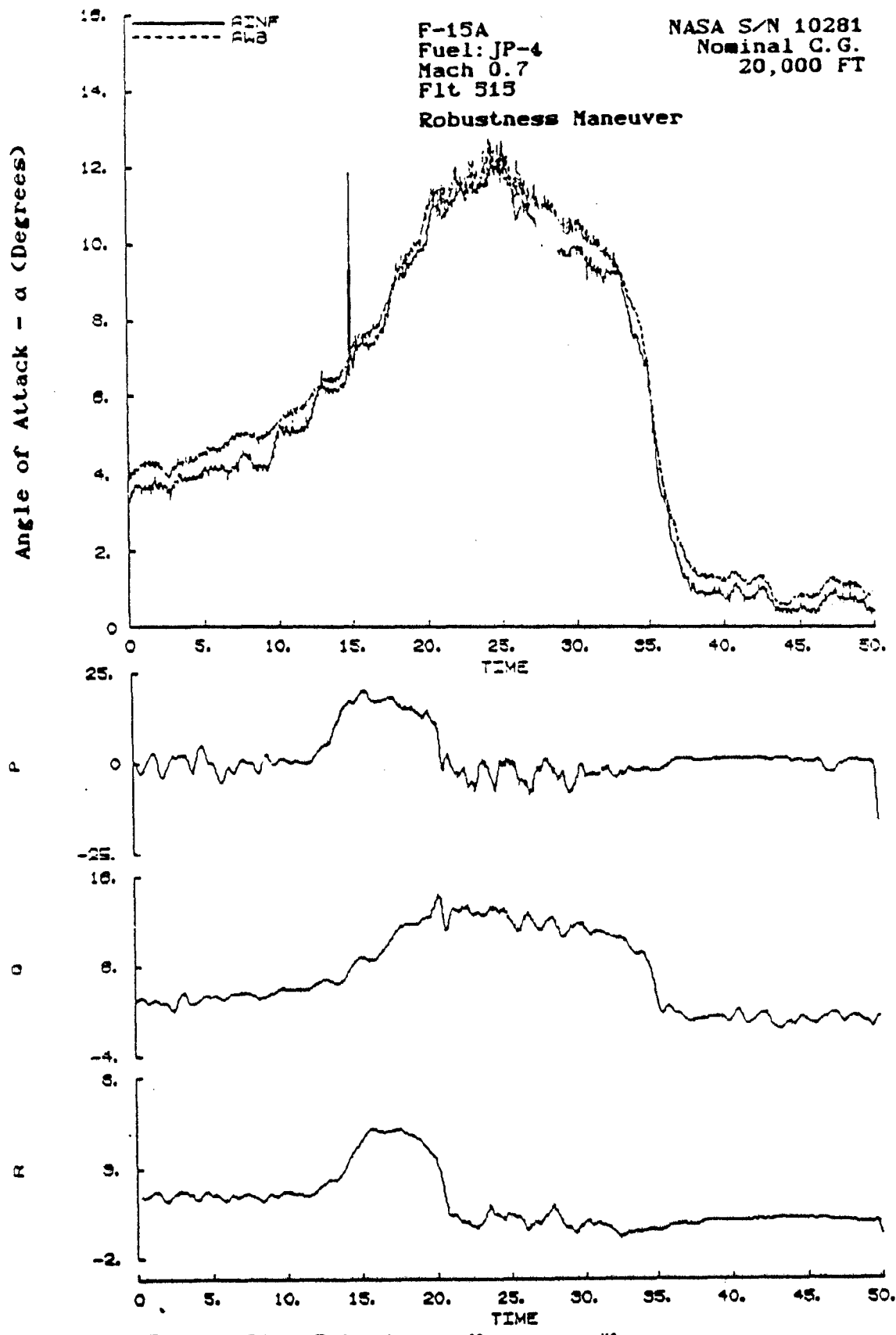
Figure 24. Robustness Maneuver #1

presented in the Wind Up Turn test, the difference between traces remains reasonably constant. However, as the roll to inverted attitude begins at 13 seconds into the trace, the curves come to within 0.2 degrees. The 4 g split-S shows very close correlation, through recovery at 38 seconds. Of note during this phase of the maneuver is the noise within the α estimator signal. While no more than approximately 0.8 degrees, it disrupts an otherwise close match under sustained g, inverted flight. The second robustness maneuver, depicted in Figure 25, shows almost the exact same results for the opposite direction maneuver, although the loaded turn portion is more distinct in this plot. Lack of a definite bias during either direction of the maneuver indicates that sign conventions in the moment correction equations are correct. The split-S maneuver in the second plot also shows YAPS boom oscillations of up to 1.5 degrees, while the estimator is smooth in relation. Again, the matching is excellent during the recovery phase at 42 seconds. In general, the only deficient area of the inflight estimator as tested is the bias noticed under sustained load factor. Note that this situation did not occur with abrupt pitch maneuvers. This deficiency, on the order of 0.3 degrees per g always occurs to the high side. Again, a trimmed lift curve at 1 g was used as the model. A higher order model of α as a function of $C_{L_{VB}}$, altitude, Mach and load factor may provide the key. However, correlation during these extreme maneuvers was quite acceptable, considering the multiple changes in plane and velocity vector during 40 seconds of robustness evaluations. The maximum difference was 2 degrees as observed in the Wind Up Turn test, and this occurred under approximately 5.5 g's. In addition, it is important to note that when in error under g, the α estimator
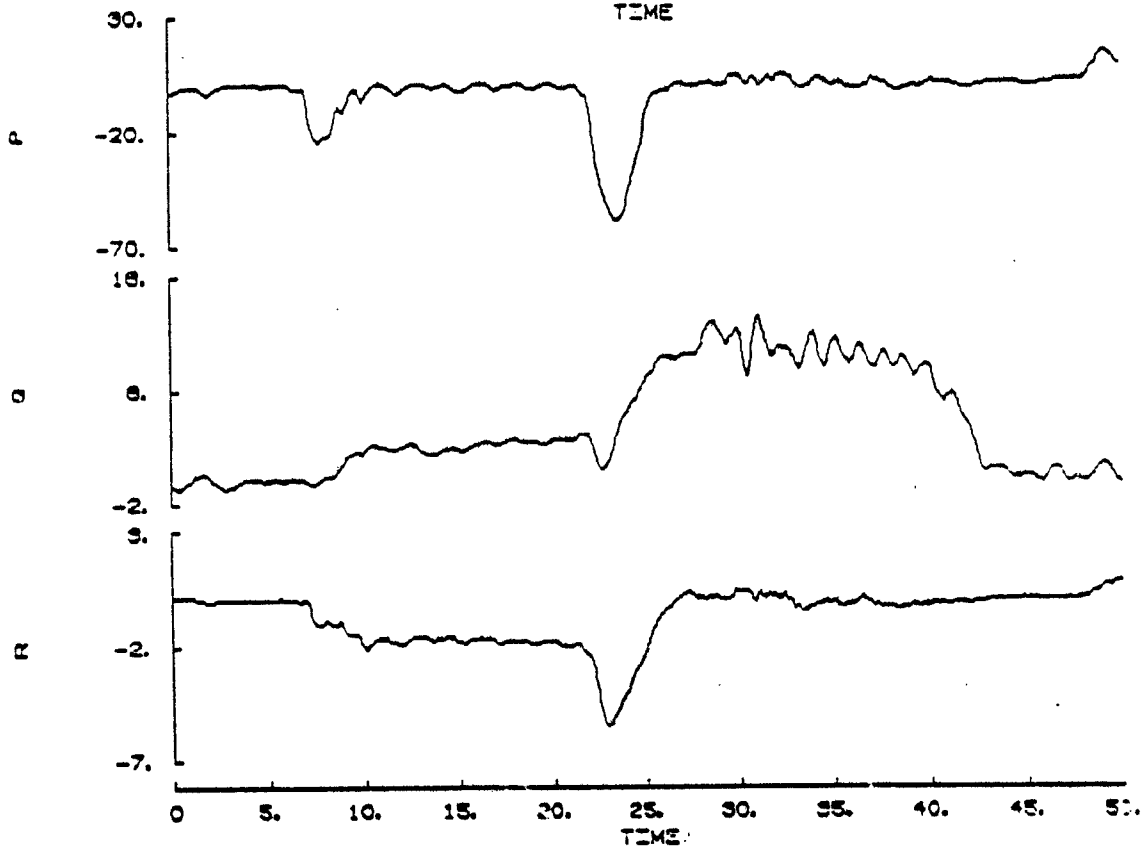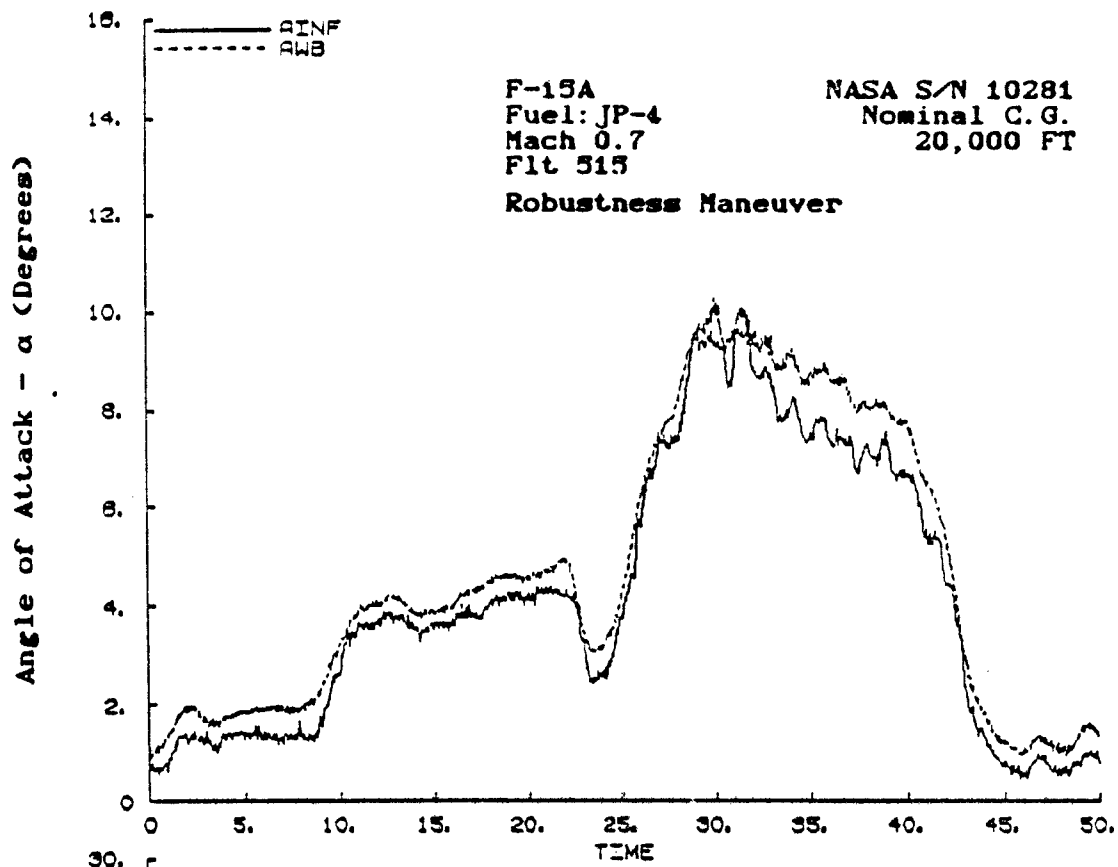
Figure 25.   Robustness Maneuver #2

was always higher than YAPS boom angles of attack.

GENERAL COMMENTS The ability to sit in the NASA control room
while the flight was in progress provided a unique
opportunity to view the α estimator performance during all
phases of flight. While it is difficult to quantify all
comments, certain qualitative observations can be made from
personal engineering notes taken during the flight.

As indicated in the Flight Test chapter, supersonic
effects were evident. In general, at subsonic speeds during
straight and level flight, the α estimator was well within
the specified 0.5 degree tolerance as compared against the
YAPS boom. At 0.72 Mach, the estimator was within 0.3
degrees of the noseboom. At 0.8 Mach, the estimator tracked
very well at 0.1 degrees off. And finally at 0.95 Mach, the
estimator was within 0.4 degrees of the YAPS boom. At
supersonic speeds, the estimator jumped to 0.8 degrees lower
than YAPS values. Again, this larger difference can be
attributed to the purely subsonic modeling of the lift curve
and pitching moment of the F-15A. However, the consistency
of the low estimator values indicates that the inflight
estimator requires some "tuning" to better approximate the
F-15A aerodynamics.

Two secondary aerodynamic effects were observed which
deserve note. At subsonic speeds, with good estimator
correlation to YAPS values of α (within .2 degrees) ,
extension of the massive F-15A speedbrake caused an immediate
jump to 0.5 degrees difference between α sources. Two
possible explanations are readily apparent. First, the large
speedbrake alters the aerodynamic characteristics of the
wing, invalidating the α_{VB} model developed for clean
configurations only. The second aerodynamic effect was a 1.2

degree estimator to YAPS boom difference during air to air refueling at 320 knots indicated airspeed. The effect here seems to be caused by tanker wake effects on the F-15A local airflow, impacting both the YAPS noseboom and the local aerodynamics as modeled by the α estimator.

Overall, the inflight α estimator performance was acceptable as qualitatively evaluated during this flight and measured against YAPS boom values.

VIII. CONCLUSIONS AND RECOMMENDATIONS

GENERAL   In broad terms, the objectives of this thesis were
met and the concept of angle of attack and sideslip
estimators using standard inertial reference platforms is
highly feasible.   Of the two estimator variations, the
inflight α estimator was the most extensively tested, and the
most widely applicable.   It served to demonstrate that the
concept of an angle of attack estimator which is accurate to
0.5 degrees is not only possible, but available for real time
inflight use, with current generation mechanical inertial
navigation systems.   Specific conclusions and
recommendations, as organized by thesis objective, follow:

Objective 1.   The linear recursive estimator lends itself
well to use as an angle of attack and sideslip estimator.
With less than full state measurements, the estimators can
easily determine a theoretical value for that missing state,
in this case α or β.   Developement of the model was quite
straightforward and required no extensive mathematics other
than formulation and discretization of the A and B matrices.
Accuracy achieved by this system is difficult to measure.
Using the noise corrupted computer model, a 0.25 degree
accuracy was easy to achieve with ring laser gyro accuracies
and variations as a model.   However, these values were only a
first guess for the actual measurement covariance matrix.   In
addition, model uncertainties were likewise only first
guesses.   However, the system can be tuned with a computer to
provide extraordinary accuracies.   Currently, the system as
designed is accurate for determining highly accurate
perturbed angles of attack and sideslip from known trimmed
conditions.   The system should be expanded to incorporate

estimation of the aerodynamic angles throughout the flight regime and independent of trimmed conditions.

R-1 DIRECT FUTURE STUDY OF α AND β LINEAR RECURSIVE ESTIMATORS TO ELIMINATE THE REQUIREMENT FOR KNOWN TRIMMED FLIGHT.

Objective 2. Both angle of attack and sideslip algorithms could easily be validated by computer simulation. Indeed, the computer simulation used by Gleason and modified for this effort was of tremendous value. Given discrete A and B matrices, a full state simulation could be run simultaneously with a noise corrupted simulation of less than full state. The degree of noise could be adjusted as required to closely model the actual lateral and longitudinal systems. The ability of the modeled system to recover α and β was then successfully demonstrated. Again, this computer simulation was restricted to small perturbations about a trimmed condition. In addition, the solution was limited to only one flight condition without extensive modeling of 27 different parameters. This is a tremendous limitation to its use in the inflight case without extensive airborne computational power.

Objective 3. An inflight angle of attack estimator was successfully developed for use. It is of note that the self imposed requirement for minimum calulations, and hence maximum computational speed, did not restrict the accuracy of the estimator as tested. Another goal under this objective was also reached. All signals used in the inflight α estimator were from standard INS or onboard data sensors carried by almost all operations military aircraft. In other words, apart from the data telemetry systems, no special

- 81 -

flight test instrumentation was required for this estimator.
In addition, mechanical INS platforms were used, allowing
incorporation of this estimator in current generation
aircraft as the need arises. Accuracy of the system was
highly dependent on the modeling of the stability
derivatives. The three moments of inertia proved to be
secondary effects, not requiring extensive mathematical
models. However, C_{m_0} was a critical factor and was used
specifically to tune the system to YAPS boom angle of attack
at the beginning of flight test data evaluation. This step
in the test process points to an area of limitation. An
aircraft still must undergo some flight testing with a YAPS
boom prior to using an α estimator. The computer program
must be "calibrated" to the aircraft. at least in the initial
flight test stages, as the α estimator requires historical
data to model the lifting system. It is then obvious that
the most critical model must be the lift curve, with α as a
function of Mach number and altitude. The most significant
limitations of the estimator as formulated for this research
was the lack of high α modeling and the lack of a supersonic
capability. This limitation was based solely on regression
algorithms available to formulate this estimator version. A
more powerful regression tool would allow incorporation of
flight regimes that were not modeled by the current
estimator.

R-2   CONDUCT SENSITIVITY ANALYSIS OF C_{m_0} ON INFLIGHT α
ESTIMATOR RESULTS.

Objective 4.   The inflight α estimator was evaluated with
flight test data, and robustness examined during real-time
flight test. Several comments can be made as a result of
this test. The primary result is that the concept is indeed

feasable. With a basic multivariable, linear regression modeling technique, accurate angle of attack estimates can be made in all attitudes to approximately 0.5 degrees, as demonstrated by the robustness maneuvers. Two areas of interest need to be highlighted. Pitch acceleration was not available in the HIDEC configuration. If it were, it could be expected to be a noisy signal due to the algorithms used in its calculation. A difference of pitch rates per time interval was used to approximate $\dot{q}$. This proved to be a satisfactory approximation of the term, which was usually very close to 0.0. The overall correction term in the primary estimator equation was subsequently small when compared to the other terms, and could actually be neglected with only limited loss of accuracy. Secondly, the rotation of the normal acceleration from body to wind axes demonstrated the difference between theoretical equations and reality. The rotation equation itself was based of c.g. accelerations of a_{BZ} and a_{BX}. In straight and level unaccelerated flight in the wind axis system, these variables should be zero, whether the aircraft is upright or inverted. However, a real accelerometer which is trimmed to read 0 ft/sec^2 a_{BZ} in upright unaccelerated flight will read 64.4 ft/sec^2 in inverted unaccelerated flight. The result is that the correction term in the rotation equation, $\cos\theta\cos\phi$, which represents the component of the earth's gravity vector, as a correction to a perfect accelerometer, is taken into account by the real accelerometer. It can be replaced simply by the constant one g acceleration of gravity, as the rotational correction is automatically applied in the real accelerometer readings.

Objective 5. The robustness maneuver demonstrated that the

concept of a simple, efficient angle of attack estimator was achievable. The estimator was accurate to within the 0.5 degree desired specification with two exceptions. First, under sustained higher g loadings, the estimator accuracy was degraded proportional to the loading. This indicates that a g correction term needs to be modeled in the α regression. Under high g, the estimator was always high, and this is the more favorable of the possibilities. Use of the trim C_{L_α} curves could be the cause of this, and simple modeling under g of the wing-body C_{L_α} should suffice to correct the estimator back to predicted values.

R-3 DIRECT INFLIGHT α ESTIMATOR EXPERIMENTATION TO LOADED FLIGHT CONDTITION RESEARCH.

Finally, in the calculation of α_{GUESS} a known singularity in the Euler angle rotations was reached at 90 degrees pitch angle. This situation could easily be rectified by reverting to an earlier guess of α, and holding that guess between the 80 to 90 degree pitch angle phases of flight. A second solution would be a hold register, allowing the previous estimated α to become α_{GUESS} for the next time segment. This would eliminate the need for Euler angle rotations to find α_{GUESS} in the first place, and seems to be the better solution.

In conclusion, the area of angle of attack and sideslip estimation is an exciting, challenging arena, encompassing many disciplines of Aeronautical Engineering and Statistical Estimation. Its uses are bounded only by imagination, and its possibilities for incorporation into current aircraft are limited only by desire.

APPENDIX A

COMPUTER PROGRAM DKF

The program DKF uses the discretized A and B matrices
of the aircraft model to create a simulation of aircraft
response to control inputs. This response is ideal. Noise
inputs for the model and the measurement are added and a
Kalman estimator then utilizes the noise corrupted θ and q
values as simulated measurements to study the ability of a
linear estimator to recover the remaining two states. The
subroutine ALPHA then calculates the angle of attack from
the estimated values.

```fortran
$STORAGE:2
C******************DKF.FOR*****************************************
C*****   DISCRETE KALMAN FILTER PROGRAM                  ********
C*****   ANGLE OF ATTACK ESTIMATOR VERSION               ********
C*****       BY D.GLEASON   MODIFIED BY J.ZEIS           ********
C*****            6 AUG 86                                ********
C****************************************************************
C****************************************************************
C*****          X = A*XD + B*W        W \ N(0,Q)          ****
C*****          Z = H*X + V           V \ N(0,R)          ****
C*****                                                    ****
C*****          XM = A*XP                                 ****
C*****          PM = A*PP*AT + B*Q*BT                     ****
C*****                                                    ****
C*****          XP = XM + KG*[ Z - H*XM !                 ****
C*****                                                    ****
C*****          PP = [ I - KG*H !*PM                      ****
C*****          KG = PM*HT*[ H*PM*HT + R   !-1            ****
C****************************************************************
C****************************************************************
C
C
C***********INPUT/OUTPUT TAPES
C   TAPE 1 = MATRIX(INPUT MATRICES A,B,H,Q,R AND XP(O),PP(O))
C   TAPE 2 = RANW(INPUT PROCESS NOISE)
C   TAPE 5 = RANV(INPUT MEASUREMENT NOISE)
C   TAPE 7 = MEAS(OUTPUT OF KALMAN FILTER RESULTS)
C   TAPE 8 = SP(OUTPUT FOR PLOTTING STATE AND STATE EST.)
C   TAPE 9 = PP(OUTPUT FOR PLOTTING COVARIANCES AND GAINS)
C   TAPE 10=AP(OUTPUT FOR ALPHA,INPUT FOR USPLO)
C***********DECLARATION STATEMENTS
C****EXACT SYSTEM
      REAL X(4),XD(4)
      REAL Z(2),U(2,600)
      REAL AE(4,4),BE(4,2),HE(2,4)
      REAL WE(2,600),SIGMAW(2),QE(2,2)
      REAL VE(2,600),SIGMAV(2),RE(2,2)
      REAL RANGE(4)
C****MODEL SYSTEM
      REAL XM(4),XP(4)
```

```
      REAL A(4,4),B(4,2),H(2,4),Q(2,2),R(2,2)
      REAL AT(4,4),BT(2,4),HT(4,2)
      REAL PM(4,4),PP(4,4),KG(4,2)
      REAL WK1(4,4),WK2(4,4),WK3(4,4),WK4(4,4)
      REAL ALPA(600,2),TIM(600)
      CHARACTER TITLE*30
      INTEGER IFLAG(1),I,IY,N,M,INC,IOPT,IER
C************PROGRAM CONSTANTS
      IFLAG(1)=60
      ITEST = IFLAG(1) + 1
      IPRINT = 0
      DT=1./30.
      ERRX=0.

      ERRV=0.
C
C************INPUT DISCRETE A(NXN),B(NXM),H(LXN) MATRICES
C************INPUT PROCESS AND MEASUREMENT NOISE COVARIANCE
C************MATRICES Q(M,M),R(L,L)
C**INPUT INITIAL STATE ESTIMATE,XM(N),AND ERROR COV,PP(N,N).
      OPEN(1,FILE='MATRIX.IN')
      READ(1,*) N,M,L
      READ(1,*)
      READ(1,*) ((AE(I,J),J=1,N),I=1,N)
      READ(1,*)
      READ(1,*) ((A(I,J),J=1,N),I=1,N)
      READ(1,*)
      READ(1,*) ((BE(I,J),J=1,M),I=1,N)
      READ(1,*)
      READ(1,*) ((B(I,J),J=1,M),I=1,N)
      READ(1,*)
      READ(1,*) ((HE(I,J),J=1,N),I=1,L)
      READ(1,*)
      READ(1,*) ((H(I,J),J=1,N),I=1,L)
      READ(1,*)
      READ(1,*) ((QE(I,J),J=1,M),I=1,M)
      READ(1,*)
      READ(1,*) ((Q(I,J),J=1,M),I=1,M)
      READ(1,*)
      READ(1,*) ((RE(I,J),J=1,L),I=1,L)
      READ(1,*)
      READ(1,*) ((R(I,J),J=1,L),I=1,L)
      READ(1,*)
```

```
        READ(1,*) (XP(I),I=1,N)
        READ(1,*)
        READ(1,*) ((PP(I,J),J=1,N),I=1,N)
C
C************INPUT GAUSSIAN(0,1) PROCESS NOISE
        OPEN(2,FILE='RANW.IN')
        OPEN(7,FILE='MEAS.OUT')
        OPEN(8,FILE='SP.OUT')
        OPEN(9,FILE='PP.OUT')
        OPEN(10,FILE='AP.OUT')
        READ(2,*) NCYCLE
        WRITE(10,*) NCYCLE
        WRITE(9,*) NCYCLE
        WRITE(7,*) 'NCYCLE =',NCYCLE
        WRITE(7,*) 'INPUT PROCESS NOISE'
        READ (2,*) ((WE(I,J),I=1,M),J=1,NCYCLE)
        WRITE(7,105)((WE(I,J),J=1,10),I=1,M)
        WRITE(7,*)
C
C************INPUT GAUSSIAN(0,1) MEASUREMENT NOISE
        WRITE(7,*)  'INPUT MEASUREMENT NOISE'
        OPEN(5,FILE='RANV.IN')
        READ(5,*)
        READ (5,*) ((VE(I,J),I=1,L),J=1,NCYCLE)
        WRITE(7,105) ((VE(I,J),J=1,10),I=1,L) WRITE(7,*)
C
C
C************MODIFY PROCESS NOISE TO GAUSSIAN(0,SIGMAW)
C************MODIFY MEASUREMENT NOISE TO GAUSSIAN(0,SIGMAV)
        CALL NOISE(WE,VE,SIGMAW,SIGMAV,QE,RE,M,L,NCYCLE)
        WRITE(7,*) 'MODIFIED PROCESS NOISE'
        WRITE(7,105) ((WE(I,J),J=1,10),I=1,M)
        WRITE(7,*)
        WRITE(7,*) 'MODIFIED MEASUREMENT NOISE'
        WRITE(7,105) ((VE(I,J),J=1,10),I=1,L)
        WRITE(7,*)
C
C************GENERATE INPUT SEQUENCE U(I,K)

        DO 20 K=1,NCYCLE
        DO 20 I=1,M
          U(I,K)=0.
   20 CONTINUE
```

```
      DO 21 K=1,NCYCLE
         U(1,K)=0.0007
   21 CONTINUE
C*****************************************************
C***********OUTPUT DISCRETE A B AND H MATRICES
      WRITE(7,*) 'N = ',N,' M = ',M,' L = ',L
      CALL MPRINT(AE,N,N,'AE MATRIX          ')
      CALL MPRINT(A,N,N,'A MATRIX           ')
      CALL MPRINT(BE,N,M,'BE MATRIX          ')
      CALL MPRINT(B,N,M,'B MATRIX           ')
      CALL MPRINT(HE,L,N,'HE MATRIX          ')
      CALL MPRINT(H,L,N,'H MATRIX           ')
C
C***********OUTPUT MEASUREMENT AND NOISE COVARIANCE MATRICES
      CALL MPRINT(QE,M,M,'PROCESS COV.-QE    ')
      CALL MPRINT(Q,M,M,'PROCESS COV.-Q     ')
      CALL MPRINT(RE,L,L,'MEASUREMENT COV.-RE ')
      CALL MPRINT(R,L,L,'MEASUREMENT COV.-R  ')
C
C***********      SIMULATION      ***********************
C*******INITIALIZE STATE AND ESTIMATE VECTORS
      DO 50 I=1,N
         X(I)=0.
         XD(I)=0.
   50 CONTINUE
      DO 52 I=1,N
         XM(I)=0.
   52 CONTINUE
      DO 55 I=1,N
      DO 55 J=1,N
         PM(I,J)=0.
   55 CONTINUE
C***********OUTPUT INITIAL CONDITIONS ON X & PP
      WRITE(7,*) '*************************************************'
      WRITE(7,*) 'CYCLE = 0       TIME = 0'
      CALL VPRINT(XP,N,'INITIAL STATE EST-XP')
      CALL MPRINT(PP,N,N,'INITIAL COVAR EST-PP')
      WRITE(7,*) '*************************************************'
C***********MAIN LOOP ON K
      DO 1000 K=1,NCYCLE
      TIME = K*DT
C*******CALCULATE STATE VECTOR
      CALL STATE(K,X,XD,WE,U,AE,BE,N,M,NCYCLE)
```

```
C
C+++++++CALCULATE MEASUREMENT VECTOR
      CALL MEASURE (K,X,Z,HE,VE,N,L,NCYCLE)
C++++++++++++++++++++++++++++++++++++++++++++++++++++++++++++++++++++++++++
C
C++++CALCULATE PREDICTED ESTIMATE & PREDICTED ERROR COVARIANCE.
      CALL XPRED(K,XM,XP,A,B,U,N,M,NCYCLE)
      CALL COVARM(A,PP,AT,B,Q,BT,N,M,PM,WK1,WK2,WK3,WK4)
C
C++CALCULATE FILTER GAIN,FILTER ESTIMATE & FILTER ERROR COVARIANCE
      CALL KGAIN(PM,HT,H,R,N,L,KG,WK1,WK2,WK3,WK4)
      CALL XFILTER(XM,KG,Z,H,N,L,XP,WK1,WK2,WK3)
      CALL COVARP(KG,H,PM,N,L,PP,WK1,WK2,WK3)
      WRITE(9,105) TIME,PP(1,1),PP(1,2),PP(2,2)
      WRITE(9,105) KG(1,1),KG(2,1)
C
C++++++++UPDATE DELAY VECTOR XD(I)
      DO 120 I=1,N
      XD(I)=X(I)
  120 CONTINUE
C+++++++++++CALCULATE ANGLE OF ATTACKS+++++++++++++++++++++++++++
      CALL ALPHA(X,XM,XP,N,K,ALPA,TIM,TIME)
C++++++++PERFORM ERROR ANALYSIS
C   CALCULATE ERROR INDICES
      EV=(X(2)-XP(2))
      EX=(X(1)-XP(1))
      ERRX=ERRX + ABS(X(1)-XP(1))
      ERRV=ERRV + ABS(X(2)-XP(2))
C WRITE PLOT VECTORS TO TAPE
      WRITE(8,130)  TIME,X(2),XP(2),X(1),XP(1),EV,EX
  130 FORMAT(8F15.5)
C++++++++++++OUTPUT FILTER RESULTS
      IPRINT =IPRINT + 1
      IF (IPRINT .EQ. ITEST) IPRINT = 1
      IF (IPRINT .LT. IFLAG(1)) GO TO 1000
      WRITE(7,*) '++++++++++++++++++++++++++++++++++++++++++++++++++++'
      WRITE(7,*) 'CYCLE = ',K,'     TIME = ',TIME
      CALL VPRINT(X,N,'STATE VECTOR-X      ')
      CALL VPRINT(Z,L,'MEASUREMENT VECTOR-Z')
      WRITE(7,*) '===================================='
CX    CALL VPRINT(XM,N,'PREDICTED EST.-XM    ')
CX    CALL MPRINT(PM,N,N,'PREDICTED COV.-PM    ')
CX    WRITE(7,*) '===================================='
```

- 91 -

```
      CALL VPRINT(XP,N,'FILTER EST.-XP        ')
      CALL MPRINT(KG,N,L,'KALMAN GAIN MATRIX  ')
      CALL MPRINT(PP,N,N,'FILTER COV.-PP       ')
      WRITE(7,*) '**************************************************'
 1000 CONTINUEC********ANGLE OF ATTACK OUTPUT*************************
      WRITE(10,*) 'TIME                    EXACT ALPHA
     CPREDICTED ALPHA'
      DO 551 K=1,NCYCLE
      WRITE(10,549)TIM(K), ALPA(K,1),ALPA(K,2)
  549 FORMAT(2X,F6.3,16X,F12.10,20X,F12.10)
  551 CONTINUE
C  OUTPUT ERROR INDICES
      ERRX=ERRX/NCYCLE
      ERRV=ERRV/NCYCLE
      WRITE(7,*) 'AVERAGE POSITION ERROR = ',ERRX
      WRITE(7,*) 'AVERAGE VELOCITY ERROR = ',ERRV
C***********FORMAT STATEMENTS
  100 FORMAT(2(F15.5,2X))
  105 FORMAT(11(F10.5,2X))
      STOP
      END
C
CCCCCCCC1CCCCCCCC2CCCCCCCCC3CCCCCCCC4CCCCCCC5CCCCCCCC6CCCCCCCC7
C                    SUBROUTINE VPRINT
C  THIS SUBROUTINE PRINTS OUT A VECTOR WITH A TITLE
CCCCCCCCCCCCCCCCCCCCCCCCCCCCCCCCCCCCCCCCCCCCCCCCCCCCCCCCCCCCCC
      SUBROUTINE VPRINT(X,N,TITLE)
      REAL X(N)
      CHARACTER TITLE*30
      WRITE(7,200)TITLE
      WRITE(7,*) X
      WRITE(7,*)
  200 FORMAT(25X,A20)
      RETURN
      END
C
CCCCCCCC1CCCCCCCCCCCCCCCC3CCCCCCCCCC4CCCCCCCC5CCCCCCCC6CCCCCCCCC7
C                    SUBROUTINE MPRINT

C  THIS SUBROUTINE PRINTS OUT MATRIX A(MXN) WITH TITLE(20 CHAR)
CCCCCCCCCCCCCCCCCCCCCCCCCCCCCCCCCCCCCCCCCCCCCCCCCCCCCCCCCCCCCC
      SUBROUTINE MPRINT(A,M,N,TITLE)
      REAL A(M,N)
```

```
          CHARACTER TITLE*30
          WRITE(7,200)TITLE
          DO 20 I=1,M
              WRITE(7,300) (A(I,J),J=1,N)
     20 CONTINUE
          WRITE(7,*)
    200 FORMAT(25X,A20)
    300 FORMAT(8(2X,E9.3))
          RETURN
          END
C
CCCCCCCCC1 CCCCCCCCCCCCC3CCCCCCCCC4CCCCCCCCC5CCCCCCCCC6CCCCCCCC7
C                         SUBROUTINE MADD
C    THIS SUBROUTINE ADDS TWO MATRICES (A(MXN) + B(MXN) = C(MXN))
CCCCCCCCCCCCCCCCCCCCCCCCCCCCCCCCCCCCCCCCCCCCCCCCCCCCCCCCCCCCCCCCC
          SUBROUTINE MADD(A,B,C,M,N)       REAL A(M,N),B(M,N),C(M,N)
          DO 10 I=1,M
          DO 10 J=1,N
              C(I,J)=A(I,J) + B(I,J)
     10 CONTINUE
          RETURN
          END
C
C
CCCCCCCCC1 CCCCCCCCCCCCCCC3CCCCCCCCC4CCCCCCCCC5CCCCCCCCC6CCCCCCCC7
C                         SUBROUTINE MTRANS
C THIS PROGRAMS TAKES THE TRANSPOSE OF MATRIX A(MXN) AND RETURNS
C AT(NXM).
CCCCCCCCCCCCCCCCCCCCCCCCCCCCCCCCCCCCCCCCCCCCCCCCCCCCCCCCCCCCCCCC
          SUBROUTINE MTRANS(A,AT,M,N)
          REAL A(M,N),AT(N,M)
          DO 10 I=1,N
          DO 10 J=1,M
              AT(I,J)=A(J,I)
     10 CONTINUE
          RETURN
          END
C
CCCCCCCCC1 CCCCCCCCCCCCCCC3CCCCCCCCC4CCCCCCCCC5CCCCCCCCC6CCCCCCCC7
C                         SUBROUTINE MMULT
C THIS ROUTINE MULTIPLIES TWO MATRICES.(A(LXM) X B(MXN) = C(LXN)).
C
CCCCCCCCCCCCCCCCCCCCCCCCCCCCCCCCCCCCCCCCCCCCCCCCCCCCCCCCCCCCCCCC
```

```
      SUBROUTINE MMULT(A,B,C,L,M,N)
      REAL A(L,M),B(M,N),C(L,N)
      DO 10 I=1,L
      DO 10 J=1,N
      C(I,J)=0.
      DO 10 K=1,M
      C(I,J)=C(I,J)+ A(I,K)*B(K,J)
   10 CONTINUE
      END
C
CCCCCCC1CCCCCCCCC2CCCCCCCCC3CCCCCCCC4CCCCCCCC5CCCCCCCC6CCCCCCCC7
C                          SUBROUTINE NOISE
CTHIS SUBROUTINE CHANGES THE GAUSSIAN(0,1) PROCESS AND MEASUREMENT
CNOISE TO GAUSSIAN(0,SIGMAW),AND GAUSSIAN(0,SIGMAV) RESPECTIVELY.
CTHIS CHANGE IS BASED ON THE PROCESS AND MESUREMENT NOISE
CCOVARIANCE MATRICES.
CCCCCCCCCCCCCCCCCCCCCCCCCCCCCCCCCCCCCCCCCCCCCCCCCCCCCCCCCCCCCCCCC
      SUBROUTINE NOISE(W,V,SIGMAW,SIGMAV,Q,R,M,L,NCYCLE)
      REAL W(M,NCYCLE),SIGMAW(M),Q(M,M)
      REAL V(L,NCYCLE),SIGMAV(L),R(L,L)
C****CALCULATE NOISE STANDARD DEVIATION FOR PROCESS NOISE
      DO 10 I=1,M
         SIGMAW(I)=SQRT(Q(I,I))
   10 CONTINUE
C****CALCULATE NOISE STANDARD DEVIATION FOR MEASUREMENT NOISE
      DO 20 I=1,L
         SIGMAV(I)=SQRT(R(I,I))   20 CONTINUE
C****CREATE GAUSSIAN(0,SIGMAW) PROCESS NOISE
      DO 30 I=1,M
      DC 30 J=1,NCYCLE
         W(I,J)=W(I,J)*SIGMAW(I)
   30 CONTINUE
C****CREATE GAUSSIAN(0,SIGMAV) MEASUREMENT NOISE
      DO 40 I=1,L
      DO 40 J=1,NCYCLE
         V(I,J)=V(I,J)*SIGMAV(I)
   40 CONTINUE
      RETURN
      END
CCCCCCCCCC1CCCCCCCCC2CCCCCCCCC3CCCCCCCC4CCCCCCCC5CCCCCCCC6CCCCCCCC7
C                          SUBROUTINE STATE
C THIS SUBROUTINE CALCULATES THE TRUE STATE VECTOR AT TIME K
C                X(K)=AE*XD(K) + BE*U(K) + BE*V(K)
```

```
CCCCCCCCCCCCCCCCCCCCCCCCCCCCCCCCCCCCCCCCCCCCCCCCCCCCCCCCCCCCCCCC
      SUBROUTINE STATE(K,X,XD,W,U,AE,BE,N,M,NCYCLE)
      REAL X(N),XD(N),W(M,NCYCLE),U(M,NCYCLE)
      REAL AE(N,N),BE(N,M)
      DO 60 I=1,N
      X(I)=0.
      DO 60 J=1,N
      X(I)=X(I)+AE(I,J)*XD(J)
   60 CONTINUE
      DO 70 I=1,N
      DO 70 J=1,M
      X(I)=X(I)+BE(I,J)*W(J,K)+BE(I,J)*U(J,K)
   70 CONTINUE
      RETURN
      END
CCCCCCCCC1CCCCCCCCC2CCCCCCCCC3CCCCCCCC4CCCCCCCC5CCCCCCCC6CCCCCCC7
C                     SUBROUTINE MEASURE
C THIS SUBROUTINE CALCULATES THE TRUE SYSTEM MEASUREMENTS
C                 Z(K)=HE*X(K) + V(K)
CCCCCCCCCCCCCCCCCCCCCCCCCCCCCCCCCCCCCCCCCCCCCCCCCCCCCCCCCCCCCCCC
      SUBROUTINE MEASURE(K,X,Z,HE,V,N,L,NCYCLE)
      REAL X(N),Z(L),HE(L,N),V(L,NCYCLE)
      DO 80 I=1,L
      Z(I)=0.
      DO 80 J=1,N
      Z(I)=Z(I)+HE(I,J)*X(J)
   80 CONTINUE
      DO 90 I=1,L
      Z(I)=Z(I)+V(I,K)
   90 CONTINUE
      RETURN
      END
CCCCCCCCC1CCCCCCCCC2CCCCCCCCC3CCCCCCCC4CCCCCCCC5CCCCCCCC6CCCCCCC7
C                     SUBROUTINE XPREDICT
CTHIS SUBROUTINE PREDICTS THE STATE VECTOR PRIOR TO THE MEASUREMENT
C                 XM(K)=A*XP(K-1) + B*U
CCCCCCCCCCCCCCCCCCCCCCCCCCCCCCCCCCCCCCCCCCCCCCCCCCCCCCCCCCCCCCCC
      SUBROUTINE XPRED(K,XM,XP,A,B,U,N,M,NCYCLE)
      REAL XM(N),XP(N),A(N,N)
      DO 10 I=1,N
         XM(I)=0.
      DO 10 J=1,N
         XM(I)=XM(I) + A(I,J)*XP(J)
```

```fortran
   10 CONTINUE
      DO 20 I=1,N
      DO 20 J=1,M
      XM(I)=XM(I)+B(I,J)*U(J,K)
   20 CONTINUE
      RETURN
      END
C
C
CCCCCCCCCC1CCCCCCCCC2CCCCCCCCCCCCCCCCCCC4CCCCCCCCC5CCCCCCCCC6CCCCCCCCC7
C                      SUBROUTINE COVARM
CTHIS SUBROUTINE CALCULATES THE ERROR COVARIANCE MATRIX PRIOR TO
CTHE MEASUREMENT
C              PM(K)=A*PP(K-1)*AT + B*Q*BT
CCCCCCCCCCCCCCCCCCCCCCCCCCCCCCCCCCCCCCCCCCCCCCCCCCCCCCCCCCCCCCCCCCCCCC
      SUBROUTINE COVARM(A,PP,AT,B,Q,BT,N,M,PM,PP1,PP2,PP3,PP4)
      REAL A(N,N),PP(N,N),PM(N,N),B(N,M),Q(M,M)
      REAL AT(N,N),BT(M,N)
      REAL PP1(N,N),PP2(N,N),PP3(N,M),PP4(N,N)
C              PP1=A*PP(K-1)
C              PP2=A*PP(K-1)*AT=PP1*AT
C              PP3=B*Q
C              PP4=B*Q*BT=PP3*BT
      CALL MTRANS(A,AT,N,N)
      CALL MMULT(A,PP,PP1,N,N,N)
      CALL MMULT(PP1,AT,PP2,N,N,N)
      CALL MTRANS(B,BT,N,M)
      CALL MMULT(B,Q,PP3,N,M,M)
      CALL MMULT(PP3,BT,PP4,N,M,N)
      CALL MADD(PP2,PP4,PM,N,N)
      RETURN
      END
C
CCCCCC1CCCCCCCCC2CCCCCCCCCC3CCCCCCCCC4CCCCCCCCC5CCCCCCCCC6CCCCCCCCC7
C                SUBROUTINE KGAIN
C  THIS SUBROUTINE CALCULATES THE KALMAN GAIN.
C              KG(K)=PM*HT*[H*PM*HT + R]-1
CCCCCCCCCCCCCCCCCCCCCCCCCCCCCCCCCCCCCCCCCCCCCCCCCCCCCCCCCCCCCCCCCCCCCC
      SUBROUTINE KGAIN(PM,HT,H,R,N,L,KG,K1,K2,K3,K4)
      REAL PM(N,N),H(L,N),HT(N,L),KG(N,L),R(L,L)
      REAL K1(N,L),K2(L,L),K3(L,L),K4(L,L)
      REAL VK(130)
C              K1=PM*HT
```

```
C            K2=H*PM*HT=H*K1
C            K3=H*PM*HT+R=K2+R
C            K4=[H*PM*HT+R! INVERSE=K3   INVERSE
C            KG=P*HT*[H*PM*HT+R!INVERSE= K1*K4
      CALL MTRANS(H,HT,L,N)
      CALL MMULT(PM,HT,K1,N,N,L)
      CALL MMULT(H,K1,K2,L,N,L)
      CALL MADD(K2,R,K3,L,L)
      CALL GMINV(L,L,K3,K4,0,0,L)
      CALL MMULT(K1,K4,KG,N,L,L)
      RETURN
      END
C
CCCCCCC1CCCCCCCCC2CCCCCCCCC3CCCCCCCC4CCCCCCCC5CCCCCCCC6CCCCCCC7
C                 SUBROUTINE COVARP
C  THIS SUBROUTINE CALCULATES THE ERROR COVARIANCE AFTER THE
C MEASUREMENT HAS BEEN MADE.
C            PP(K)=[II-KG(K)*H!*PM
CCCCCCCCCCCCCCCCCCCCCCCCCCCCCCCCCCCCCCCCCCCCCCCCCCCCCCCCCCCCCC
      SUBROUTINE COVARP(KG,H,PM,N,L,PP,II,PP1,PP2)
      REAL KG(N,L),H(L,N),PM(N,N),PP(N,N)
      REAL II(N,N),PP1(N,N),PP2(N,N)
C            PP1= -KG*H
C            PP2=II-KG*H=II+PP1
C CREATE IDENTITY MATRIX II(NXN)
      DO 10 I=1,N
      DO 10 J=1,N
        II(I,J)=0.
        IF(I.EQ.J) II(I,J)=1.0
   10 CONTINUE
      CALL MMULT(KG,H,PP1,N,L,N)
C NEGATE PP1 MATRIX
      DO 20 I=1,N
      DO 20 J=1,N
        PP1(I,J)= -PP1(I,J)
   20 CONTINUE
      CALL MADD(II,PP1,PP2,N,N)
      CALL MMULT(PP2,PM,PP,N,N,N)
      RETURN
      END
C
CCCCCCC1CCCCCCCCC2CCCCCCCCC3CCCCCCCC4CCCCCCCC5CCCCCCCC6CCCCCCC7
C                 SUBROUTINE XFILTER
```

```fortran
C  THIS SUBROUTINE CALCULATES THE STATE VECTOR ESTIMATE AFTER
C  THE MEASUREMENT OCCURS.
C                    XP(K)=XM(K) + KG[Z-H*XM(K)!
CCCCCCCCCCCCCCCCCCCCCCCCCCCCCCCCCCCCCCCCCCCCCCCCCCCCCCCCCCCCCCCCC
       SUBROUTINE XFILTER(XM,KG,Z,H,N,L,XP,HXM,RZ,KGR)
       REAL XM(N),KG(N,L),Z(L),H(L,N),XP(N)
       REAL HXM(L,1),RZ(L,1),KGR(N,1)
C       HXM=H*XM
C       RZ=Z-H*XM=Z-HXM=RESIDUALS
C       KGR=KG*(Z-H*XM!=KG*R
       CALL MMULT(H,XM,HXM,L,N,1)
C NEGATE HXM
      DO 10 I=1,L
         HXM(I,1)=-HXM(I,1)
   10 CONTINUE
       CALL MADD(Z,HXM,RZ,L,1)
       CALL MMULT(KG,RZ,KGR,N,L,L)
       CALL MADD(XM,KGR,XP,N,1)
       RETURN         END
```

```fortran
*
*
*
*          SUBROUTINE ALPHA                          *
*      THIS ROUTINE CALCULATES THE EXACT,MEASURED AND    *
*      PREDICTED ANGLE OF ATTACK, AND STORES THE VALUES   *
*      IN ARRAYS.  VTRIM IS THE TRIM VELOCITY, AND ALFT   *
*      IS THE TRIM ANGLE OF ATTACK.                      *
```

```fortran
       SUBROUTINE ALPHA(X,XM,XP,N,K,ALPA,TIM,TIME)
       REAL X(N),XM(N),XP(N),TIM(600)
       REAL ALPA(600,2)
       VTRIM=570.0
       ALFT=.014
       UO=VTRIM*COS(ALFT)
       WO=VTRIM *SIN(ALFT)
       ARG1=(WO+X(2))/(UO+X(1))
       ARG3=(WO+XP(2))/(UO+XP(1))
C  ALPHA CALCULATION
       ALPA(K,1)=ATAN(ARG1)
C   ALPHA PREDICTED CALCULATION
       ALPA(K,2)=ATAN(ARG3)
       TIM(K)=TIME
       RETURN
```

- 98 -

```
        END
$INCLUDE:  'GMINV.FOR'
$INCLUDE:  'VADD.FOR'
$INCLUDE:  'DOT.FOR'
```

APPENDIX B

COMPUTER PROGRAM DKFLAT

SUBROUTINE BETA

The program DKFLAT is identical to DKF with the exception of the subroutine BETA instead of ALPHA as in DKF. Input and output is change to accomodate the different variables, but all logic is the same. BETA will calculate the modeled and predicted angle of sideslip from the lateral equations of motion as described in the program and text.

```
**************************************************************
*                                                            *
*                                                            *
*          SUBROUTINE BET                                    *
*     THIS ROUTINE FINDS ACTUAL AND                          *
*     PREDICTED ANGLE OF SIDESLIP AND STORES THE VALUES      *
*     IN ARRAYS.  VTRIM IS THE TRIM VELOCITY, AND ALFT       *
*     IS THE TRIM ANGLE OF ATTACK.                           *
**************************************************************
      SUBROUTINE    BET(X,XM,XP,N,K,BETA,TIM,TIME)
      REAL X(N),XM(N),XP(N),TIM(600)
      REAL BETA(600,2)
      VTRIM=570.0
      ALFT=.014
      UO=VTRIM*COS(ALFT)
      WO=VTRIM *SIN(ALFT)
      ARG1=X(1)/VTRIM
      ARG2=XP(1)/VTRIM
C  BETA  CALCULATION
      BETA(K,1)=ASIN(ARG1)
C     BETA  PREDICTED CALCULATION
      BETA(K,2)=ASIN(ARG2)
      TIM(K)=TIME
      RETURN
```

APPENDIX C

COMPUTER PROGRAM LONG

LONG

The program LONG provides an independent source to compute modeled angle of attack to verify DKF derived angle of attack. This program takes the continuous stability and control matrices and calculates through a Taylor series expansion the response of the system to step control inputs.

```
C*********************LONG.FOR(1000 DATA POINT VERSION)***********
C*************************(100 SECONDS MAX)***********************
C**************************************************************
C*******************AERONAUTICAL ENGINEERING PROGRAM***********
C***************BY: J.E. ZEIS  VERSION 5(9 APRIL 86)***********
C
C
C
C
C***************TIME RESPONSE OF AIRCRAFT (FORCED AND UNFORCED)*********
C                 IN THE LONGITUDINAL MODES
C*********************       ASSUMPTIONS      ***********************
C       1. BODY AXIS SYSTEM
C       2. FLIGHT PATH ANGLE IS SMALL
C       3. XWDOT=0.0
C       4. XQ=0.0
C**************************************************************
C
C****************DATA STORAGE INSTRUCTIONS*********************
C       1. DATA FOR DIFFERENT AIRCRAFT IS STORED IN SEPERATE FILES
C            i.e. F-4C.DAT OR A-4D.DAT
C       2. THIS PROGRAM USES PLANE.DAT AS ITS INPUT FILE.  COPY AN
C          AIRCRAFT FILE AS "PLANE.DAT".   THEIR FORMATS ARE EXACTLY
C          THE SAME.
C       3. THE OUTPUT FILE IS "LONG.PRN"  TO SEE THE OUTPUT ON
C          YOUR TERMINAL, "TYPE LONG.PRN".
C       4. TO CHANGE THE TIME OVER WHICH RESPONSE IS COMPUTED, JUST
C          CHANGE TIME IN FILE "PLANE.DAT".
C
C**************************************************************
C
C
10        REAL MU,MWDOT,MW,MQ,ME,MT
110       DIMENSION A(4,4),B(4,2),EAT(4,4),E(4,4),G(4,4),AINV(4,4)
111       DIMENSION P(4,4),PP(4,4),ASUB(4,4)
112       DIMENSION U(2005),W(2005),THET(2005),Q(2005),CON(4),
          CALPA(2005)
113       DIMENSION EATI(4,4)
20        DIMENSION EVR(4),EVI(4),VECR(4,4),VECI(4,4)
30        DIMENSION INDIC(4)
C*********************** DATA INPUT *************************
114       DATA TAU/0.0333333/
C****************** READ INPUT LOGIC ***********************
```

```
C****************************************************************
300       OPEN(2,FILE='PLANE.DAT')
310       READ(2,320)V,ALF,TJ,XU,XW,XE,XT
320       FORMAT(/,/,/,9X,F6.1,28X,F7.3,/,/,5X,F9.6,/,5X,F9.6,/,5X,
          CF7.4,/,10X,F7.4,/,10X,F9.6,/)
330       READ(2,340)ZQ,ZU,ZWDOT,ZW,ZE,ZT
340       FORMAT(5X,F7.3,/,5X,F7.4,/,9X,F9.6,/,5X,F7.4,/,10X,F7.2,/,
          C10X,F7.2,/)
350       READ(2,360)MU,MWDOT,MW,MQ,ME,MT
360       FORMAT(5X,F9.6,/,9X,F9.6,/,5X,F9.6,/ 5X,F5.2,/,10X,F7.2,/,
          C10X,F9.6,/)
370       READ(2,380)U(1),W(1),THET(1),Q(1),ELEV,THROT,TI
380     FORMAT(/,/,5X,F7.2,/,5X,F7.2,/,9X,F7.3,/,5X,F7.3,/,/,/,6X,
          CF7.4,/,6X,F7.1,/,/,33X,F5.1)
C*************************INITAL VELOCITY AND TIME ***************
400       WO=V*SIN(ALF)
410       UO=V*COS(ALF)
420       IT=TI*30+1
500       A(1,1)=XU
510       A(1,2)=XW
520       A(1,3)=-32.194
530       A(1,4)=-WO
540       A(2,1)=ZU/(1.0-ZWDOT)
550       A(2,2)=ZW/(1.0-ZWDOT)
560       A(2,3)=0.0
570       A(2,4)=(V+ZQ)/(1.0-ZWDOT)
580       A(3,1)=0.0
590       A(3,2)=0.0
600       A(3,3)=0.0
610       A(3,4)=1.0
620       A(4,1)=ZU*MWDOT/(1.0-ZWDOT) + MU
630       A(4,2)=ZW*MWDOT/(1.0-ZWDOT) + MW
640       A(4,3)=0.0
650       A(4,4)=(V+ZQ)*MWDOT/(1.0-ZWDOT) + MQ
C*******************B-MATRIX CALCULATIONS************************
660       B(1,1)=XE
670       B(1,2)=XT
680       B(2,1)=ZE/(1.0-ZWDOT)
690       B(2,2)=ZT/(1.0-ZWDOT)
700       B(3,1)=0.0
710       B(3,2)=0.0
720       B(4,1)=ZE*MWDOT/(1.0-ZWDOT) +ME
730       B(4,2)=ZT*MWDOT/(1.0-ZWDOT) +MT
```

```
C*****************IDENTITY MATRIX INPUT*************************
450      DATA E/1.,.0,.0,.0,.0,1.,.0,.0,.0,.0,1.,.0,.0,.0,.0,1./
C*****************OPEN OUTPUT FILE LONG.PRN********************
100      OPEN(4,FILE='LONG.PRN')
C*****************SERIES EXPANSION FOR UNFORCED RESPONSE********
C*****************EXP(AT)=I+AT+1/2(ASQ)(TSQ)+... ***************
1000     DO 1040 I=1,4
1010     DO 1030 J=1,4
1020     G(I,J)=A(I,1)*A(1,J)+A(I,2)*A(2,J)+A(I,3)*A(3,J)+A(I,4)*
         CA(4,J)
1030     CONTINUE
1031     J=1
1040     CONTINUE
1050     DO 1110 I=1,4
1060     DO 1100 J=1,4
1070     EAT(I,J)=E(I,J)+TAU*A(I,J)+.5*TAU*TAU*G(I,J)
1100     CONTINUE
1101     J=1
1110     CONTINUE
C*********************CALCULATION OF "A INVERSE"***************
3000     NR=4
3010     NC=4
3020     MT=0
3030     MR=0
3040     NCOL=43045    DO 3049 I=1,4
3046     DO 3049 J=1,4
3047     ASUB(I,J)=A(I,J)
3049     CONTINUE
3050     CALL GMINV(NR,NC,ASUB,AINV,MR,MT,NCOL)
C*********************CALCULATION OF "EAT - I"*****************
3200     EATI(1,1)=EAT(1,1)-1.0
3210     EATI(1,2)=EAT(1,2)
3220     EATI(1,3)=EAT(1,3)
3230     EATI(1,4)=EAT(1,4)
3240     EATI(2,1)=EAT(2,1)
3250     EATI(2,2)=EAT(2,2)-1.0
3260     EATI(2,3)=EAT(2,3)
3270     EATI(2,4)=EAT(2,4)
3280     EATI(3,1)=EAT(3,1)
3290     EATI(3,2)=EAT(3,2)
3300     EATI(3,3)=EAT(3,3)-1.0
3310     EATI(3,4)=EAT(3,4)
3320     EATI(4,1)=EAT(4,1)
```

```
3330      EATI(4,2)=EAT(4,2)
3340      EATI(4,3)=EAT(4,3)
3350      EATI(4,4)=EAT(4,4)-1.0
C*********************MULTIPLY AINV TIMES EATI*************************
3400      DO 3450 I=1,4
3410      DO 3440 J=1,4
3420      P(I,J)=AINV(I,1)*EATI(1,J)+AINV(I,2)*EATI(2,J)+AINV(I,3)
     C*EATI(3,J)+AINV(I,4)*EATI(4,J)
3440      CONTINUE
3441      J=1
3450      CONTINUE
C*********************MULTIPLY P TIMES B MATRIX***********************
3510      DO 3600 I=1,4
3520      DO 3590 J=1,2
3530      PP(I,J)=P(I,1)*B(1,J)+P(I,2)*B(2,J)+P(I,3)*B(3,J)+P(I,4)*
     CB(4,J)
3590      CONTINUE
3591      J=1
3600      CONTINUE
C*****************FINAL MULTIPLICATION FOR AINV*(EAT - I)*B*U(T)***
4000      CON(1)=PP(1,1)*ELEV+PP(1,2)*THROT
4010      CON(2)=PP(2,1)*ELEV+PP(2,2)*THROT
4020      CON(3)=PP(3,1)*ELEV+PP(3,2)*THROT
4030      CON(4)=PP(4,1)*ELEV+PP(4,2)*THROT
C*********************STATIC OUTPUT*********************************
8000      WRITE(4,8010)
8010      FORMAT(5X,'FORCED AIRCRAFT RESPONSE TO ELEVATOR/THROTTLE
     C INPUT')
8020      WRITE(4,8030)
8030      FORMAT(/,8X,'INITIAL CONDITIONS ARE AS FOLLOWS:')
8040      WRITE(4,8050)U(1),W(1),THET(1),Q(1)
8050      FORMAT(4X,'DELTA U=',F8.3,/,4X,'DELTA W=',F8.3,/,4X,'THETA=',
     CF8.4,/,4X,'Q=',F8.4)
8051      WRITE(4,8052)ELEV,THROT
8052      FORMAT(/,'ELEVATOR INPUT IS:',F6.3,4X,'THROTTLE CHANGE:',
     C F6.1)
8060      WRITE(4,8070)
8070      FORMAT(/,6X,'STATE-SPACE SYSTEM OF THE FORM X(DOT)=AX + BU')
8080      WRITE(4,8090)8090    FORMAT(/,23X,'"A" MATRIX')
8100      DO 8130 I=1,4
8110      WRITE(4,8120)A(I,1),A(I,2),A(I,3),A(I,4)
8120      FORMAT(3X,F10.6,4X,F10.6,4X,F10.6,4X,F12.6)
8130      CONTINUE
```

```
8140      WRITE(4,8150)
8150      FORMAT(/,23X,'"A INVERSE" MATRIX')
8160      DO 8190 I=1,4
8170      WRITE(4,8180)AINV(I,1),AINV(I,2),AINV(I,3),AINV(I,4)
8180      FORMAT(3X,F10.6,4X,F10.6,4X,F15.3,4X,F10.6)
8190      CONTINUE
8200      WRITE(4,8210)
8210      FORMAT(/,16X,'"B" MATRIX')
8220      DO 8250 I=1,4
8230      WRITE(4,8240)B(I,1),B(I,2)
8240      FORMAT(3X,F10.6,4X,F10.6)
8250      CONTINUE
C************************EIGENVALUE AND EIGENVECTOR CALL************************
8500      N=4
8510      NM=4
8520      CALL EIGEN(N,NM,A,EVR,EVI,VECR,VECI,INDIC)
8530      WRITE(4,8540)
8540      FORMAT(/,/,8X,'EIGEN ANALYSIS')
8550      WRITE(4,8560)
8560      FORMAT(/,10X,'EIGENVALUES')
8570      DO 8600 I=1,4
8580      WRITE(4,8590)EVR(I),EVI(I)
8590      FORMAT(5X,E13.6,2X,'+',E13.6,'i')
8600      CONTINUE
8610      WRITE(4,8620)
8620      FORMAT(/,10X,'EIGENVECTORS')
8630      DO 8700 I=1,4
8640      WRITE(4,8641)I
8641      FORMAT(/,5X,'VECTOR #',I3)
8642      DO 8699 J=1,4
8643      WRITE(4,8644)VECR(J,I),VECI(J,I)
8644      FORMAT(2X,E11.4,1X,'+',E11.4,'i')
8699      CONTINUE
8700      CONTINUE
C************************FREQENCY AND DAMPING RATIO************************
8710      OMEG1=SQRT(EVR(1)**2 + EVI(1)**2)
8720      OMEG2=SQRT(EVR(3)**2 + EVI(3)**2)
8730      IF (OMEG1 .LT.OMEG2) GOTO 8800
8740      OMEGP=OMEG2
8750      DAMPP=ABS(EVR(3)/OMEGP)
8760      OMEGS=OMEG1
8770      DAMPS=ABS(EVR(1)/OMEGS)
8780      GOTO 8850
```

```
8800      OMEGP=OMEG1
8810      DAMPP=ABS(EVR(1)/OMEGP)
8820      OMEGS=OMEG2
8830      DAMPS=ABS(EVR(3)/OMEGS)
8850      WRITE(4,8860)OMEGS,DAMPS
8860      FORMAT(/,5X,'OMEGA(SHORT PERIOD)=',E11.4,4X,
      C'SHORT PERIOD DAMPING =',E11.4)
8870      WRITE(4,8880)OMEGP,DAMPP
8880      FORMAT(5X,'OMEGA(PHUGOID)=',E11.4,4X,'PHUGOID DAMPING =',
      CE11.4,/)
C*********************OUTPUT HEADER*********************
9000      WRITE(4,9010)
9010      FORMAT(/,8X,'AIRCRAFT RESPONSE (STABILITY AXIS SYSTEM)')
9020      WRITE(4,9030)
9030      FORMAT(5X,'T',7X,'U',11X,'W',8X,'THETA',8X,'Q',8X,'ALPHA')
C*********************UNFORCED TIME RESPONSE*********************
1500      N=1
1510      T=N*TAU
1520      M=N+1
C*********************X(N+1)=EXP(AT)*X(N)*********************
2000      U(M)=EAT(1,1)*U(N)+EAT(1,2)*W(N)+EAT(1,3)*THET(N)+
      C EAT(1,4)*Q(N)
2010      W(M)=EAT(2,1)*U(N)+EAT(2,2)*W(N)+EAT(2,3)*THET(N)+
      C EAT(2,4)*Q(N)
2020      Q(M)=EAT(4,1)*U(N)+EAT(4,2)*W(N)+EAT(4,3)*THET(N)+
      C EAT(4,4)*Q(N)
2030      THET(M)=EAT(3,1)*U(N)+EAT(3,2)*W(N)+EAT(3,3)*THET(N)+
      C EAT(3,4)*Q(N)
2100      CONTINUE
C*********************FORCED TIME RESPONSE*********************
C*********************X(N+1)=X(N+1) + CONTROL VALUE*********************
2200      U(M)=U(M)+CON(1)
2210      W(M)=W(M)+CON(2)
2220      THET(M)=THET(M)+CON(3)
2230      Q(M)=Q(M)+CON(4)
2240      ARG=(WO+W(M))/(UO+U(M))
2250      ALPA(M)=ATAN(ARG)
C*********************INCREMENTAL TIME RESPONSE OUTPUT*********************
9050      WRITE(4,9060) T,U(M),W(M),THET(M),Q(M),ALPA(M)
9060      FORMAT(2X,F5.2,4X,F8.3,3X,F7.3,3X,F7.4,4X,F6.4,4X,F7.5)
9070      N=N+1
9080      IF (N.LT.IT) GOTO 1510
9090      CONTINUE
```

```
9100      END
$INCLUDE:  'EIGEN.FOR'
$INCLUDE:  'GMINV.FOR'
$INCLUDE:  'VADD.FOR'
$INCLUDE:  'DOT.FOR'
```

APPENDIX D

COMPUTER PROGRAM LAT

LAT

LAT is the lateral response equivalent of the program LONG. Again, the continuous stability and control matrices are input, along with the prscribed step control input to find the modeled response of the aircraft in the lateral modes. This is used to verify the operation of the lateral estimator program, DKFLAT.

```
C*********************LAT.FOR(1000 DATA POINT VERSION)****************
C***********************(100 SECONDS)********************************
C******************************************************************
C*******************AERONAUTICAL ENGINEERING PROGR. ***************
C*****************BY: J.E. ZEIS   VERSION 1(8 APRIL 86)************
C
C
C
C***************TIME RESPONSE OF AIRCRAFT (FORCED AND UNFORCED)*****
C                  IN THE LATERAL MODES
C******************************************************************
C******************            ASSUMPTIONS        ****************
C      1. BODY AXIS SYSTEM
C      2. ASSUME SMALL FLIGHT PATH ANGLE.
C      3. ASSUME YAW RATE IS SMALL.
C      4. Y(V DOT)=L'(V DOT)=N'(V DOT)=0
C******************************************************************
C
C****************DATA STORAGE INSTRUCTIONS************************
C      1. DATA FOR DIFFERENT AIRCRAFT IS STORED IN SEPERATE FILES
C            i.e. F-4C.LAT OR A-4D.LAT
C      2. THIS PROGRAM USES PLANE.DAT AS ITS INPUT FILE.  COPY AN
C         AIRCRAFT FILE AS "PLANE.DAT".  THEIR FORMATS ARE EXACTLY
C         THE SAME.
C      3. THE OUTPUT FILE IS "LATERAL.PRN"  TO SEE THE OUTPUT ON
C         YOUR TERMINAL, "TYPE LATERAL.PRN".
C      4. TO CHANGE THE TIME OVER WHICH RESPONSE IS COMPUTED, JUST
C         CHANGE THE TIME IN THE LAST LINE OF THE INPUT PROGRAM
C         PLANE.DAT.
C******************************************************************
C
C
10       REAL LB,LR,LP,LVDOT,LA,LRD,NB,NVDOT,NP,NR,NA,NRD
110      DIMENSION A(4,4),B(4,2),EAT(4,4),E(4,4),G(4,4),AINV(4,4)
111      DIMENSION PPP(4,4),PP(4,4)
112      DIMENSION V(2005),P(2005),PHI(2005),R(2005),CON(4),
         CBETA(2005)
113      DIMENSION EATI(4,4),ASUB(4,4)
20       DIMENSION EVR(4),EVI(4),VECR(4,4),VECI(4,4)
30       DIMENSION INDIC(4)
C*********************** DATA INPUT *******************************
114      DATA TAU/0.033333/
C******************** READ INPUT LOGIC ***************************
```

```
C***************************************************************
300       OPEN(2,FILE='PLANE.DAT')
310       READ(2,320)VEL,ALF,YP,YB,YR,YA,YRD
320       FORMAT(/,/,/,9X,F6.1,28X,F7.3,/,/,40X,F9.6,/,40X,F9.4,/,40X,
      CF7.4,/,15X,F7.4,/,45X,F9.6,/)
330       READ(2,340)LR,LP,LVDOT,LB,LA,LRD
340       FORMAT(41X,F7.3,/,41X,F7.4,/,45X,F9.6,/,41X,F7.2,/,46X,
      CF7.2,/,46X,F7.2,/)
350       READ(2,360)NB,NVDOT,NP,NR,NA,NRD
360       FORMAT(41X,F9.6,/,45X,F9.6,/,41X,F9.6,/,41X,F5.2,/,46X,
      CF7.2,/,46X,F9.6,/)
370       READ(2,380)V(1),P(1),PHI(1),R(1),AIL,RUD,TI
380       FORMAT(/,/,40X,F7.2,/,40X,F7.2,/,42X,F7.3,/,40X,F7.3,/,/,
      C/,41X,F7.4,/,41X,F7.4,/,/,33X,F5.1)
C***********************INITIAL VELOCITY AND TIME***************
400       WO=VEL*SIN(ALF)
410       UO=VEL*COS(ALF)
420       IT=TI*30+1
C***********************A-MATRIX CALCULATIONS*******************
500       A(1,1)=YB/UO
510       A(1,2)=WO
520       A(1,3)=-32.194
530       A(1,4)=-UO
540       A(2,1)=LB/UO
550       A(2,2)=LP
560       A(2,3)=0.0
570       A(2,4)=LR
580       A(3,1)=0.0
590       A(3,2)=1.0
600       A(3,3)=0.0
610       A(3,4)=0.0
620       A(4,1)=NB/UO
630       A(4,2)=NP
640       A(4,3)=0.0
650       A(4,4)=NR
C***********************B-MATRIX CALCULATIONS*******************
660       B(1,1)=YA
670       B(1,2)=YRD
680       B(2,1)=LA
690       B(2,2)=LRD
700       B(3,1)=0.0
710       B(3,2)=0.0
720       B(4,1)=NA
```

```
730        B(4,2)=NRD
C*******************IDENTITY MATRIX INPUT**********************************
450        DATA E/1.,.0,.0,.0,.0,1.,.0,.0,.0,.0,1.,.0,.0,.0,.0,1./
C*******************OPEN OUTPUT FILE RESPOND.OUT**************************
100        OPEN(4,FILE='LATERAL.PRN')
C*******************SERIES EXPANSION FOR UNFORCED RESPONSE***************
C*******************EXP(AT)=I+AT+1/2(ASQ)(TSQ)+... ***********************
1000       DO 1040 I=1,4
1010       DO 1030 J=1,4
1020       G(I,J)=A(I,1)*A(1,J)+A(I,2)*A(2,J)+A(I,3)*A(3,J)+A(I,4)*
           CA(4,J)
1030       CONTINUE
1031       J=1
1040       CONTINUE
1050       DO 1110 I=1,4
1060       DO 1100 J=1,4
1070       EAT(I,J)=E(I,J)+TAU*A(I,J)+.5*TAU*TAU*G(I,J)
1100       CONTINUE
1101       J=1
1110       CONTINUE
C**** ********************CALCULATION OF "A INVERSE"*********************
3000       NRW=4
3010       NC=4
3020       MR=0
3030       MT=0
3040       NCOL=43045    DO 3049 I=1,4
3046       DO 3049 J=1,4
3047       ASUB(I,J)=A(I,J)
3049       CONTINUE
3050       CALL GMINV(NRW,NC,ASUB,AINV,MR,MT,NCOL)
C*******************CALCULATION OF "EAT - I"***************************
3200       EATI(1,1)=EAT(1,1)-1.0
3210       EATI(1,2)=EAT(1,2)
3220       EATI(1,3)=EAT(1,3)
3230       EATI(1,4)=EAT(1,4)
3240       EATI(2,1)=EAT(2,1)
3250       EATI(2,2)=EAT(2,2)-1.0
3260       EATI(2,3)=EAT(2,3)
3270       EATI(2,4)=EAT(2,4)
3280       EATI(3,1)=EAT(3,1)
3290       EATI(3,2)=EAT(3,2)
3300       EATI(3,3)=EAT(3,3)-1.0
3310       EATI(3,4)=EAT(3,4)
```

- 116 -

```
3320      EATI(4,1)=EAT(4,1)
3330      EATI(4,2)=EAT(4,2)
3340      EATI(4,3)=EAT(4,3)
3350      EATI(4,4)=EAT(4,4)-1.0
C********************MULTIPLY AINV TIMES EATI***********************
3400      DO 3450 I=1,4
3410      DO 3440 J=1,4
3420      PPP(I,J)=AINV(I,1)*EATI(1,J)+AINV(I,2)*EATI(2,J)+AINV(I,3)
     C*EATI(3,J)+AINV(I,4)*EATI(4,J)
3440      CONTINUE
3441      J=1
3450      CONTINUE
C********************MULTIPLY PPP TIMES B MATRIX*******************
3510      DO 3600 I=1,4
3520      DO 3590 J=1,2
3530      PP(I,J)=PPP(I,1)*B(1,J)+PPP(I,2)*B(2,J)+PPP(I,3)*B(3,J)
     C+PPP(I,4)*B(4,J)
3590      CONTINUE
3591      J=1
3600      CONTINUE
C******************FINAL MULTIPLICATION FOR AINV*(EAT - I)*B*U(T)***
4000      CON(1)=PP(1,1)*AIL+PP(1,2)*RUD
4010      CON(2)=PP(2,1)*AIL+PP(2,2)*RUD
4020      CON(3)=PP(3,1)*AIL+PP(3,2)*RUD
4030      CON(4)=PP(4,1)*AIL+PP(4,2)*RUD
C************************STATIC OUTPUT****************************
8000      WRITE(4,8010)
8010      FORMAT(5X,'FORCED AIRCRAFT RESPONSE TO AILERON/RUDDER
     C INPUT')
8020      WRITE(4,8030)
8030      FORMAT(/,8X,'INITIAL CONDITIONS ARE AS FOLLOWS:')
8040      WRITE(4,3050)V(1),P(1),PHI(1),R(1)
8050      FORMAT(4X,'DELTA V=',F8.3,/,4X,'DELTA P=',F8.3,/,4X,'PHI=',
     CF8.4,/,4X,'R=',F8.4)
8051      WRITE(4,8052)AIL,RUD
8052      FORMAT(/,'AILERON  INPUT IS:',F6.3,4X,'RUDDER INPUT IS:',
     CF6.3)
8060      WRITE(4,8070)
8070      FORMAT(/,6X,'STATE-SPACE SYSTEM OF THE FORM X(DOT)=AX + BU')
8080      WRITE(4,8090)
8090      FORMAT(/,23X,'"A" MATRIX')
8100      DO 8130 I=1,4
8110      WRITE(4,8120)A(I,1),A(I,2),A(I,3),A(I,4)
```

```
8120      FORMAT(3X,F10.6,4X,F10.6,4X,F10.6,4X,F12.6)
8130      CONTINUE
8140      WRITE(4,8150)
8150      FORMAT(/,23X,'"A INVERSE" MATRIX')
8160      DO 8190 I=1,4
8170      WRITE(4,8180)AINV(I,1),AINV(I,2),AINV(I,3),AINV(I,4)
8180      FORMAT(3X,F14.6,4X,F14.6,4X,F15.3,4X,F14.6)
8190      CONTINUE
8200      WRITE(4,8210)
8210      FORMAT(/,16X,'"B" MATRIX')
8220      DO 8250 I=1,4
8230      WRITE(4,8240)B(I,1),B(I,2)
8240      FORMAT(3X,F10.6,4X,F10.6)
8250      CONTINUE
C**********************OUTPUT HEADER*****************************
9000      WRITE(4,9010)
9010      FORMAT(/,8X,'AIRCRAFT RESPONSE (BODY AXIS SYSTEM)')
9020      WRITE(4,9030)
9030      FORMAT(5X,'T',7X,'V',11X,'P',8X,'PHI  ',8X,'R',8X,'BETA')
C**********************UNFORCED TIME RESPONSE*******************
1500      N=1
1510      T=N*TAU
1520      M=N+1
C**********************X(N+1)=EXP(AT)*X(N)**********************
2000      V(M)=EAT(1,1)*V(N)+EAT(1,2)*P(N)+EAT(1,3)*PHI(N)+EAT(1,4)
          C*R(N)
2010      P(M)=EAT(2,1)*V(N)+EAT(2,2)*P(N)+EAT(2,3)*PHI(N)+EAT(2,4)
          C*R(N)
2020      R(M)=EAT(4,1)*V(N)+EAT(4,2)*P(N)+EAT(4,3)*PHI(N)+EAT(4,4)
          C*R(N)
2030      PHI(M)=EAT(3,1)*V(N)+EAT(3,2)*P(N)+EAT(3,3)*PHI(N)+EAT(3,4)
          A*R(N)
2100      CONTINUE
C**********************FORCED TIME RESPONSE*********************
C**********************X(N+1)=X(N+1) + CONTROL VALUE***********
2200      V(M)=V(M)+CON(1)
2210      P(M)=P(M)+CON(2)
2220      PHI(M)=PHI(M)+CON(3)
2222      ARG=V(M)/VEL
2225      BETA(M)=ASIN(ARG)
2230      R(M)=R(M)+CON(4)
C**********************INCREMENTAL TIME RESPONSE OUTPUT*********
9050      WRITE(4,9060) T,V(M),P(M),PHI(M),R(M),BETA(M)
```

```
9060      FORMAT(2X,F5.2,4X,F8.3,3X,F7.3,3X,F7.4,4X,F6.3,4X,F7.5)
9070      N=N+1
9080      IF (N.LT.IT) GOTO 1510
9090      CONTINUE
9100      END
$INCLUDE: 'GMINV.FOR'
$INCLUDE: 'VADD.FOR'
$INCLUDE: 'DOT.FOR'
```

APPENDIX E

F-15A AIRCRAFT DESCRIPTION

F-15A AIRCRAFT DESCRIPTION

The following data and diagram were extracted from AFFTC TR-76-48 [18].
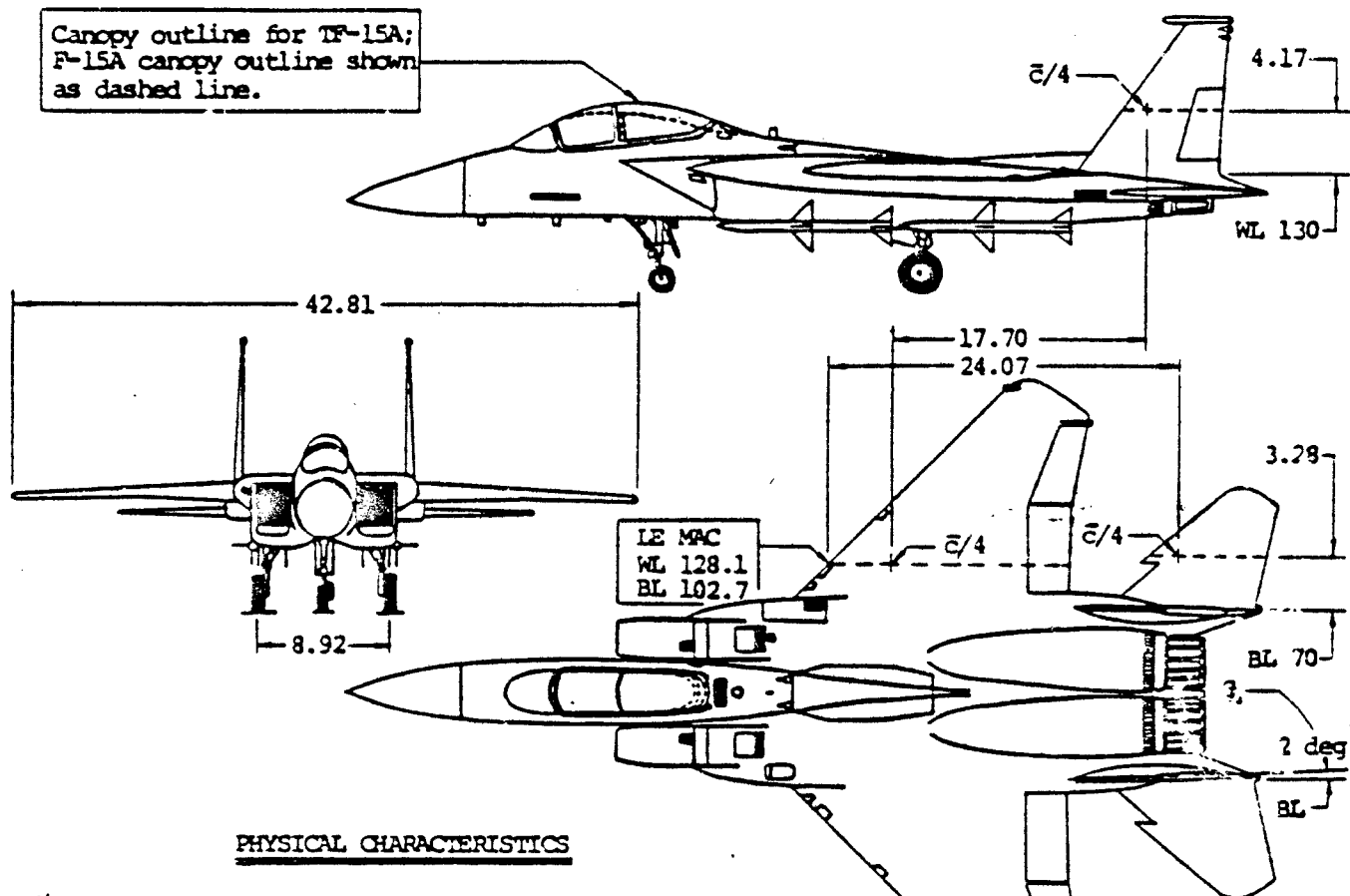
PHYSICAL CHARACTERISTICS

Wings:
    Theoretical Area _____ 608.0 sq ft
    Mean Aerodynamic Chord (MAC) _____ 15.94 ft
    Span _____ 42.81 ft

Horizontal Stabilators:
    Area (Total) _____ 111.36 sq ft
    MAC _____ 8.28 ft
    Span _____ 28.25 ft

Vertical Tails (Each):
    Area _____ 62.61 sq ft
    MAC _____ 6.75 ft
    Span (Exposed) _____ 10.32 ft

CONTROL SURFACE AREAS

Flaps (Total) _____ 35.84 sq ft
Ailerons (Total) ____ 26.48 sq ft
Rudders (Total) _____ 19.94 sq ft
Speedbrake _____ 31.50 sq ft

Figure E1.   F-15 General Aircraft Layout

F-15A Aircraft Data

Aircraft

Length	62.52 Ft
Height	18.63 Ft
Wetted Area	2668.8 Ft
Takeoff Gross Weight	39,770 Lbs
Internal Fuel Capacity	11,138 Lbs

Wing

Reference Area	608 Ft^2
Span	42.81 Ft
Aspect Ratio	3.0
Taper Ratio	0.25
Incidence	0 Deg
Leading Edge Sweep	45 Deg
Mean Aerodynamic Chord	15.94 Ft
Theoretical Root Chord	22.77 Ft

Horizontal Stabilators

Area	120 Ft
Span	28.25 Ft
Deflection Limits	+15 to -29 Deg
Mean Aerodynamic Chord	8.27 Ft
Root Chord	11.43 Ft
Tail Length $(.25\ \bar{c}_w$ to $.25\ \bar{c}_T)$	20.08 Ft

Vertical Stabilizers

Area	125.22 Ft
Span	10.32 Ft
Mean Aerodynamic Chord	6.75 Ft
Root Chord	9.58 Ft
Tail Length (.25 $\bar{c}_v$ to .25 $\bar{c}_v$	17.69 Ft

APPENDIX F

KEY INS/AIR DATA OUTPUTS

KEY INS/AIR DATA OUTPUTS

INERTIAL MEASURING UNIT
CN-1376/ASN-109

IMU EQUIPMENT RACK
MT-4390/ASN-109
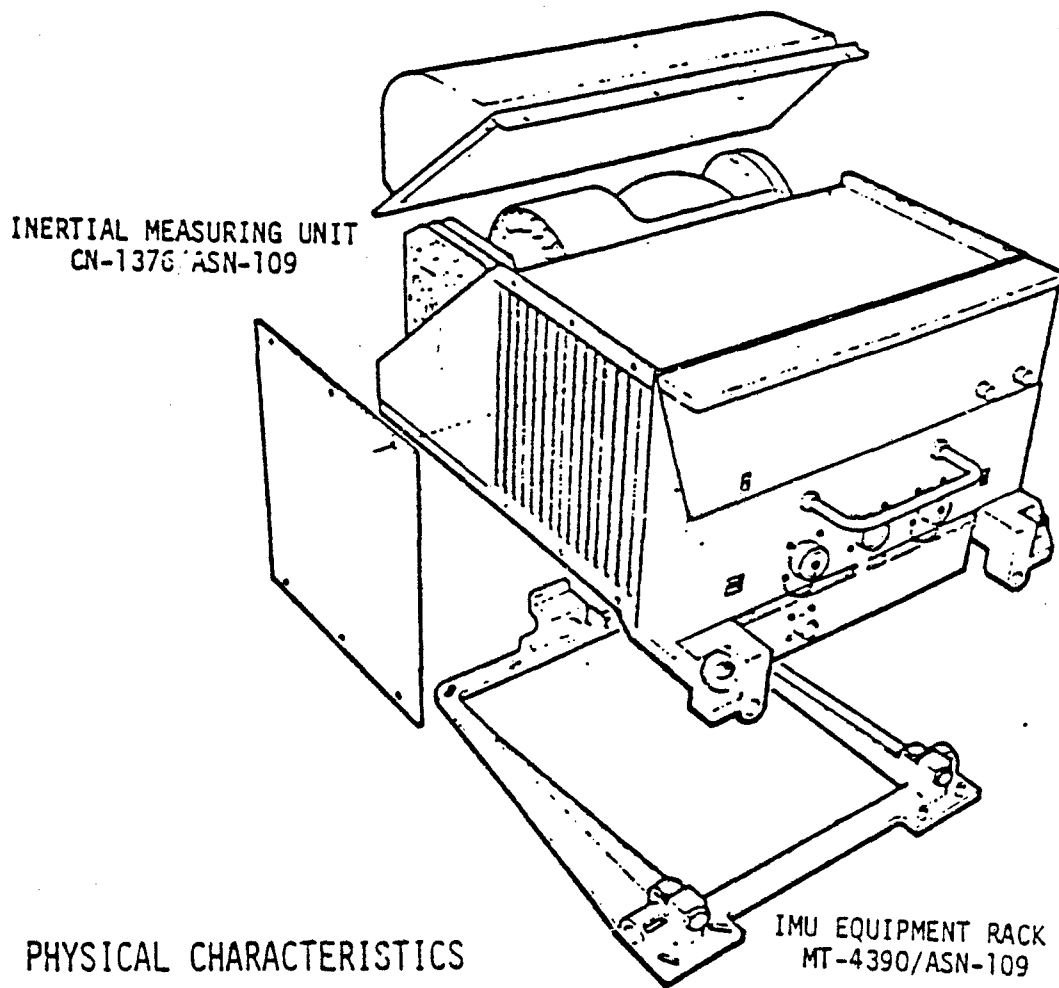
PHYSICAL CHARACTERISTICS

- Weight - 36.5 pounds.

- Volume - 1658 cubic inches.

- Power Required - 115v, 3 phase, 400 Hz, 285 watts.

Figure F1.   F-15A HIDEC INS

AIR DATA COMPUTER
(SPERRY)
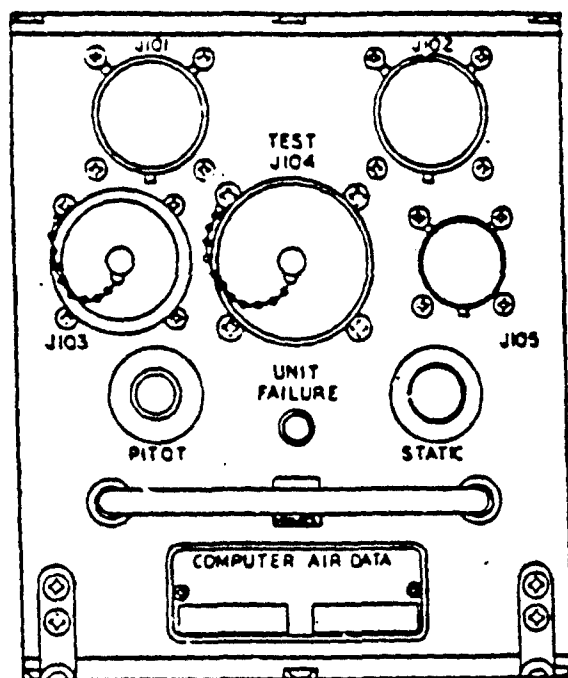
AIR DATA COMPUTER
AN/ASK-6

CHARACTERISTICS

- Digital Computer.
- Continuous BIT and Initiated BIT capability provided.
- Initiated BIT available on ground ONLY.
- Weight - 12 pounds.
- Volume - 508 cubic inches.
- Power Required - 115v, 400 Hz, 53 watts.

Figure F2.   F-15A HIDEC Air Data Computer System

TABLE F1

KEY SENSOR OUTPUTS

Quantity	Source
θ	INS
ϕ	INS
ψ	INS
p	Flight Control Computer
q	Flight Control Computer
r	Flight Control Computer
a_x	INS
a_y	INS
a_z	Flight Control Computer
v_E	INS
v_N	INS
v_{DWN}	INS
v_T	ADC
h	INS/ADC
Mach	ADC
ρ	ADC
$\dot{q}$	Computed
w	Computed from Fuel Totalizer and Basic Weight

APPENDIX G

F-15A STABILITY DERIVATIVE MODELS

F-15 STABILITY DERIVATIVE MODELS

The following figures depict the developmental flight test data used to formulate stability derivative models for the F-15A Inflight α Estimator. In all cases, flight test data precedes modeled parameters used in the estimator. References for documents from which the actual flight test data plots were extracted from are included immediately following the figure title. All data and graphs are unclassified.
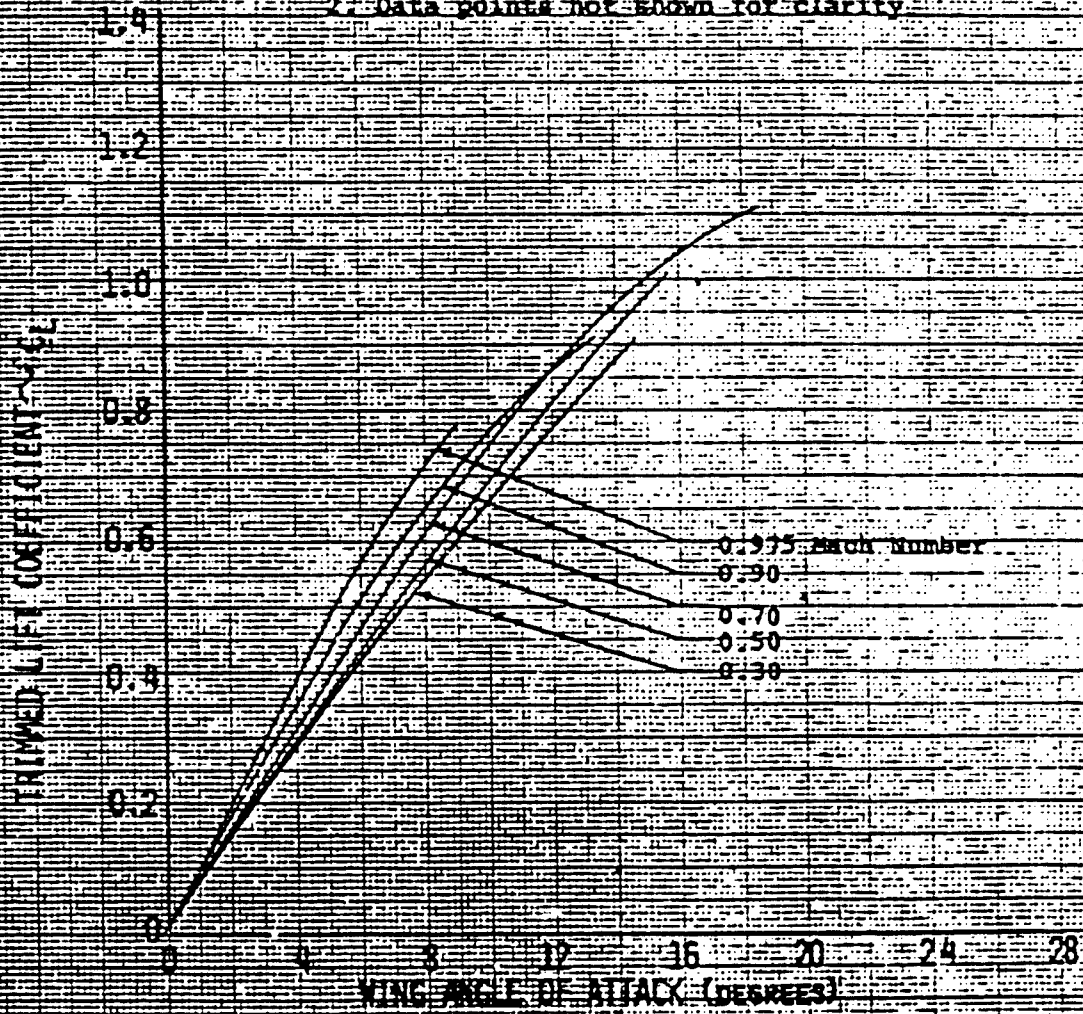
Figure G1. F-15A Subsonic Trimmed Lift Curve (U)[19]
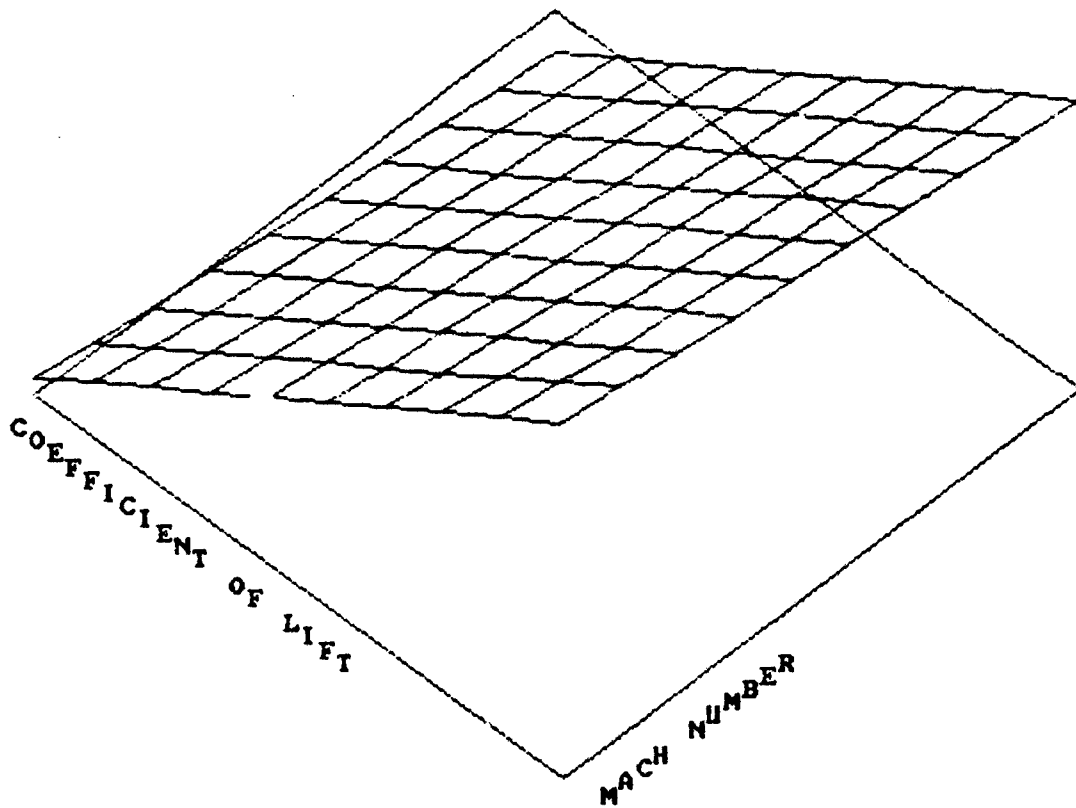
Figure G2.   F-15A Three Dimensional α Estimator Model

DYNAMIC
SYMBOL PRESSURE   Notes:

◻   200 psf   1. Solid symbols denote data
◯   400 psf   obtained with F-9 during con-
▢   800 psf   stant g level accelerations and
                            decelerations.
                            2. Zero-lift AOAs were not cal-
                            culated for data obtained with
                            F-9; trim AOAs did not differ
                            significantly from those obtained
                            with TF-1 for corresponding flight
                            conditions.
                            3. Dashed lines represent pre-
                            dicted values from reference 7.

ZERO - LIFT ANGLE OF ATTACK (DEGREES)

2

0

200 psf

-2

800 psf

400 psf

-4

ZERO-LIFT PITCHING MOMENT - C_{m_o}

.08   TF-15A

C_{m_o}

.04   F-15A

800 psf

400 psf

0

-.04

0   0.5   1.0   1.5   2.0   2.5

MACH NUMBER
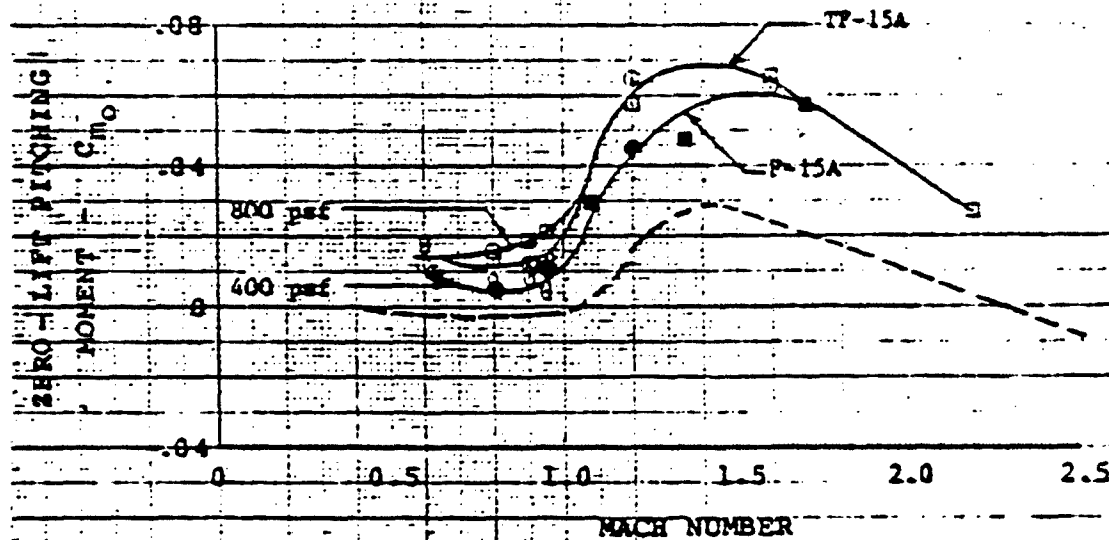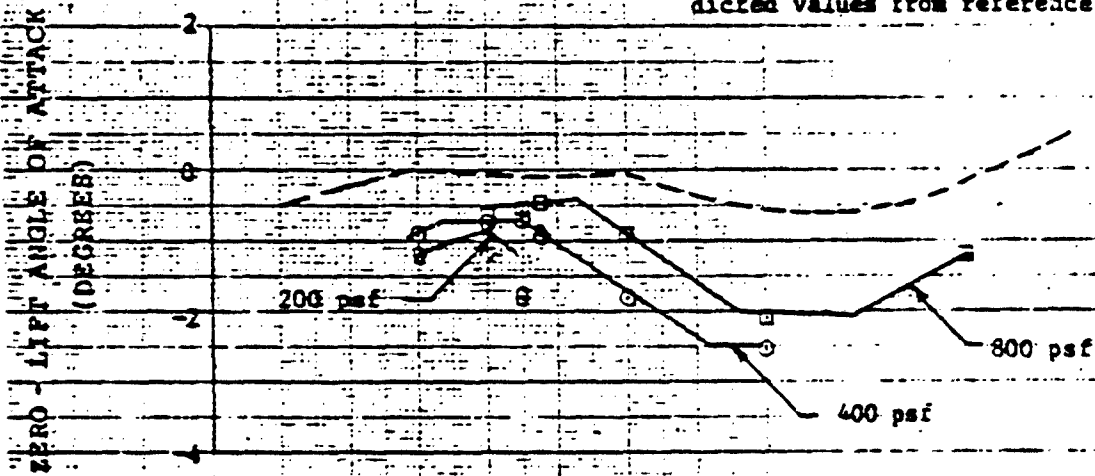
Figure G3.   F-15A Zero Lift Angle of Attack and Pitching
Moment Characteristics [18]
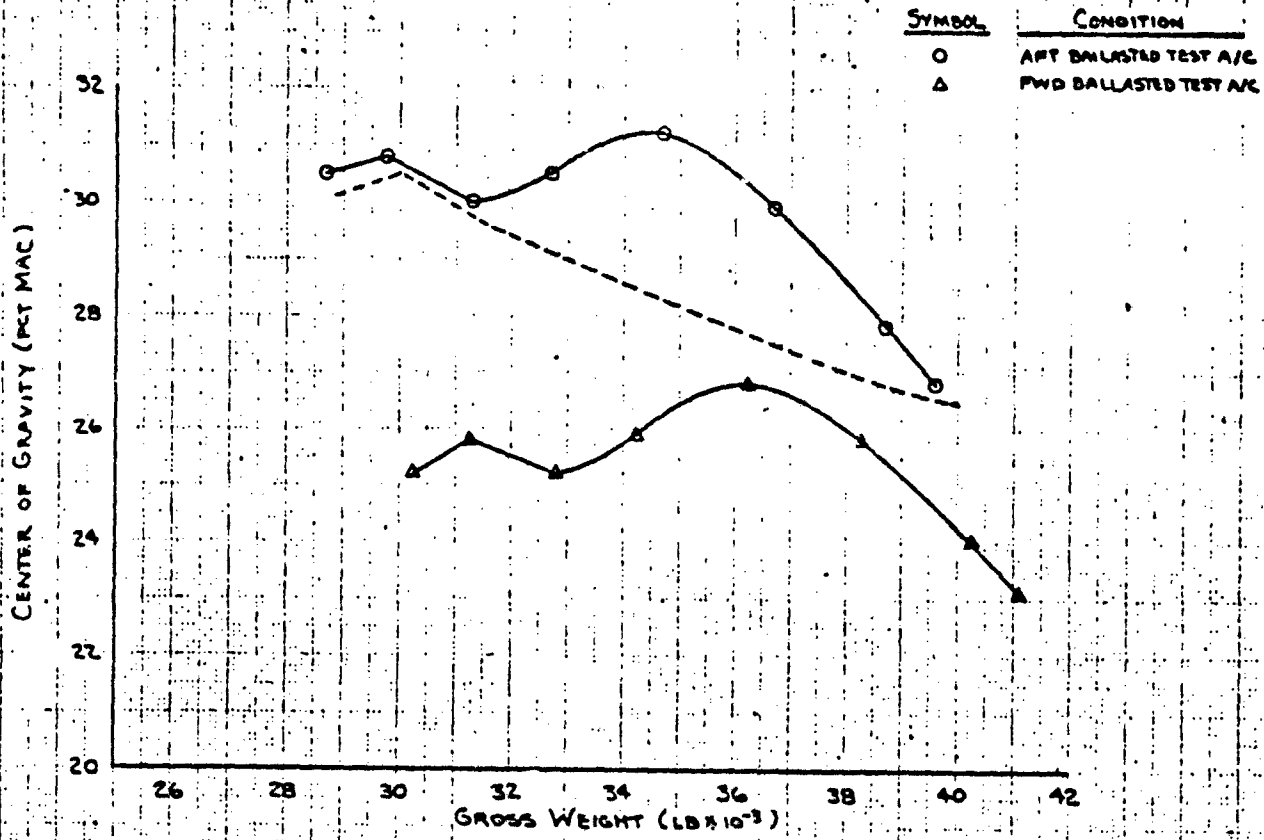
Figure G4.   F-15A Gross Weight vs. Center of Gravity (U)[20]
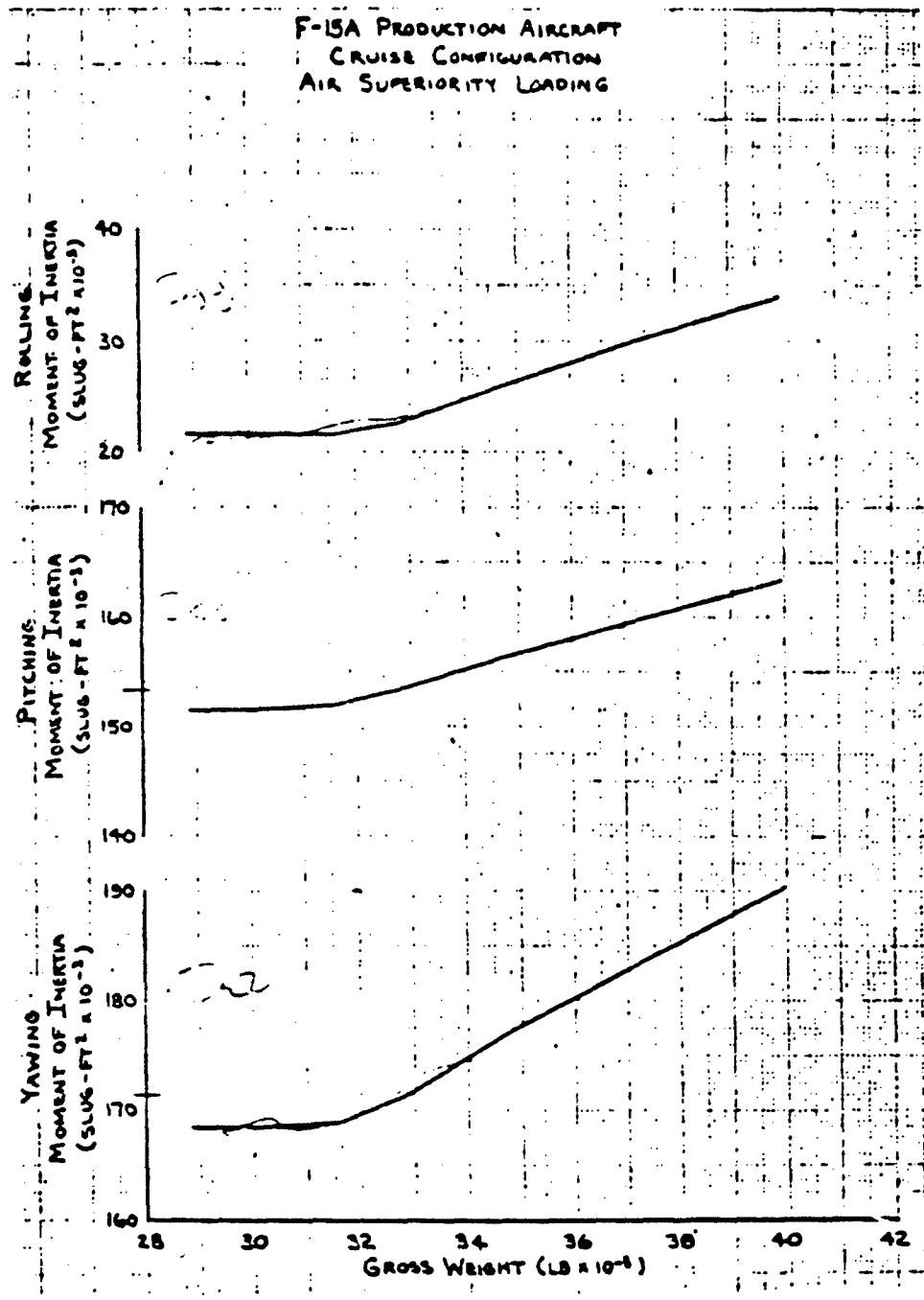
Figure G5.   F-15A Moments of Inertia (U)[20]

F-15A ANGLE OF ATTACK ESTIMATOR
IXX PROGRAM CODE MODEL
SECOND ORDER POLYNOMIAL FIT
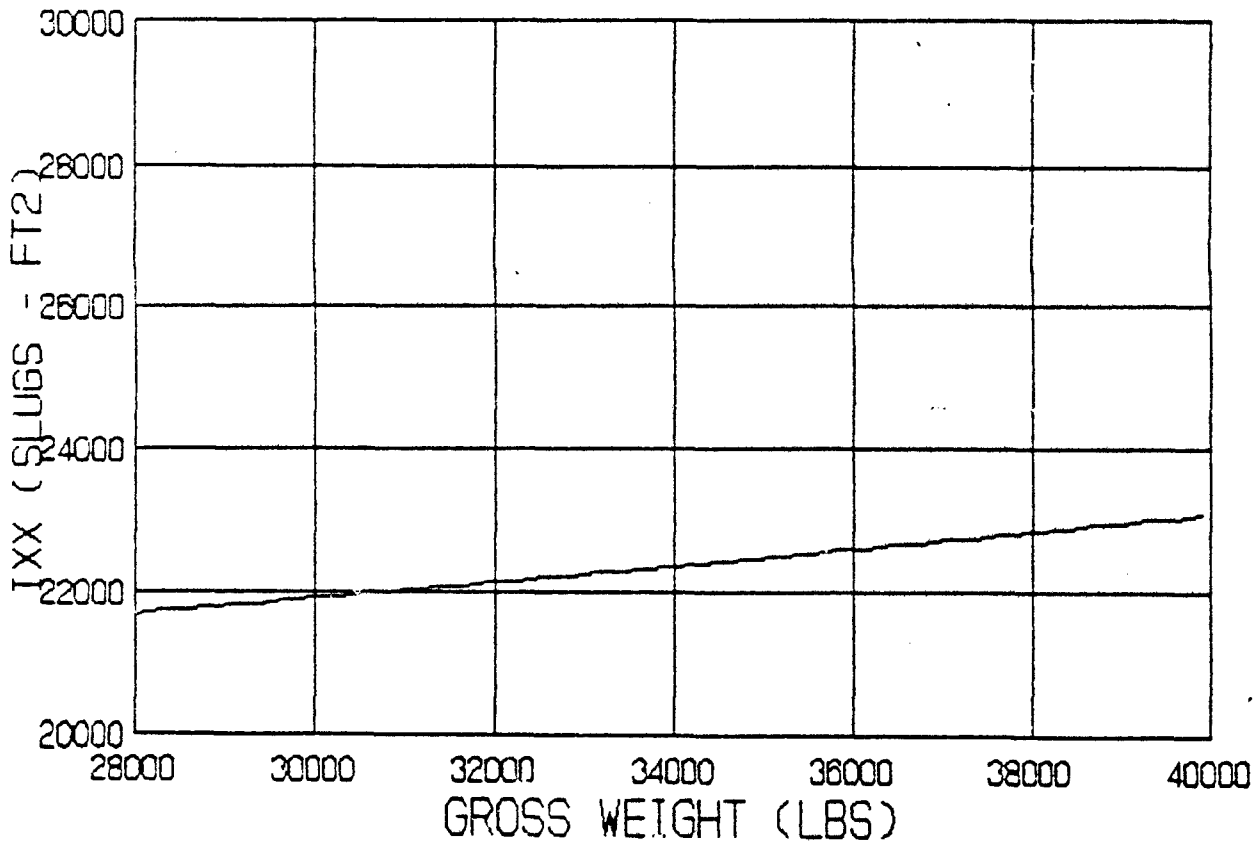
Figure G6.   F-15A Estimator IXX Model

F-15A ANGLE OF ATTACK ESTIMATOR

IYY PROGRAM CODE MODEL
SECOND ORDER POLYNOMIAL FIT
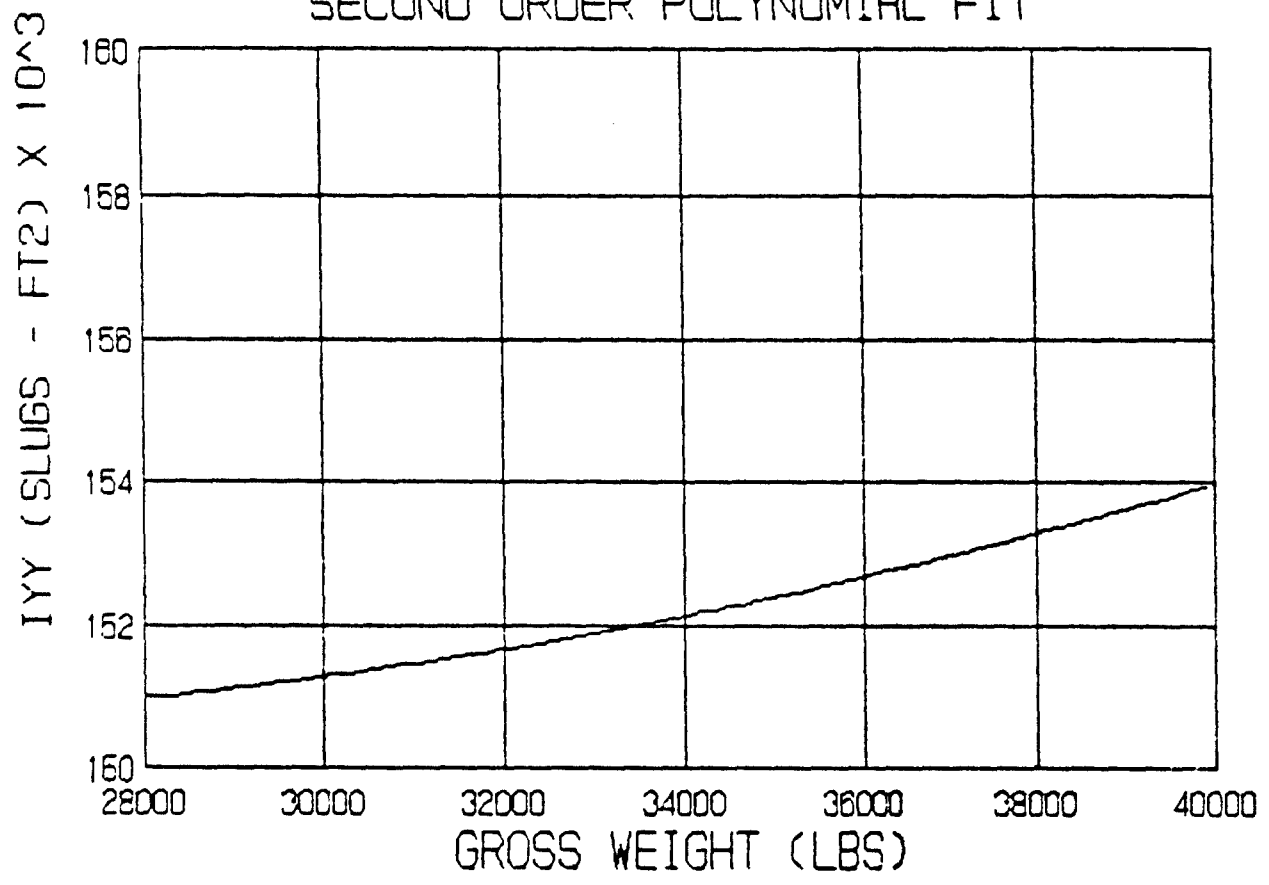
Figure G7. F-15A Estimator IYY Model

F-15A ANGLE OF ATTACK ESTIMATOR
IZZ PROGRAM CODE MODEL
SECOND ORDER POLYNOMIAL FIT
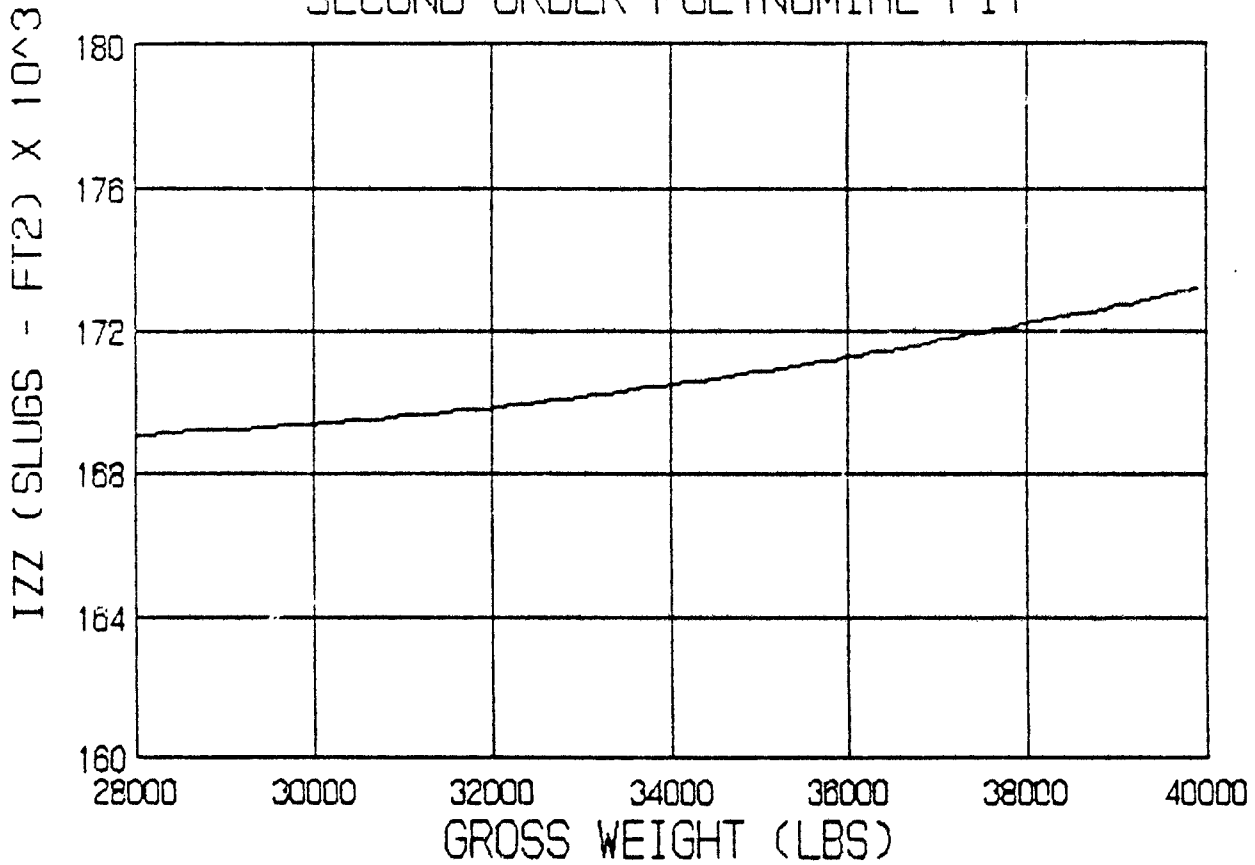
Figure G8.   F-15A Estimator IZZ Model

APPENDIX H

ELEXI PROGRAM AOA

ELEXI PROGRAM AOA

The program AOA is the modification of the basic inflight
α estimator, altered for implementation on the NASA ELEXI
computer.   The computer allows both post flight and actual
real time inflight data reduction.   The enumerated input
signals are read in and the program then sequentially reduces
each time segment of data before moving on to the next
increment.   The result is similar to onboard implementation of
the algorithm for real time estimation of angle of attack.

```
....................................................................
.
      PROGRAM AOA
.
....................................................................
.
* THIS PROGRAM UTILIZES AIRCRAFT GEOMETRY, 6 STABILITY DERIVATIVES, AND
* INPUTS FROM THE INS AND CADC TO CALCULATE ANGLE OF ATTACK OF THE
* AIRCRAFT IN ANY FLIGHT CONDITION.  (VERSION 2 CLEAN CONFIGURATION).
.
....................................................................
.
*   INPUTS FROM FLIGHT DATA FORMAT:
.
*      FUEL        - FUEL WT ON BOARD (LBS)
*                  - currently a calculated parameter
.
*      THETA       - PITCH ANGLE
*                  - en03, ADC/INS (DEG)
.
*      PHI         - BANK ANGLE
*                  - nno4, ADC/INS (DEG)
.
*      PSI         - HEADING ANGLE
*                  - eno7, ADC/INS (DEG)
.
*      P           - ROLL RATE
*                  - dd25, DFCC     (DEG/SEC)
.
*      Q           - PITCH RATE
*                  - dd01, DFCC     (DEG/SEC)
.
*      R           - YAW RATE
*                  - dd26, DFCC     (DEG/SEC)
.
*      AX          - BODY X ACCELERATION
*                  - lb50, INDICATED LONGITUDINAL ACCELERATION AT C.G. (G)
.
*      AY          - BODY Y ACCELERATION
*                  - dd27, LATERAL ACCEL  (FT/SEC**2)
.
*      AZ          - BODY Z ACCELERATION
*                  - dd02, NORMAL ACCEL DFCC    (DEG/SEC)
.
*      VE          - VELOCITY EAST
*                  - en05, INS     (FT/SEC)
.
*      VN          - VELOCITY NORTH
*                  - en06, INS     (FT/SEC)
.
*      VDWN        - VELOCITY DOWN
*                  - en10, INS     (FT/SEC)
.
*      VT          - TRUE AIRSPEED
*                  - lg22, ADC/INS    (KTS)
.
*      H           - ALTITUDE
*                  - en09, ADC/INS    (FT)
.
*      RMACH       - MACH NUMBER
*                  - lg23, ADC/INS
.
*      RHO         - AIR DENSITY ()
*                  - lg25 * s.l.s. density
.
*      QDOT        - PITCH ACCELERATION, OFF INS (DEG/SEC) ** ESTIMATED
*                  -- ESTIMATED FROM Q
.
....................................................................
.
      EXTERNAL OPENR, OPENW, FREAD, FWRITE, CLOSER, CLOSEW
      LOGICAL OPENR, OPENW, FREAD, FWRITE
      CHARACTER*16 SIGS(50)
      REAL*8  RDATA(50), N
      INTEGER*4 UNITI, UNITO, NIN, NOUT, NAVAIL
.
```

```
      PARAMETER ( UNITI = 6, UNITO = 7, NIN = 18, NOUT = 29)
      DATA SIGS /  'FUEL',  'THETA',    'PHI',   'PSI',     'P',      'Q',
     .              'R',     'AX',      'AY',    'AZ',      'VE',    'VN',
     .            'VDWN',    'VT',      'H','RMACH',      'RHO', 'AINF',
     .             'AWB',    'VW',      'VV',   'DIR','ALPHAG',
     .             'VWN',   'VWE',     'VWZ', 'QDOT',      'VX',    'VZ',
     .            21*' ' /
*
*****************************************************************************
*
*   OPEN DATA FILES AND SET UP OUTPUT FILES
*
      IF( .NOT. OPENR(UNITI,'FLDT.IN',NAVAIL)) THEN
         WRITE(7,100)
         STOP
      END IF

      IF( .NOT. OPENW(UNITO,'FLDT.OUT',NOUT,SIGS,'CMP2')) THEN
         WRITE(7,200)
         STOP
      END IF
  100 FORMAT(///'OOPS 1'/)
  200 FORMAT(///'OOPS 2'/)
*
*****************************************************************************
*
*   INITIALIZE PROGRAM PARAMETERS
*
      QL       = 0.0
*
 1000 S        = 608.0
 1100 XT       = 17.7
 1110 XSM      = 0.0300 * 15.94
 1200 CBAR     = 15.94
 1300 B        = 42.81
 1400 WTDRY    = 29503.00
 1500 STORES   = 0.0
*
      PI       = 3.141592654
      DTOR     = PI / 180.0
*
*****************************************************************************
*
*   READ IN FLIGHT DATA PARAMETERS FOR SPECIFIC TIME INCREMENT.
*
  300 IF( FREAD(UNITI,TIME,RDATA)) THEN
*
         FUEL    = RDATA( 1)
         THETA   = RDATA( 2)
         PHI     = RDATA( 3)
         PSI     = RDATA( 4)
         P       = RDATA( 5)
         Q       = RDATA( 6)
         R       = RDATA( 7)
         AX      = RDATA( 8) * 32.174
         AY      = RDATA( 9)
         AZ      = -1.0 * RDATA(10)
         VE      = RDATA(11)
         VN      = RDATA(12)
         VDWN    = RDATA(13)
         VT      = RDATA(14) * 1.687778
         H       = RDATA(15)
         RMACH   = RDATA(16)
         RHO     = RDATA(  ) * 0.0023769
         AINF    = RDATA(18)
*
         WT      = WTDRY + STORES + FUEL
*
*****************************************************************************
*
*   CHANGE ANGULAR PARAMETERS FROM DEGREES TO RADIANS AND CALCULATE
*   TRIGOMETRIC FUNCTIONS.  CALCULATE QDOT.
*
         PHI     = PHI * DTOR
         PSI     = PSI * DTOR
         THETA   = THETA * DTOR
         P       = P * DTOR
         Q       = Q * DTOR
         R       = R * DTOR
*
```

```
          COSPHI = COS(PHI)
          COSPSI = COS(PSI)
          COSTHA = COS(THETA)
          SINPHI = SIN(PHI)
          SINPSI = SIN(PSI)
          SINTHA = SIN(THETA)
    .

          QDOT = (Q - QL) * 20.0
          QL = Q
    .
    .......................................................................
    .
    . MODEL STABILITY DERIVATIVES
    .
          WTS  = WT/1.0E+05
    4200  RIXX = 1.119E+04 * (WTS**2) + 4.067E+03 * WTS + 2.025E+04
          RIYY = 7.428E+03 * (WTS**2) + 6.723E+03 * WTS + 1.502E+05
          RIZZ = 1.454E+04 * (WTS**2) + 8.908E+03 * WTS + 1.678E+05
          CMO  = 0.016
    .
    .......................................................................
    .
    . ESTIMATE VX AND VZ
    .
          VX = ( COSTHA * COSPSI ) * VN +
    .          ( COSTHA * SINPSI ) * VE -
    .          ( SINTHA ) * VDWN
          VX = ABS(VX)
          VZ = ( (SINPHI * SINPSI) + (COSPHI * SINTHA * COSPSI) ) * VN +
    .          ( (-SINPHI * COSPSI) + (COSPHI * SINTHA * SINPSI) ) * VE +
    .          ( COSPHI * COSTHA ) * VDWN
    .
    .......................................................................
    .
    . COMPUTE NO WIND ESTIMATE OF ALPHA BASED ON INERTIAL VELOCITIES IN THE
    . BODY DIRECTIONS.
    .
          VZABS = ABS(VZ)
          ALPHAG = ATAN(VZABS/VX)
          IF (VZ .LT. 0.0) ALPHAG = -ALPHAG
    C
    .
    .......................................................................
    .
    . DERIVE LOAD FACTOR FROM AZ
    .
    .
    6000  N = ( -1.0 * ( COS(ALPHAG) * AZ + SIN(ALPHAG) * AX ) / 32.2 )
    .          + 1.0
    .
    .......................................................................
    .
    . CALCULATION OF ALPHA ESTIMATED
    .
    .
    7000  CL      = ( (N*WT*XT) + (QDOT*RIYY) + (P*R*(RIXX-RIZZ)) +
    .                 CMO*(0.5*RHO*(VT**2))*S*CBAR ) /
    .                 ( (0.5*RHO*(VT**2)) * S * XT * (1.0+(XSM/XT)) )
          AWB = 0.79 + 15.44*CL - 2.75*RMACH
          AWBR = AWB * DTOR
    .
    .......................................................................
    .
    . 3 - D WIND CALCULATION
    .
          COSAWB = COS(AWBR)
          SINAWB = SIN(AWBR)
    .
          VAN = ( COSPSI * COSTHA * COSAWB +
    .            COSPSI * SINTHA * COSPHI * SINAWB +
    .            SINPSI * SINPHI * SINAWB ) * VT
    .
          VAE = ( SINPSI * COSTHA * COSAWB +
    .            SINPSI * SINTHA * COSPHI * SINAWB -
    .            COSPSI * SINPHI * SINAWB ) * VT
    .
          VAZ = ( -1.0 * SINTHA * COSAWB +
    .            COSTHA * COSPHI * SINAWB ) * VT
```

- 142 -

```
      .
                VWN = VN - VAN
      .
                VWE = VE - VAE
      .
                VWZ = VDWN - VAZ
      .
.........................................................................
      .
. STANDARD WIND CALCULATIONS
      .
                VW = SQRT(VWN**2 + VWE**2)
                ARG = VWN/VT
                DIR = ACOS(ARG) + 3.1714
                IF (VWE .LT. 0.0) DIR = DIR - 3.174
                VV = -1.0*VWZ
      .
.........................................................................
      .
. SET UP NEW OUTPUT PARAMETERS AND WRITE OUTPUT FILE.
      .
                RDATA(19) = AWB
                RDATA(20) = VW
                RDATA(21) = VV
                RDATA(22) = DIR
                RDATA(23) = ALPHAG / DTOR
                RDATA(24) = VWN
                RDATA(25) = VWE
                RDATA(26) = VWZ
                RDATA(27) = QDOT
                RDATA(28) = VX
                RDATA(29) = VZ
      .
                CALL FWRITE(UNITO,TIME,RDATA)
      .
          GO TO 300
          END IF
      .
.........................................................................
      .
          CALL CLOSER(UNITI)
          CALL CLOSEW(UNITO)
      .
.........................................................................
      .
          STOP
          END
      .
.........................................................................
```

APPENDIX I

FLIGHT TEST CARD

FLIGHT TEST CARD

The following is the actual NASA flight test card used for the robustness test on the NASA F-15A HIDEC aircraft. Test point 22 is the modified split-S maneuver designed specifically to test the α estimator. The test point was flown once as printed and repeated once, substituting a 30 degree left wing down bank at 2 g's for step 22B.

20K'/0.5 - 0.9M

16. MIL THRUST ACCEL. 0.5 - 0.9M COUPLED
                (228 - 423 KCAS)

17. MIL THRUST 5 - 6g TURN, 0.9M COUPLED -
    10 SECONDS

20K'/0.4 - 0.9M

18. MAX THRUST ACCEL. 0.4 - 0.9M UNCOUPLED
                (182 - 423 KCAS)

19. REPEAT COUPLED

20K'/0.6M   (275 KCAS)

20. MIL THRUST 3 - 4g TURN, 0.6M UNCOUPLED -
    30 SECONDS

21. REPEAT COUPLED

20K'/0.7M   (324 KCAS)

22. PERFORM THE FOLLOWING MODIFIED SPLIT-S
    MANEUVER.

        A. HDG TRUE NORTH
        B. 30 DEG RWD BANK / 2g's
        C. ROLL INVERTED
        D. MOD. SPLIT-S MANEUVER / 4-5g's

23. RTB

Figure I1.   NASA F-15A HIDEC Flight Test Card -
             Robustness Test

BIBLIOGRAPHY

1. Thacker, Thomas. Use of State Estimation to Calculate Angle of Attack Postion Error From Flight Test Data. M.S. Thesis, GAE/AA/85J-3, Wright-Patterson AFB, Ohio: Air Force Institute of Technology, Oct 85.

2. McRuer, Duane, Irving Ashkenas, and Dunstan Graham. Aircraft Dynamics and Automatic Control. New Jersey: Princeton University Press, 1973.

3. Laerus, Mel, YPEA. Personal interview, Aeronautical Systems Division, Wright-Patterson AFB, Ohio, 25 Jul 85.

4. Department of the Air Force. USAF Series F-111F Flight Manual. T.O.1F-111F-1. McClellan AFB, CA: Sacramento ALC/MMSRB, 1 Aug 83.

5. Department of the Air Force. Specification for USAF Standard Form, Fit and Function (F3) Medium Accuracy Inertial Navigation Set/Unit. SNU 84-1. Aeronautical Systems Division, Wright-Patterson AFB, Ohio, 15 Oct 84.

6. Griffiths, Barry and E. Michael Geyer. Interfacing Kalman Filters with the Standard INS. AFWAL-TR-84-1139. Wright-Patterson AFB, Ohio: Avionics Laboratory, September 84.

7. Freeman, Duane. Angle of Attack Computation System. AFFDL-TR-73-89. Wright-Patterson AFB, Ohio: Air Force Flight Dynamics Laboratory, Oct 73.

8. Petrov, B. and R. Studnev et al. *Determining Angles of Attack and Sideslip by Signals from Accelerometers Installed On Board an Aircraft.* FTD-ID(RS)T-1657-77. "Izvestiya Vysshikh Uchebnykh Zavedeniy, 'Priborostroyeniye'," Vol 18, Nr 10, 1975.

9. Olhausen, J. "Use of a Navigation Platform for Performance Instrumentation on the YF-16". *AIAA 13th Aerospace Sciences Meeting.* AIAA-75-32. American Institute of Aeronautics and Astronautics, Pasedena, CA, Jan 75.

10. Costigan, Michael, AFIT/USAFTPS. Personal interview, Air Force Institute of Technology, Wright-Patterson AFB, Ohio, Mar 86.

11. Maybeck, Peter S., AFIT/ENE. Personal interview, Air Force Institute of Technology, Wright-Patterson AFB, Ohio, Sept 86.

12. Gelb, Arthur, ed. *Applied Optimal Estimation.* Massachusetts: The M.I.T. Press, 86.

13. Gleason, Daniel, AFIT/ENY. Personal interview, Air Force Institute of Technology, Wright-Patterson AFB, Ohio, Aug 86.

14. Maybeck, Peter S. *Stochastic Models, Estimation, and Control, Volume 1.* New York: Academic Press, Inc., 79.

15. Heffley, R.K. et al. *Aircraft Handling Qualities Data.* NASA CR-2144. Systems Technology, Inc., Dec 72.

16. Jumper, Eric J., S.J. Schreck, and R.L. Dimmick. "Lift-Curve Characteristics for an Airfoil Pitching at Constant Rate". AIAA 24th Aerospace Sciences Meeting. AIAA-86-0117. American Institute of Aeronautics and Astronautics, Reno, NV, Jan 86.

17. Department of the Air Force. USAF Series F-15A Flight Manual. T.O.1F-15A-1. Robins AFB, GA: WR -ALC/MMEDT, Nov 87.

18. Tanaka, Arthur Y. and Rodrigo J. Huete. F/TF-15A Flying Qualities Air Force Development Test and Evaluation. AFFTC-TR-76-48. Edwards AFB, CA: Air Force Flight Test Center, Jul 77.

19. Zaloga, Thomas. F-15A Performance Air Force Development Test and Evaluation. AFFTC-TR-77-7. Edwards AFB, CA: Air Force Flight Test Center, Jul 77. CONFIDENTIAL

20. Jones, Gerald L. and Charles P. Winters. Initial Air Force Development Test and Evaluation of the Flying Qualities of the F-15A Aircraft. AFFTC-TR-74-8. Edwards AFB, CA: Air Force Flight Test Center, Apr 74. CONFIDENTIAL

CAPTAIN JOSEPH E. ZEIS. JR.

214-48-9715

AFSC:2871B. FLIGHT TEST NAVIGATOR. FIGHTER

Captain Joseph E. Zeis. Jr. is a Flight Test Navigator
assigned to the 6510 Test Wing, F-15 Combined Test Force,
Edwards Air Force Base, California.   He is 29 years old.

Captain Zeis was born in Washington, D.C. on 20 September
1958.   He attended Montgomery Blair High School in Silver
Spring. Maryland, where he was involved in numerous
activities. including debating team, band,and National Honor
Society.   He graduated third in the Class of 1976.

Following graduation, Captain Zeis attended Syracuse
University, where he majored in Aerospace Engineering.   He
obtained an appointment to the United States Air Force
Academy in the Class of 1981 and entered on 27 June 1977.   As
a Cadet, he was actively involved in the USAFA Debate Team,
earning four letters in that intercollegiate organization.
He graduated 56 out of 875 and was designated a distinguished
graduate, with a Bachelor of Science degree in Aeronautical
Engineering.

Following graduation, Captain Zeis attented Undergraduate
Navigator Training, where he won the ATC Commander's Trophy
and the Husik Memorial Trophy as top graduate in the class.
Following upgrade training at Cannon Air Force Base. New
Mexico. he was assigned to Royal Air Force Station Lakenheath
as a Weapon Systems Officer in the F-111F.   Captain Zeis
served as an Instructor WSO in the 48 Tactical Fighter Wing
there until returning stateside in August 1985 to participate
in the Joint AFIT/Test Pilot School Program.

Captain Zeis attented the Air Force Institute of Technology
at Wright-Patterson Air Force Base, Ohio, for Master's of

Science in Aeronautical Engineering course work. Upon completion, he attended the United States Air Force Test Pilot School, where he was designated a Distinguished Graduate in December 1987. He is currently serving as Chief, F-15E Armament Branch, in the F-15 Test Force and actively flying F-15 and F-4 test missions.

Captain Zeis is a member of the American Institute of Aeronautics and Astronautics and the Air Force Association. He is also a member of the Edwards AFB Catholic parish and in his free time, he flies sailplanes and plays golf. He is a recipient of the Air Force Commendation Medal and Air Force Combat Readiness Medal.

Permanent Address: 1606 White Oak Drive

Silver Spring, Maryland

20910

REPORT DOCUMENTATION PAGE

Form Approved
OMB No. 0704-0188

1a. REPORT SECURITY CLASSIFICATION UNCLASSIFIED	1b. RESTRICTIVE MARKINGS

2a. SECURITY CLASSIFICATION AUTHORITY	3. DISTRIBUTION/AVAILABILITY OF REPORT
2b. DECLASSIFICATION/DOWNGRADING SCHEDULE	Approved for public release; distribution unlimited.

4. PERFORMING ORGANIZATION REPORT NUMBER(S) AFIT/GAE/AA/88J-2	5. MONITORING ORGANIZATION REPORT NUMBER(S)

6a. NAME OF PERFORMING ORGANIZATION School of Engineering	6b. OFFICE SYMBOL (If applicable) AFIT/ENY	7a. NAME OF MONITORING ORGANIZATION

6c. ADDRESS (City, State, and ZIP Code) Air Force Institute of Technology Wright-Patterson AFB, Ohio 45433-6583	7b. ADDRESS (City, State, and ZIP Code)

8a. NAME OF FUNDING/SPONSORING ORGANIZATION USAF Test Pilot School	8b. OFFICE SYMBOL (If applicable) TENX	9. PROCUREMENT INSTRUMENT IDENTIFICATION NUMBER

8c. ADDRESS (City, State, and ZIP Code) USAF Test Pilot School Edwards AFB, California 93523	10. SOURCE OF FUNDING NUMBERS			
	PROGRAM ELEMENT NO.	PROJECT NO.	TASK NO	WORK UNIT ACCESSION NO.

11. TITLE (Include Security Classification)
ANGLE OF ATTACK AND SIDESLIP ESTIMATION USING AN INERTIAL REFERENCE PLATFORM

12. PERSONAL AUTHOR(S)
Joseph E. Zeis, Jr., B.S., Capt, USAF

13a. TYPE OF REPORT MS Thesis	13b. TIME COVERED FROM _____ TO _____	14. DATE OF REPORT (Year, Month, Day) 1988 June	15. PAGE COUNT 168

16. SUPPLEMENTARY NOTATION

17. COSATI CODES			18. SUBJECT TERMS (Continue on reverse if necessary and identify by block number)
FIELD	GROUP	SUB-GROUP	F-15, Parameter Estimation, Angle of Attack, Angle of Sideslip, Angle of Attack Estimation, Inertial Navigation System, Inertial Reference System
1	04		

19. ABSTRACT (Continue on reverse if necessary and identify by block number)

Thesis Chairman: Dr. Robert Calico
Professor of Aeronautical Engineering

Approved for public release: IAW AFR 190-1
E. WOLAVER   15 Jun 88
Dean for Research and Professional Development
Air Force Institute of Technology (AU)
Wright-Patterson AFB OH 45433

20. DISTRIBUTION/AVAILABILITY OF ABSTRACT ☒ UNCLASSIFIED/UNLIMITED ☒ SAME AS RPT. ☐ DTIC USERS	21. ABSTRACT SECURITY CLASSIFICATION UNCLASSIFIED
22a. NAME OF RESPONSIBLE INDIVIDUAL Dr. Robert Calico	22b. TELEPHONE (Include Area Code) AV 785-2362	22c. OFFICE SYMBOL AFIT/ENY

DD Form 1473, JUN 86   Previous editions are obsolete.   SECURITY CLASSIFICATION OF THIS PAGE

Recent advances in the stability, accuracy and reliability of inertial navigation and reference systems now allow angle of attack and sideslip information to be calculated from internal aircraft systems and a central air data computer. Conflicting demands for inflight angle of attack information and post-flight angle of attack and sideslip data reduction requires that two separate methods be developed. Inflight algorithms require fast, accurate angle of attack, with no assumptions on vertical wind. Post-flight usage, however, demands great accuracy with no assumptions on either sideslip or vertical windage. From the aircraft equations of motion, angle of attack and sideslip algorithms will be developed, with velocity and angular rate inputs of the type expected from an aircraft central air data computer and inertial navigation system. A computer program will then be developed to validate these equations. A Kalman filter algorithm will also be designed to aid in estimating data output from these sources.

Flight test will consist of two parts. Initially, signals will be picked of a standard inertial reference system on a NASA F-15A aircraft. These signals will be processed using the inflight algorithm developed. The estimated angle of attack output will then be compared to angle of attack as measured by a flight test boom. Finally, a demonstration will be conducted on the NASA F-15A to determine usability and accuracy of inertially derived angle of attack information in a highly maneuvering environment.